
TECHNICAL APPLICATION PAPERS No.14

Faults in LVDC microgrids with front-end converters

Low voltage direct current distribution systems



Index

| | |
|----------------|---|
| 002–005 | Introduction |
| 006–010 | 1. Advantages of Low Voltage DC distribution systems |
| 006 | 1.1 Sensitive electronic loads |
| 006 | 1.2 Distributed generation |
| 006 | 1.3 Cables and maximum transmissible power |
| 007–008 | 1.4 DC in data centers |
| 009 | 1.5 Hazard of direct current vs alternating current |
| 010 | 1.6 Elimination of synchronization |
| 010 | 1.7 Perspective of LVDC distribution |
| 011–014 | 2. System configuration |
| 011 | 2.1 Front-End Converter (FEC) |
| 011 | 2.2 System description |
| 015–050 | 3. Fault analysis |
| 015–027 | 3.1 Short circuit on DC side of the front-end converter |
| 028–041 | 3.2 Ground fault on DC side of the front-end converter |
| 042–043 | 3.3 Short circuit on AC side of the front-end converter |
| 044–050 | 3.4 Ground fault on AC side of the front-end converter |
| 051–061 | 4. DC fault protection – The ABB offer |
| 051 | 4.1 Air circuit breakers |
| 052–055 | 4.2 Molded-case circuit breakers |
| 056–058 | 4.3 Miniature circuit breakers |
| 059 | 4.4 Fuse-disconnectors |
| 060 | 4.5 Fuse-holder |
| 061 | 4.6 GE Rapid |
| 062–065 | Annex A – Description of the main power-electronic-switches |
| 066–067 | Annex B – Switch-mode three-phase converters |
| 068–069 | Annex C – DC fault contribution of other types of converters |

Introduction

New scenarios in electrical distribution networks, with increasing presence of distributed generation and loads with strict power quality requirements, include DC microgrids with energy storage systems as a replacement for traditional AC systems.

DC electrical distribution offers several advantages compared to AC in many applications, such as data centers, marine installations and in addition in low voltage distribution in the presence of distributed generation and storage.

Battery energy storage systems and distributed generation such as PV plants or wind microtur-

bines, and their related electronic converters, affect system behavior both during normal operation and in the presence of faults, in different ways depending on different possible grounding schemes. Most converter systems are actually based on double conversion: a DC-Bus is intercDC data centers).

In these cases, probability of a fault in the DC sec-



tion is no longer negligible, and such faults need to be dealt with by proper analysis and protection design.

Conventional wisdom is that converters limit currents in any situation, hence the fault current level is no longer a concern in circuit design. While this might indeed be the case for some specific situations, there are others in which converters are not able to limit fault currents.

This depends on type and connection of converters, as will be shown.

Some most common types of power converters are shown in Figure I.1. Each has defined features and applications:

- three phase thyristor rectifier, which converts the whole of the input waveform to one of constant polarity (positive or negative) at its output. Thyristors are commonly used instead of diodes to create a circuit that can regulate the output voltage (application example: feed and control of DC motors – Figure I.1a);
- AC/DC IGBT converter, which is a forced commutated three-phase converter that can be used as a rectifier or as an inverter. Electronic component commutation (from ON to OFF position) occurs hundreds of times per period, which guarantees performances that could not be reached with thyristors, such as: current or voltage may be modulated (PWM – Pulse Width Modulation) producing a low harmonic contribution; the power factor may be controlled and it may follow an established profile (application examples: HVDC light transmission, DC/AC converter in drives, front-end converter in LVDC microgrids – Figure I.1b). Power reversal occurs by means of voltage reversal in thyristor rectifiers, while forced commutated rectifiers may be used for current reversal.
- step up converter (boost converter), which is a DC/DC converter with an output voltage higher than its input voltage (application example: PV plants connected to DC systems – Figure I.1c);
- step down converter (buck converter), which is a DC/DC converter with an output voltage lower than its input voltage (application example: DC loads connected to DC systems – Figure I.1d);
- DC/DC bidirectional converter (buck boost converter), which is obtained by the combination of the previous two converters. This configuration allows the bidirectional power flow (application example: charging and discharging of energy storage systems connected to DC systems – Figure I.1e).

As shown in pictures, semiconductors with free-wheeling diodes are widely employed. Purpose of such diodes is to prevent overvoltages and coun-

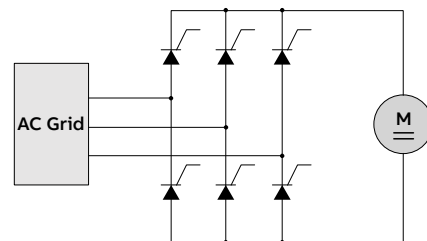
tervoltages when semiconductor is switched off. Because of the presence of such diodes, in case of fault, different effects may occur, depending on type of converter and type and location of fault.

A common situation frequently described is the connection of a DC active microgrid (e.g. with PV plant or energy storage system) to the AC grid by means of an IGBT converter.

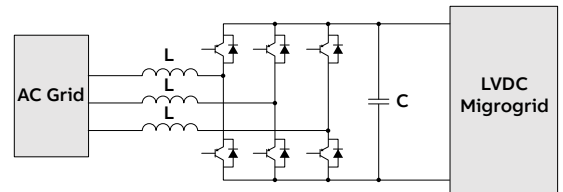
If a short circuit occurs on AC side, the converter is able to limit the fault current.

Figure I.1 – Most common types of power converters

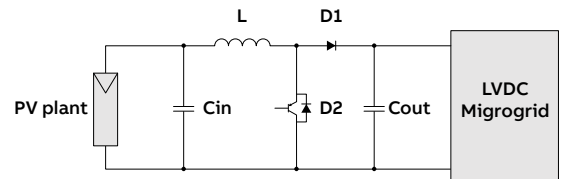
I.1a - Thyristor rectifier



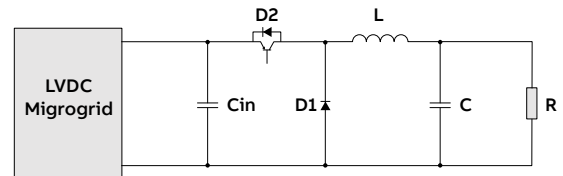
I.1b - AC/DC IGBT converter



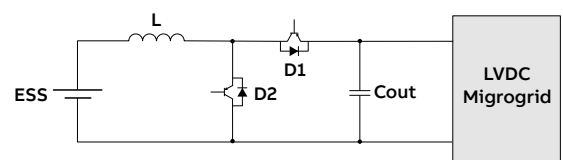
I.1c - Step up converter



I.1d - Step down converter



I.1e - Bidirectional converter



Introduction

If, on the other hand, the fault is on the DC side, fault current flows in the freewheeling diodes without any possibility for the IGBTs to limit it, even if an IGBT block signal is sent by the control system (Figure I.2).

Similar situations occur in all cases in which short circuit current path can include freewheeling diodes, hence all AC/DC IGBT converter, step-up and DC/DC bidirectional converters may suffer from this effect.

Moreover, a similar effect may take place in the case of a DC ground fault in a microgrid with the neutral point of the MV/LV transformer grounded or DC negative pole grounded. Both grounding configurations are widely used as they guarantee operation safety from overvoltages.

However, when a ground fault occurs, the front-end converter may not be able to limit the AC grid contribution to the fault current, even if the DC generators contribution may be switched off by IGBT block (Figure I.3).

It must be pointed out that ground faults are far more frequent than short circuits in electrical installations, hence DC ground faults are expected to become more and more frequent as DC section of installations extend.

Similar cases can be made for several other configurations of converters.

Thyristor rectifiers, which are immune from this issue, can't be applied as front-end converters in DC distribution with distributed generation, be-

cause in case of reversal of power flow, they require voltage polarity to be switched, with serious problems to devices connected to the DC-Bus.

It is thus apparent that the naive statements that fault currents are of no concern and that protection can be fully implemented by converters is not generally true. A number of realistic cases exist in which converters can't limit ground- or short circuit fault current.

A thorough analysis of fault conditions and dedicated protection devices must therefore be used to safeguard installation and operator safety.

This Technical Application Paper deals with fault analysis and protection in LVDC microgrids with front-end converters. In particular, Chapter 1 explains the main advantages of LVDC microgrids; Chapter 2 shows the description of the system configuration; Chapter 3 deals with the short circuit and ground fault analysis both in case they occur on DC and AC front-end converter side, highlighting the situations in which the converter cannot limit fault currents; finally, Chapter 4 presents the solutions offered by ABB to protect the plants against DC fault.

This Technical Application Paper includes three annexes with the description of the main power-electronicswitches, of the main converter control methods, and of the DC fault contribution of other types of converters.

Figure I.2 – DC short circuit current components in an active LVDC microgrid

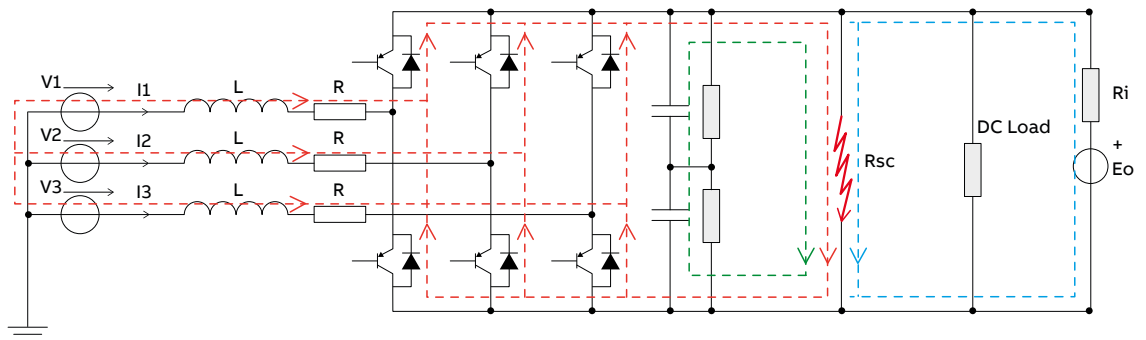
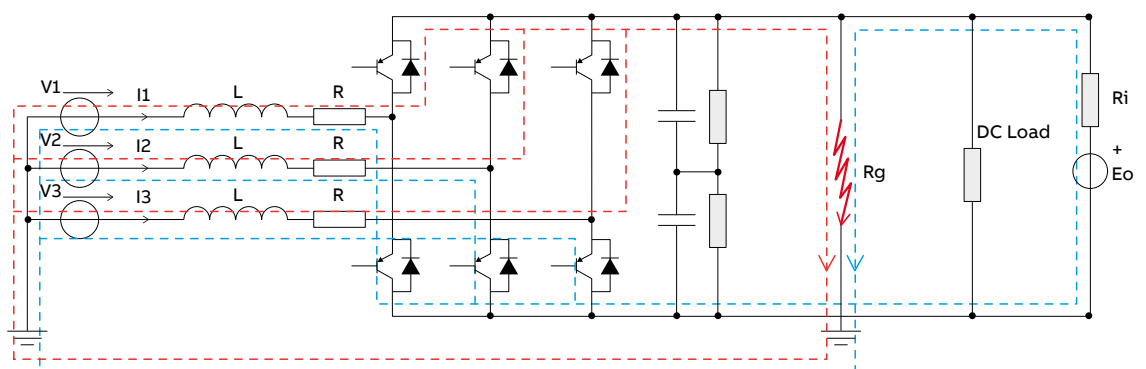


Figure I.3 – DC positive pole ground fault current path in an active LVDC microgrid with the neutral point of the MV/LV transformer grounded



1. Advantages of Low Voltage DC distribution systems

At the end of the 19th century, AC started replacing DC in power distribution, mainly because AC was more easily transformed between different voltage levels and transmitted over long distances.

These conversions allow high-voltage, low-current power distribution that minimizes losses and enables central power plants with sufficient scale to be maximally cost-effective.

Advances in power conversion technology, including DC power rectification, however, have eroded the dominance of AC power because of conversion advantages. When AC was introduced, loads were mostly resistive. Today, however, many loads utilize power electronics.

Most power-electronic loads contain a diode rectifier to convert the supplying AC voltage to DC. This introduces non-sinusoidal currents into the grid, which in turn deteriorates power quality. By using appropriate DC voltages to supply these loads, the rectifier can be removed from the loads. This reduces energy losses and brings savings without lowering power quality.

A low-voltage distribution network is traditionally based on a three-phase 400 V AC system. Because of the low voltage, 20/0.4 kV transformers have to be installed close enough to the customer to avoid too high transmission losses. The use of a higher AC or DC voltage in the LV network increases the power transmission capacity and permits longer distances.

The use of a higher AC voltage level increases the transmission capacity of an aerial or underground cable with the same cross-section area. With DC, this capacity can be further increased.

The main reason is the higher voltage level allowed, because the effective value with DC voltage can be 1500 V, while it is 1000 V in AC. Besides, some other losses can be reduced by using DC voltage. The inductance of the transmission line does not have an impact in the steady-state condition, when the voltage drop in the line is smaller. With DC there is also no skin effect, so transmission line resistance and voltage drop decrease. Moreover, considering the transition from AC to DC systems, most of the loads used today can operate equally well with a DC supply as with an AC supply. For example, universal machines, which are used in household appliances such as electric mixers and vacuum cleaners, have the same configuration as a series magnetized DC machine and work both in AC and DC.

Electronic loads, which can be found in computer equipment, battery chargers and lighting, work properly in the ranges 100-240 V and 50-60 Hz, and this is accomplished by using a switch mode

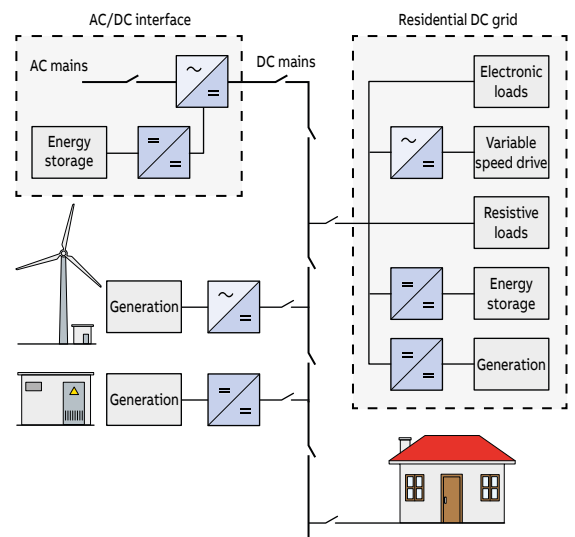
power supply (SMPS). SMPS first rectifies the voltage and then adjusts the rectified voltage to the load using a DC/DC converter. SMPS can be operated with both AC and DC without any design modifications since the actual frequency range typically includes 47-63 Hz and DC.

With DC distribution, it is also possible to improve the customer-end power quality. The main reason is that inverters on the customer-side are able to maintain the voltage level at the defined values, even if the DC link voltage varies, as long as the voltage is above the minimum value. Tolerance to voltage variation is therefore improved. It is also possible to eliminate power outages resulting from reconnections in the electrical power system, but this requires some energy to supply the inverter or inverters during the loss-of-mains situation. These energy storages can be directly connected to the DC link, and it is possible to use a common storage for all inverters or a separate storage for every inverter. This also makes it possible for a customer to individually select the size of the energy storage.

Considering a DC-distribution system with centralized AC/DC power conversion like in Figure 1.1, the proposed AC/DC interface does not affect the utility power quality in terms of low-frequency harmonics, and it has voltage-dip ride-through capability.

Furthermore, the chosen topology allows bi-directional power flow, which can be of interest if the DC system includes power sources, and allows easy connection of energy storage as a countermeasure for power outages.

Figure 1.1 – A DC distribution system with centralized AC/DC power conversion



1. Advantages of Low Voltage DC distribution systems

1.1 Sensitive electronic loads

Commercial buildings, such as office buildings, often have a large amount of nonlinear electronic loads, such as lighting, computers, monitors, and adjustable-speed drives for air conditioning.

Special office buildings, such as banks and data centers, have critical computer systems which must be operating “24-7” and must not be affected by transients and outages on the utility power grid.

A common way to protect these loads is to install online uninterruptible power supplies (UPSs) and standby diesel-generator sets. The UPSs are used to protect the loads from transients and short interruptions with duration up to approximately 0.5 h. The losses of a UPS are in the range 5–10%.

The installed UPSs must also be able to handle distorted currents from nonlinear loads, and they must therefore be overrated.

If, instead, DC distribution is used, a single converter is utilized to supply the loads, and additional losses can be reduced. Since loads are supplied with DC, the rectifiers inside the loads can be removed and the losses can be lowered.

1.2 Distributed generation

The number of alternative generation sources connected to the distribution system increases. Some of them, such as photovoltaic and fuel cells, produce DC, and they can easily be connected to a DC distribution system directly, or through a DC/DC converter. Microturbines generating high-frequency AC are also easier to connect to a DC system than to an AC system, where generating a synchronized sinusoidal AC current is required. The electric power output of a wind turbine can be kept at a maximum if the speed of the turbine is allowed to vary. If the shaft is connected to the generator through a gearbox, the ability to vary the speed is limited. To increase the speed range, an AC/DC/AC converter can be used, which is an expensive solution. A cheaper and simpler solution is to connect an AC/DC converter to a DC grid. Other types of generators operating with varying speed are small hydro and tidal generators. Using a DC distribution system makes it easier to incorporate more local energy storage and sources, either standby power generation, which is used only

when there is a fault on the utility grid, or distributed generation (DG) (small-scale energy sources) which are operated more or less continuously.

To connect an energy source to a DC system only the voltage has to be controlled.

1.3 Cables and maximum transmissible power

A grounded three-phase AC system requires five wires—three phase conductors, one neutral, and one ground. A DC system requires three wires—two phase conductors and one ground. An existing five-wire AC cable in a retrofit DC system can be used in two different configurations. The first is to use two wires for each pole and one for ground.

The other alternative is to use one for each pole, two for neutral and one for ground, with the load connected between one pole and neutral.

Considering the maximum transmissible power, the DC distribution solutions (distribution with 2 or 3 conductors) may be compared with the traditional AC distribution, that in Italy is usually made by three-phase cable lines with 4 conductors (3 phase conductors and the neutral with a smaller cross section), with a nominal voltage of 400V.

The transmissible power for the various systems can be expressed as follows:

- traditional AC - $P_{AC} = \sqrt{3} \cdot V_{AC} \cdot I_{AC} \cdot \cos\varphi$
- DC with 3 conductors - $P_{DC3} = 2 \cdot V_{DC3} \cdot I_{DC3}$
- DC with 2 conductors - $P_{DC2} = V_{DC2} \cdot I_{DC2}$

where V_{DC3} is the voltage between the positive or negative pole and neutral conductor, while V_{DC2} is the voltage between the two poles. Assuming $V_{AC} = 400$ V; $V_{DC3} = 400$ V; $V_{DC2} = 800$ V, for the comparison between the AC and DC distribution, the following hypotheses are made:

- the cables, with the same section in all the examined cases, are loaded up to their thermal limit current, so that $I_{AC} = I_{DC3} = I_{DC2}$;
- the whole load is connected at the end of the line and the possible presence of DG is neglected;
- the power factor of the AC loads is 0.9.

The comparison between the two systems, AC and DC with 3 conductors, shows that in DC a power 1.28 times larger than that in AC can be transported. The same result is obtained in case of 2-wire DC distribution system.

The relationships between the AC and DC transmissible powers are the following:

[1.1]

$$\frac{P_{DC3}}{P_{AC}} = \frac{2 \cdot V_{DC3}}{\sqrt{3} \cdot V_{AC} \cdot \cos\varphi} \quad \frac{P_{DC2}}{P_{AC}} = \frac{V_{DC2}}{\sqrt{3} \cdot V_{AC} \cdot \cos\varphi}$$

By increasing the length of the line, the DC solutions can transport an amount of electric power up to 2.2÷3.9 times the one in AC. It can be concluded that with the same extension of the distribution network, the DC solutions can supply a larger load, while with the same load, the DC distribution systems can have a greater extension than the AC one.

1.4 DC in data centers

Commercial data centers have traditionally distributed AC in their facilities.

But all information technology (IT) equipment operates on DC power.

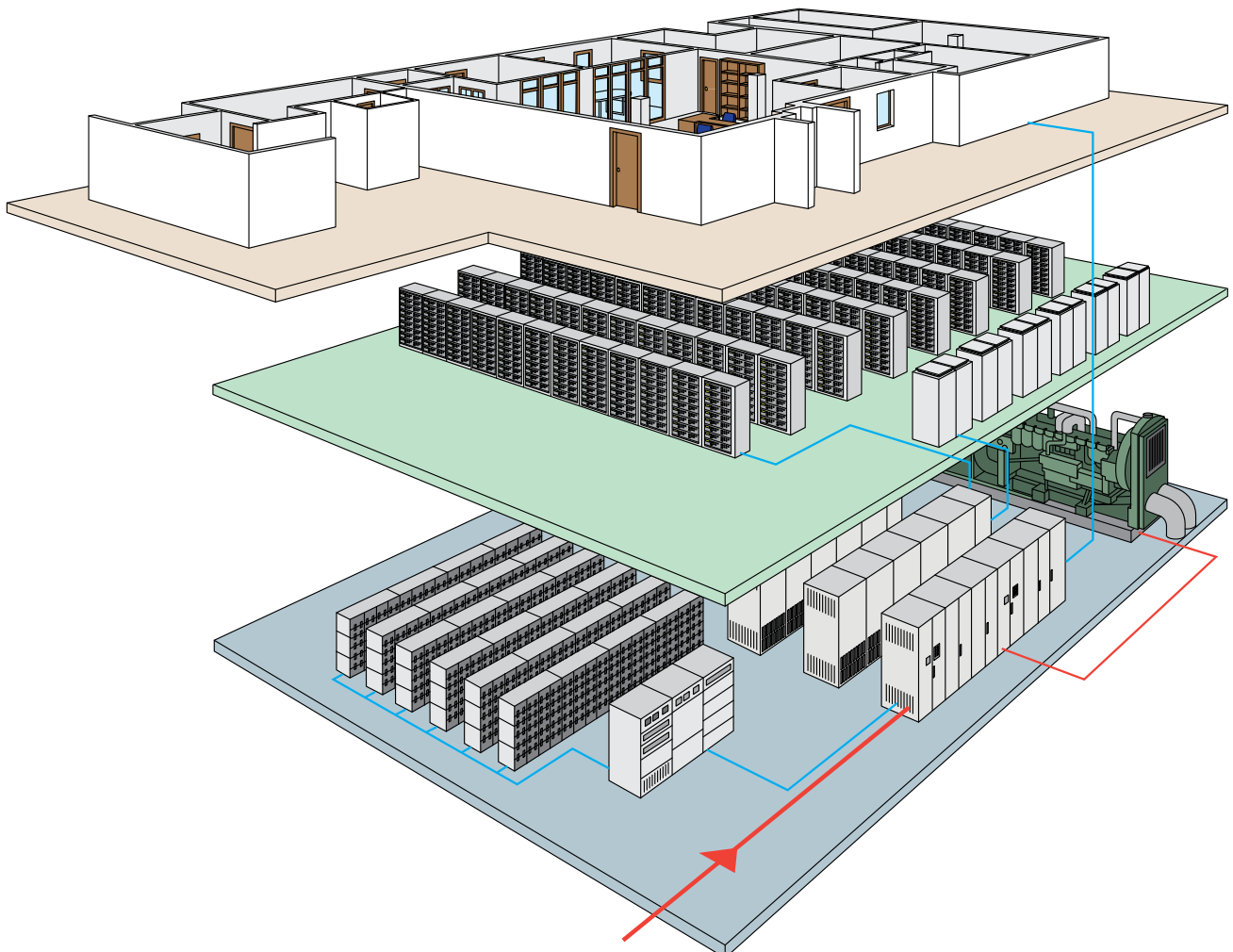
Therefore, a typical data center power distribution system incorporates multiple power conversion stages from AC to DC and from higher to lower voltages .

The servers and other IT devices are powered with AC and immediately convert this to DC power inside their power supply. The DC voltage is then converted to lower DC voltages as required by the IT equipment. The typical AC power distribution system results in five to seven conversion steps, with each step resulting in power losses, heat generation, and reductions in the end-to-end system reliability.

The advantage of a DC architecture is evident in the reduced number of critical system components. Fewer components result directly in a lower installation cost, a smaller footprint, and higher system reliability. The efficiency gains result from fewer energy conversions and enabling the use of DC server power supplies that are more efficient at lower load levels. These efficiency gains also drive reduced cooling demand, resulting in additional energy savings.

Figure 1.2 shows a modern data center with the different electric components supporting the racks housing the servers/routers.

Figure 1.2 – Data center layout



1. Advantages of Low Voltage DC distribution systems

Distribution in such a plant can be carried out in DC at 380V, with the advantages shown in Figure 1.3.

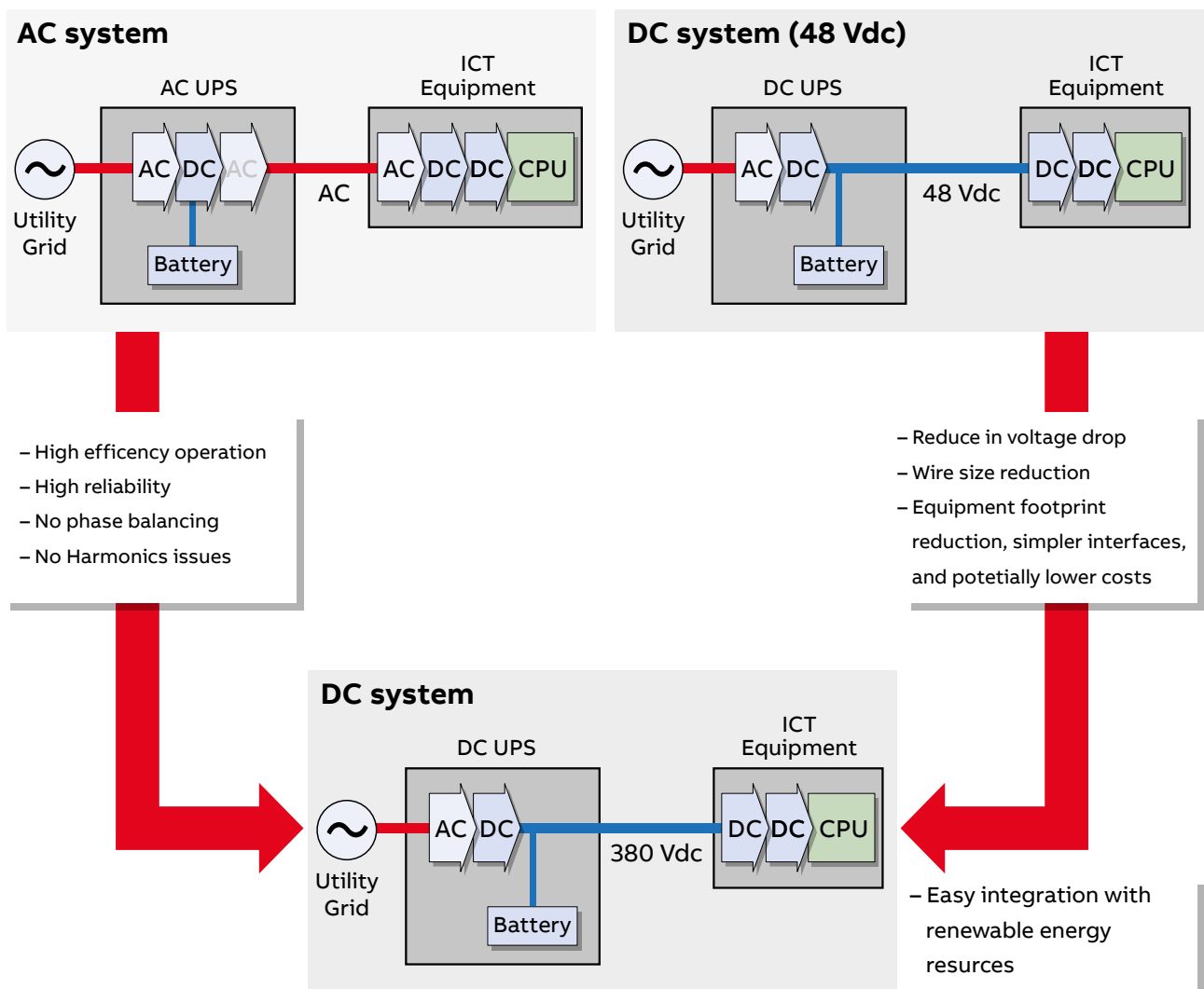
In particular, thanks to power supply at 380V DC distribution, the following advantages can be obtained:

- higher reliability, since there is a lower number of conversions and less points at which failures/breakdowns may occur, with a consequent decrease in the likelihood of fault occurrence

- higher efficiency, due to minor losses in the converters and cables. In particular:

- energy saving $\cong 28\%$ compared to a “typical” AC system
- energy saving $\cong 7\%$ compared to a “best in class” AC system
- smaller overall dimensions ($\cong 33\%$ reduction in the occupied space)
- easier integration of renewable sources
- easier energy storage.

Figure 1.3 – DC distribution advantages in a data center

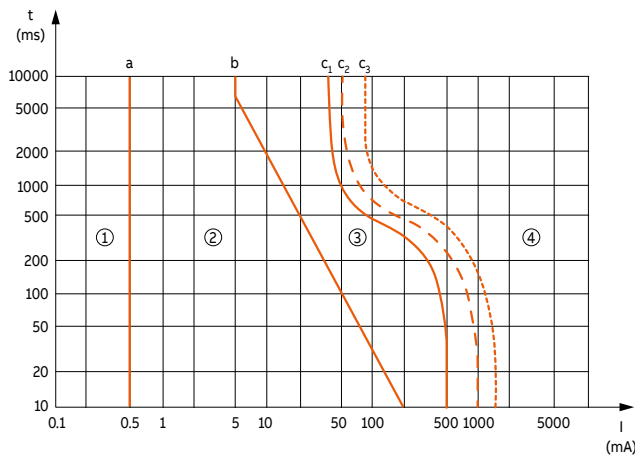


1.5 Hazard of direct current vs alternating current

Direct current is less dangerous than alternating current. This according to the general principle that the human body is more sensitive to time-variable stresses with respect to continuous ones (“accommodation” phenomenon).

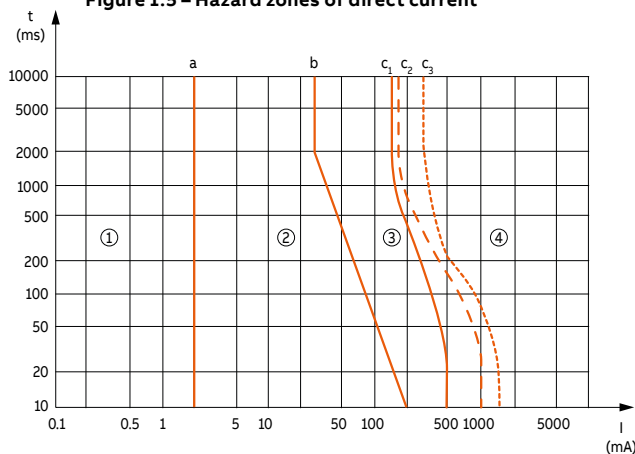
The hazardous zones of the electric current according to the time of current flow through the human body are shown in Figure 1.4 for alternating current 50Hz and in Figure 1.5 for direct current.

Figure 1.4 – Hazard zones of alternating current (15-100 Hz)



- ① usually absence of reactions up to the threshold of perception (fingers)
- ② usually no harmful physiological effects up to the threshold of tetanization
- ③ generally reversible physiological effects may occur; they increase as current intensity and time increase. They are: muscular contractions, breathing difficulties, increase in the blood pressure, troubles in the formation and transmission of cardiac electrical impulses, atrial fibrillation and temporary cardiac arrest included, but without ventricular fibrillation
- ④ likelihood of ventricular fibrillation, cardiac arrest, breathing arrest, serious burns. Curves c2 and c3 correspond to a probability of ventricular fibrillation of 5% and 50% respectively.

Figure 1.5 – Hazard zones of direct current

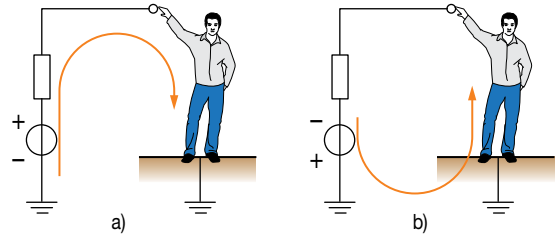


Direct current can flow from head to foot (descending current) or vice versa (ascending current), considering by convention the direction of the current that of the positive charges.

In Figure 1.5 the curves c1, c2, and c3 refer to the as-

ending current, which is more hazardous than the descending one, since a descending current twice the ascending one is necessary to start ventricular fibrillation. Therefore, for electrical safety, in the DC systems with grounded pole, it is advisable to connect to ground the negative pole (Figure 1.6).

Figure 1.6 – The descending direct current is less hazardous than the ascending one, therefore it is better to ground the negative pole of the generator



Besides, the transverse path hand-to-hand is less dangerous than the longitudinal path hand-to-foot, independently of the direction of the direct current: to start ventricular fibrillation in the hand-to-hand path the current required is 250% of the ascending current with hand-to-foot path.

On the whole, direct current is however less dangerous than alternating current as it can be deduced also by the voltage values reported in Table 1.1 and considered as safe: they are higher in DC than in AC.

Table 1.1 – Safety voltages

| | Direct contact | Indirect contact |
|---------------------------|----------------|------------------|
| Alternating current (rms) | 25V | 50V |
| Direct current | 60V | 120V |

The DC systems at a voltage lower than 60V are to be regarded as safe if they are either SELV or PELV, namely, if they are separated from the network through an insulation transformer and by the other circuits through a double or reinforced insulation or by a shield connected to earth.

The limit of 60V is to be referred to the voltage between the pole of the system in a two-terminal contact. In case of one-terminal contacts, the hazard would depend on the voltage to earth. In principle, at the same voltage level, a ground-isolated system is less dangerous than a system with one pole earthed, but it is dangerous anyway, due to the leakage currents, which grow as the DC system expands.

1. Advantages of Low Voltage DC distribution systems

1.6 Elimination of synchronization

Last, but not least, the elimination of synchronization is a significant advantage of a DC system when compared with AC.

AC current sources must be carefully synchronized before they can be connected.

A failure to synchronize can result in catastrophic current and forces, as two sources work against one another.

At best, such events result in shutdown of the power system; at worst, there is significant damage to the generation, distribution, and control components.

Preventing this damage requires the installation of synchronization relays and control schemes.

This is a straightforward task with two sources, but it can become complex and unstable with increasing numbers of sources.

DC systems, because of their constant voltage, do not exhibit this issue. Paralleling multiple sources in a DC system requires no control.

Thus, a DC system is uniquely suited for applications where multiple sources must work together.

Systems that include utility power, batteries for back up, and variable “green” sources such as solar, wind, and fuel cells can be easily and reliably integrated in a DC architecture.

1.7 Perspective of LVDC distribution systems and microgrids

With the several advantages explained in the previous sections, LVDC distribution systems and microgrids are becoming a good alternative, since they perform better in terms of efficiency, scalability and stability. Moreover, by observing the residential energy consumption pattern, we may discover that major part of our consumption loads are becoming more and more DC, e.g., laptops, cellphones, LED lights, displays, etc.

Even the conventional AC loads driven by AC motors, such as washing machines, refrigerators, air conditioners, and industrial equipment, are being gradually replaced by AC motors with inverters to

control the motor speed and save energy.

Therefore, the electric grid is conceived in AC since the grid has been designed to support conventional loads for more than a century, basically induction motors and other AC appliances.

Furthermore, in order to transmit electricity with minimum losses, the voltage has to be increased, which was previously only possible by using AC transformers. After one century, the contemporary residential loads have been changed a lot, but the electric grid practically stayed intact.

This implies that every time we plug-in one of these new loads to the grid, a conversion stage from AC to DC is required. Besides, generation also changed from big synchronous generators in power plants to small solar panels, fuel cells, or batteries, which are essentially DC sources.

Even micro-wind or gas turbines are more efficient by using only one converter (AC/DC) instead of two back-to-back converters (AC/DC and DC/AC).

This will naturally lead to an emerging grid in which microgrids and distribution systems at homes and buildings would be done in DC.

With home microgrids, now AC and in the future DC, electrical vehicles will be also playing an important appliance role at home, given the DC onboard energy storage systems and emerging DC charging stations. A new scenario could be to build a hybrid DC and AC grid at distribution levels, to couple DC sources with DC loads and AC sources with AC loads.

This hybrid structure would reduce the multiple conversions to a minimum.

Moreover, the connection of all DC loads to the DC side of the hybrid grid would make it easy to control harmonic injections into the AC side through the main converters, thus guaranteeing high-quality AC in the utility grid.

Finally, the DC grid could solve negative and zero sequence current problems caused by unbalanced loads in AC distribution systems, and the neutral wire in subtransmission might be eliminated and the related transmission losses reduced.

This revolution can be seen as a “back-to-Edison” phenomenon, which is already happening in high-voltage direct current (HVDC) systems and is becoming a reality in LV and MV distribution systems.

2. System configuration

In order to carry out a deep analysis on the several faults that may occur in a LVDC microgrid, first of all it is important to describe its configuration with the several electrical devices that are connected.

This is the topic of this Chapter, along with the description of the system arrangements regarding the ground connection combinations that will be considered during a ground fault.

2.1 Front-End Converter (FEC)

Forced commutated three-phase rectifiers are AC/DC converters using IGBTs (Insulated Gate Bipolar Transistor), i.e. electronic components with both closing and opening commands that allow the converter control depending on needs (see Annex A). Electronic component commutation (from ON to OFF position) occurs hundreds of times per period, so it guarantees performances that otherwise could not be reached with thyristors. This characteristic gives the following advantages:

- current or voltage may be modulated (PWM – Pulse Width Modulation, see Annex B) producing a low harmonic contribution;
- the power factor may be controlled and it may follow an established profile;
- power reversal occurs by means of voltage reversal in thyristor rectifiers, while forced commutated rectifiers may be used both for current reversal.

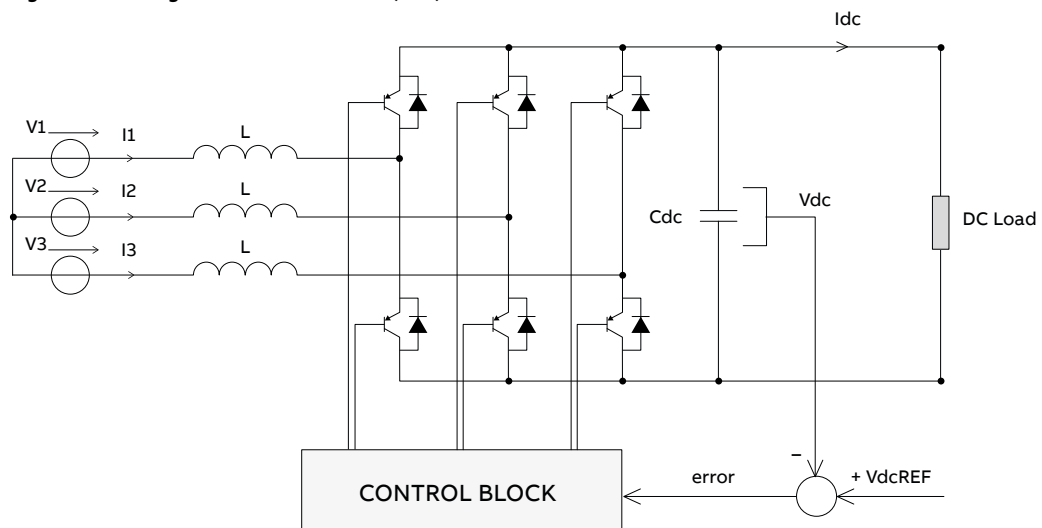
Usually, the FEC works by maintaining the DC voltage at a desired reference value, using a feedback control loop, as shown in Figure 2.1.

In order to perform this task, the actual DC voltage V_{dc} is compared with the reference voltage V_{dcREF} . The error signal, created by the comparison, represents the main input of the whole control system; the error signal is used to manage the ON/OFF control of the six electronic components. In this manner, the power may flow from the AC side to the DC side and vice versa, depending on the DC voltage requirements. When I_{dc} is positive (rectifier operation mode), the C_{dc} capacitor discharge occurs and the error signal requires by means of the control block a higher power from the AC source.

The control block allows a power absorption from the AC source by creating an adequate PWM signal for the electronic components control. In this manner, a higher current flows from the AC side to the DC side to fulfil the higher power request of DC loads and the DC voltage is brought back to the desired value. On the contrary, when the I_{dc} becomes negative (inverter operation mode), the DC voltage tends to increase, so the capacitor is overloaded and the error signal requires the capacitor discharge by means of the control block, returning power to the AC source. The PWM control logic permits not only active power control but also the reactive one, allowing power factor correction by means of the converter. Moreover, the AC current waveform may be maintained almost sinusoidal, reducing the harmonic contribution.

It is important to note that, while the IGBTs can be opened and closed by the control system, the freewheeling diodes cannot be controlled.

Figure 2.1 – Voltage Front-End Converter (FEC)



2. System configuration

2.2 System description

The analyzed electric plant is composed by an AC section and a LVDC microgrid fed by a front-end converter. On the AC side there are a MV/LV transformer connecting the system to the MVAC Utility and a generic purely resistive passive load.

The analyzed LVDC microgrid includes the following components:

- bidirectional FEC, which controls the DC-Bus voltage, keeping it to the preset value. The converter, usually based on PWM, exchanges sinusoidal wave currents with the grid at the unit power factor, i.e., with no exchange of reactive power;
- Energy Storage System (ESS), which provides continuity of supply to the priority loads during short power interruptions, connected to the DC-Bus by a DC/DC bidirectional converter;
- PhotoVoltaic (PV) plant, connected to the DC-Bus by a DC/DC step-up converter;
- DC load that can be considered as a purely resistive passive element.

Moreover, on the AC side an AC three-phase load is installed, working at $\cos\phi = 1$.

The generic passive DC load is represented by means of a resistance R_L , the parasitic capacitances by means of the concentrated capacitances C_p , the ESS by means of a voltage DC generator (E_o, R_i), whereas the PV plant is modeled by means of a controlled current source ($I_{pv} = P/V_{dc}$ with a maximum short circuit equal to 1.25 times the short circuit current $I_{SC\ STC}$ under standard conditions¹, according to the Standard IEC 60364-7-712 [15]).

For simulation purpose, the DC poles short circuit and the AC three-phase short circuit are respectively represented by means of the resistances R_{sc} and R_{sc}' , while DC and AC ground faults by means of R_g and R_g' , sum of fault and protective ground system resistances.

Figures 2.2-2.5 depict the scheme of the electrical plant analyzed with the several ground system configurations. In particular, the configurations in Figures 2.2-2.4 will be used for DC ground faults, while the configuration in Figure 2.5 for an AC ground fault. The configuration with the AC exposed conductive parts connected to the same grounding arrangement of the transformer neutral point will not be analyzed in this Technical Application Paper since it is the well-known usual configuration.

We consider the DC negative pole grounded configuration, not the DC positive pole, for safety reason. Without a galvanic isolation transformer, it is not possible to have both the transformer neutral point and the DC negative pole grounded, since it would create a permanent short circuit fault through ground that would prevent the system normal operation.

The fictitious switches S_x in Figures 2.2-2.5 show the connection possibilities of the exposed conductive parts to a protective grounding system that can be distinct from the operational grounding or the same.

¹ A standard set of reference conditions used for the testing and rating of photovoltaic cells and modules. The standard test conditions are:
 a) PV cell temperature of 25 °C;
 b) irradiance in the plane of the PV cell or module of 1000 W/m²;
 c) light spectrum corresponding to an atmospheric air mass of 1.5.

Figure 2.2 – Microgrid scheme with MV/LV transformer neutral point grounded for DC ground fault analysis

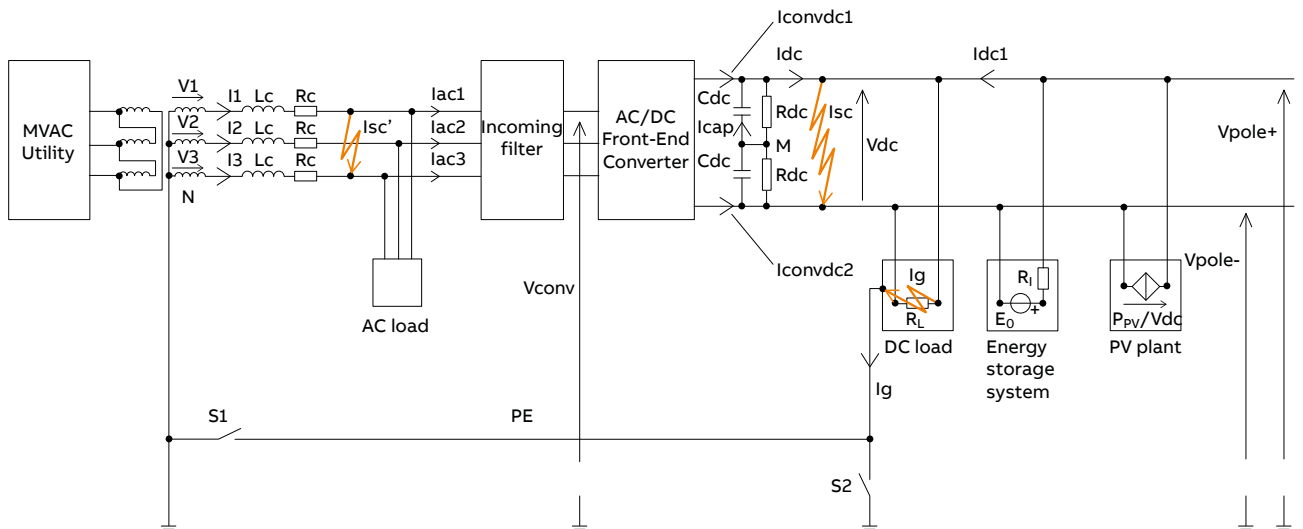


Figure 2.3 –Microgrid scheme with DC negative pole grounded for DC ground fault analysis

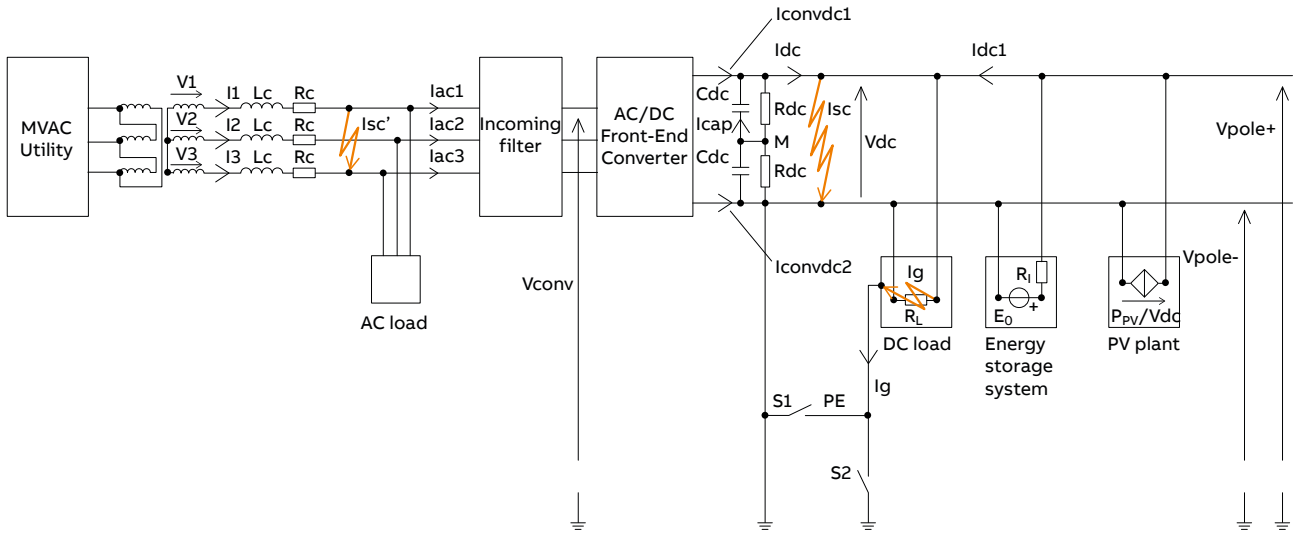
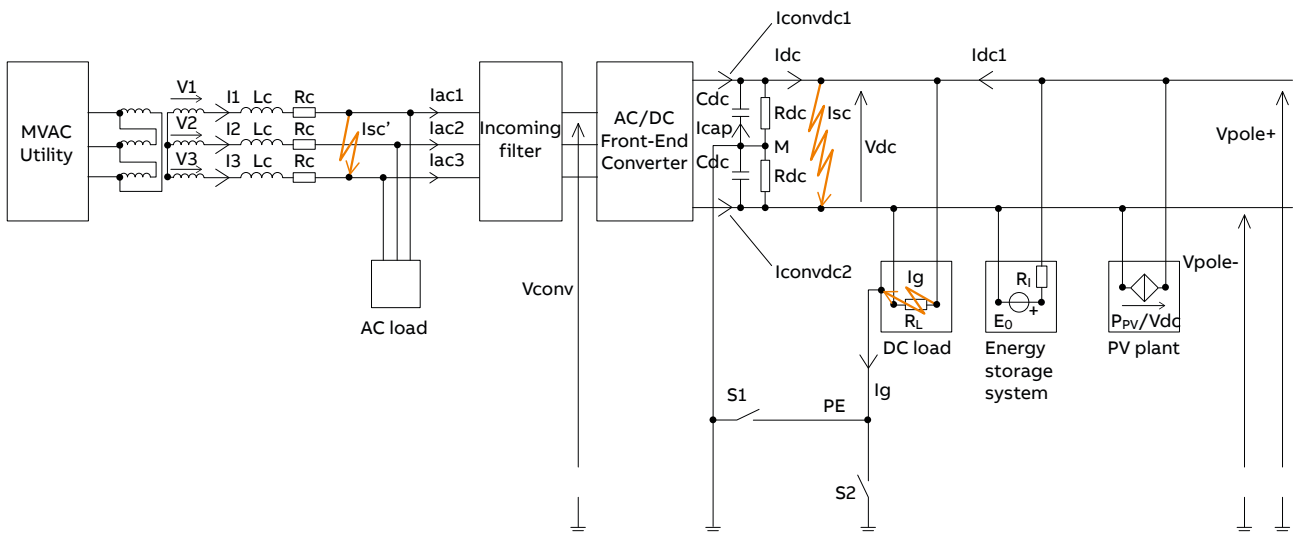


Figure 2.4 –Microgrid scheme with DC mid-point grounded for DC ground fault analysis



2. System configuration

Figure 2.5 – Microgrid scheme with DC negative pole grounded for AC ground fault analysis

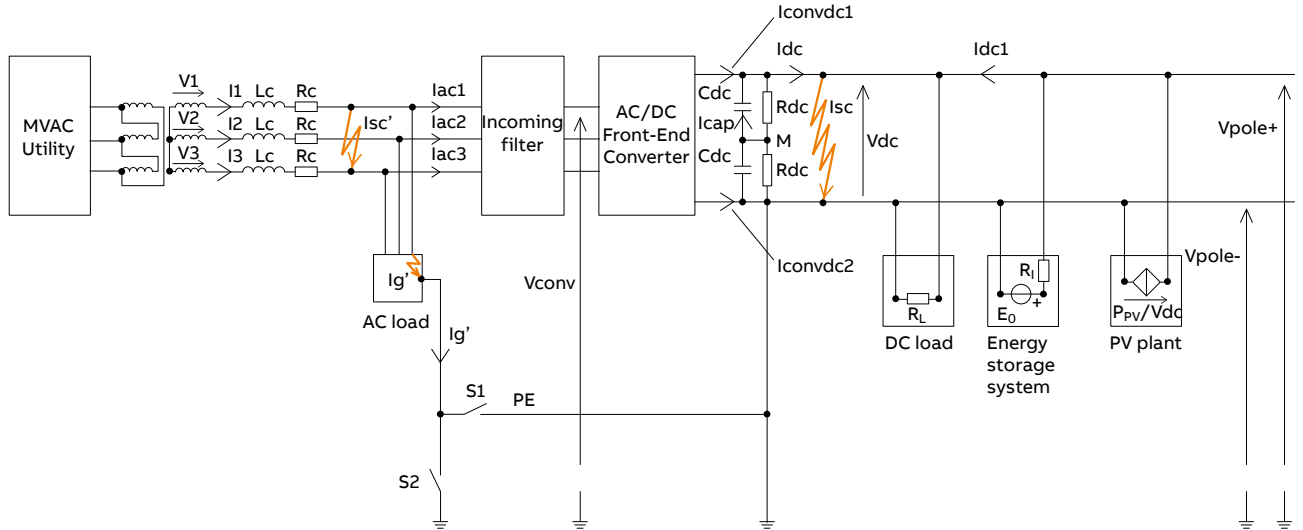


Table 2.1 summarizes electrical plant data.

Table 2.1 – Plant characteristic data

| | |
|--|----------------|
| MV Utility nominal voltage U_{1n} | 20 kV |
| Rated frequency | 50 Hz |
| Utility short-circuit power S_{sc} ($R_{sc}=0.1Z_{sc}$, $X_{sc}=0.995Z_{sc}$) | 500 MVA |
| MV/LV transformer nominal power S_n | 200 kVA |
| LVAC nominal voltage U_{2n} | 400 V |
| V_{sc} % | 4% |
| P_{sc} % | 2.5% |
| LVAC cable resistance R_c | 85 m Ω |
| LVAC cable inductance L_c | 100 μ H |
| LVAC Load nominal power P_n ($\cos\phi=1$) | 50 kW |
| Incoming filter inductance ($V=6\%$ absorbed voltage) L_f | 300 μ H |
| FEC nominal power P_{nFEC} ($\cos\phi=1$) | 100 kW |
| Switching frequency f_{sw} | 10 kHz |
| DC nominal voltage V_{dcn} | 800 V |
| DC link resistance R_{dc} | 1000 Ω |
| DC link capacitance C_{dc} | 15 mF |
| DC Load resistance R_L ($P_{nL} = 90$ kW) | 7.1 Ω |
| ESS no-load voltage E_o | 803 V |
| ESS internal resistance R_i | 200 m Ω |
| PV plant short circuit current I_{PVmax} ($P_{PV} = 50$ kW) | 78 A |
| Total resistance R | 110 m Ω |
| Total inductance L | 500 μ H |

3. Fault analysis

In the Chapter the LVDC microgrid behavior is analyzed in presence of either DC or AC fault (both short circuit and ground fault) in order to highlight the trends of voltage and currents quantities in the several parts of the electrical plant and in the FEC electronic components; since there are situations in which the FEC is not able to control and limit the fault currents, such currents will have to be detected and interrupted by means of protection devices.

On the DC side, we'll consider in detail the conditions of DC poles short circuit and ground fault of one pole in the several grounding configurations explained in Chapter 2. In particular, the theoretical fault contribution of the ESS and PV plant and the repercussions on the FEC will be analyzed.

On the AC side, we'll consider the fault contribution supplied by the LVDC microgrid through the FEC during a three-phase short circuit and single-phase ground fault conditions, in case of the neutral point of the transformer isolated from the ground and the DC negative pole directly connected to the ground and in presence of both the ESS and PV plant.

3.1 Short circuit on DC side of the front-end converter

3.1.1 Behavior without ESS and PV plant

The short circuit on DC side, independently from grounding configurations, may be considered as an additional load with low resistance.

This fault typology doesn't cause currents toward ground, so the FEC operation will be free from effects due to the circulation of a zero-sequence current in its electronic components. It is assumed that the short circuit occurs immediately downstream the FEC DC terminals at the DC-Bus beginning point, which is the worst case as usual considered in short circuit calculations. With decreasing values of fault resistance R_{sc} , different effects occur as described as follows. We first neglect the presence of IGBT self-protection based on detection of VCEsat, (DE-SAT protection) which is normally implemented by converters sold on the market and blocks IGBTs. Such hypothesis allows current analysis in electronic components without self-protection: they may be used in future architectures of FECs, relying on innovative external devices for fault protection.

Case 1a

If the fault resistance R_{sc} has a value such that the AC current absorbed is lower than the maximum value

set inside the FEC control to preserve the electronic components, the FEC control itself is able to maintain the V_{dc} voltage at the nominal value.

As a consequence, the FEC fault contribution is close to the nominal current value of the FEC itself.

With an $R_{sc} = 100 \Omega$, as a result of the short circuit that occurs at $t = 0.5s$, we may note how the V_{dc} voltage is brought back to the nominal value by the FEC control (Figure 3.1) and how the presence of the fault causes an increase of the AC current absorbed I_{ac1} (Figure 3.2) and consequently of the DC current supplied I_{dc} (Figure 3.3);

however, both I_{ac1} and I_{dc} remain lower than their respective nominal currents, i.e. $I_{acn} = 144A$ (and $\cos\phi = 1$) e $I_{dcn} = 125A$.

Figure 3.1 – Trend of V_{dc} voltage during a short circuit on DC side in Case 1a

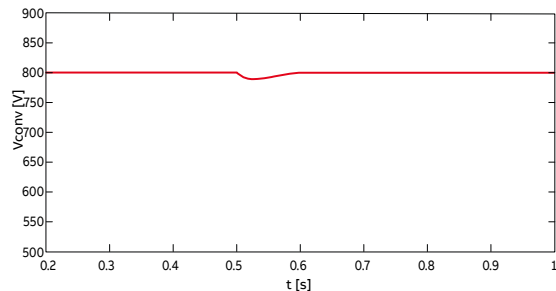


Figure 3.2 – Trend of I_{ac1} current during a short circuit on DC side in Case 1a

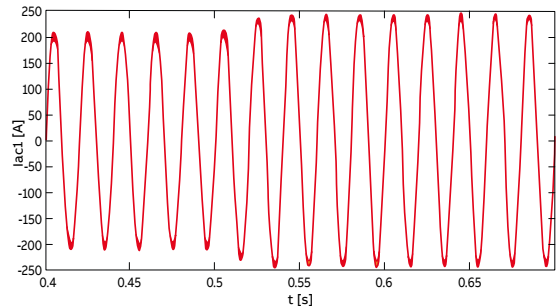
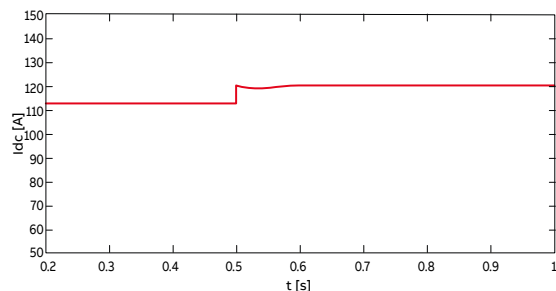


Figure 3.3 – Trend of I_{dc} current during a short circuit on DC side in Case 1a



3. Fault analysis

The FEC control remains in linear modulation and, with reference to the conventional current paths of Figure 3.4, the electronic components are still PWM controlled; in particular, the current in the electronic components of the first leg of cathodic star I_{sw1} and of the anodic star I_{sw2} (positive current through the IGBT, negative one through the freewheeling diode) are respectively shown in Figures 3.5-3.6. Instead the zooms of such currents are depicted in Figures 3.7-3.8 so as to highlight the PWM control.

Figure 3.4 – Conventional currents direction into the FEC electronic components

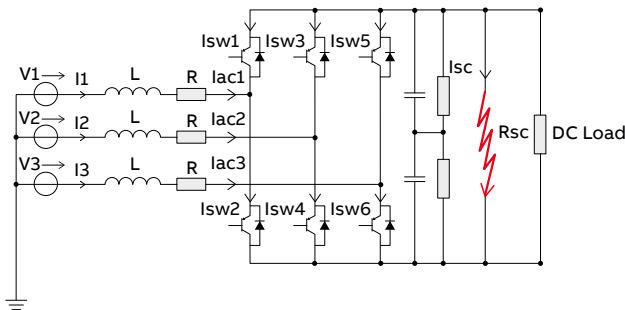


Figure 3.5 – Trend of the current in the electronic component of the first leg of the cathodic star during a short circuit on DC side in Case 1a

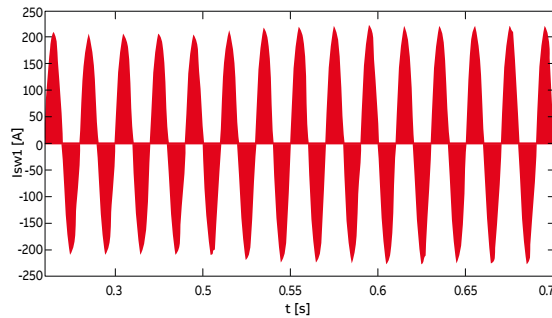


Figure 3.6 – Trend of the current in the electronic component of the first leg of the anodic star during a short circuit on DC side in Case 1a

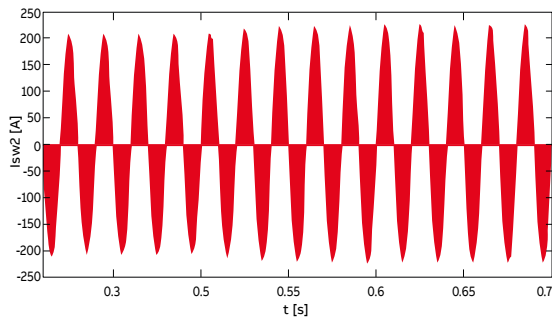


Figure 3.7 – Zoom of the current in electronic component of the first leg of the cathodic star during a short circuit on DC side in Case 1a

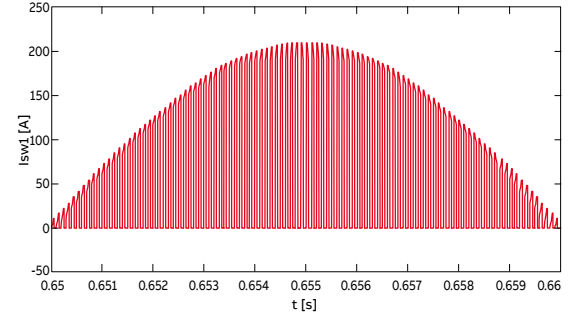
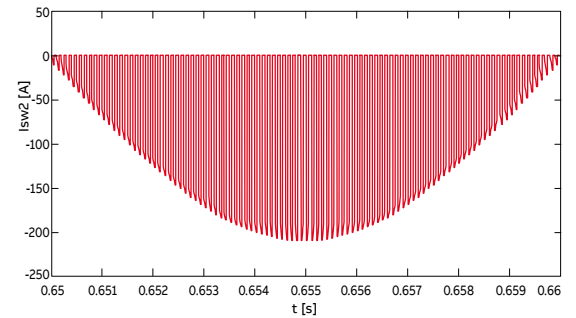
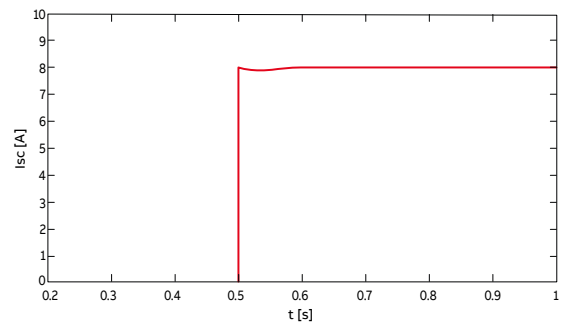


Figure 3.8 – Zoom of the current in electronic component of the first leg anodic star during a short circuit on DC side in Case 1a



The short circuit current I_{sc} may be calculated by the ratio $V_{dc}/R_{sc} = 800/100 = 8$ A (Figure 3.9): it is a low current that cannot be detected by the usual overcurrent protection systems, but it may create arcing and fire hazard.

Figure 3.9 – Trend of I_{sc} current during a short circuit on DC side in Case 1a



Case 2a

If the R_{sc} values are lower than in previous case, the converter control system limits the current absorbed from the AC side to a preset maximum value; hence, active power transferred to DC side is limited as well: as a consequence, V_{dc} cannot be maintained to its rated value, but decreases with decreasing values of R_{sc} .

With $R_{sc} = 30 \Omega$, as we can see in Figure 3.10 in steady-state condition, the V_{dc} (774V) is adjusted by the FEC control at a value such that the transferred power to the DC side corresponds to the maximum current that can be absorbed on the AC side without creating any problem to the electronic components (Figure 3.11). Indeed, the AC power absorbed is equal to ($\cos\phi=1$):

$$[3.1] \quad P_{AC} = \frac{3 \cdot V_1 \cdot V_{conv50Hz}}{X} \cdot \sin \delta = \frac{3 \cdot 230 \cdot 209.5}{0.16} \cdot \sin(6.3^\circ) = 106.6 kW$$

where $V_{conv50Hz}$ is the rms-value of the fundamental frequency component of the phase to ground incoming FEC voltage waveform shown in Figure 3.13. As we can see from (3.1), $V_{conv50Hz}$ value is lower than the AC grid phase to ground voltage V_1 and in addition $V_{conv50Hz}$ is phase-delayed by 6.3° respect to V_1 (Figure 3.13) in order to allow an active power absorption from the AC grid like in a synchronous motor. The (3.1) corresponds, apart of the FEC internal power losses, to the power transferred to the DC side:

$$[3.2] \quad P_{DC} = \frac{V_{dc}^2}{R_L} + \frac{V_{dc}^2}{R_{sc}} = \frac{774^2}{7.1} + \frac{774^2}{30} = 104 kW$$

Figure 3.10 – Trend of V_{dc} voltage during a short circuit on DC side in Case 2a

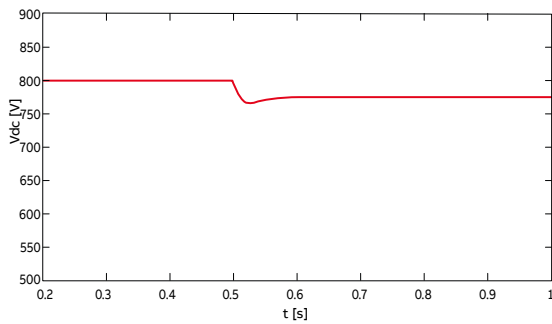


Figure 3.11 – Trend of I_{ac1} current during a short circuit on DC side in Case 2a

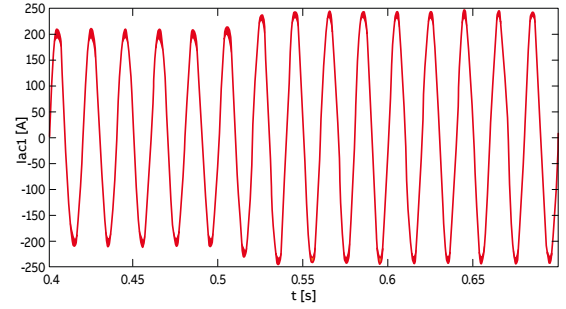


Figure 3.12 – Trend of I_{sc} current during a short circuit on DC side in Case 2a

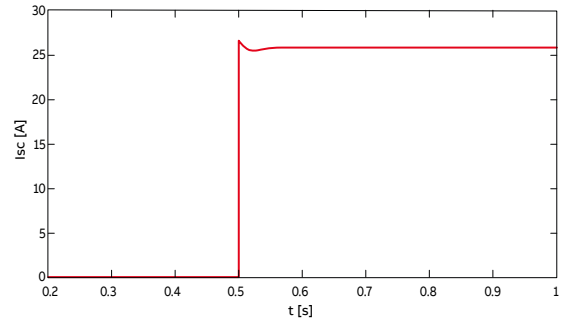
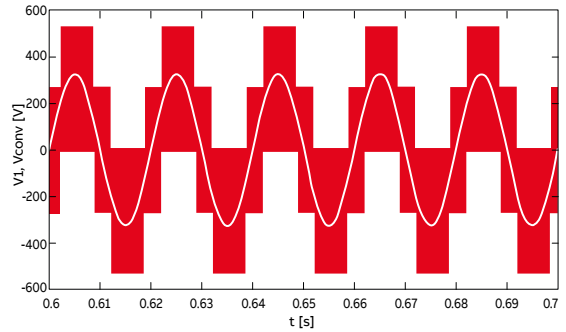


Figure 3.13 – Phase shift between V_1 e V_{conv} during a short circuit on DC side in Case 2a



3. Fault analysis

The FEC control system works correctly in linear modulation (Figure 3.14) and also the trend of the phase-to-ground voltage at AC converter terminals remains unchanged (Figure 3.15).

Figure 3.14 – PWM Control linear modulation during a short circuit on side in Case 2a

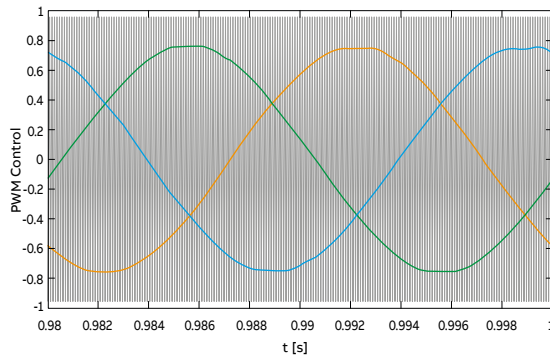
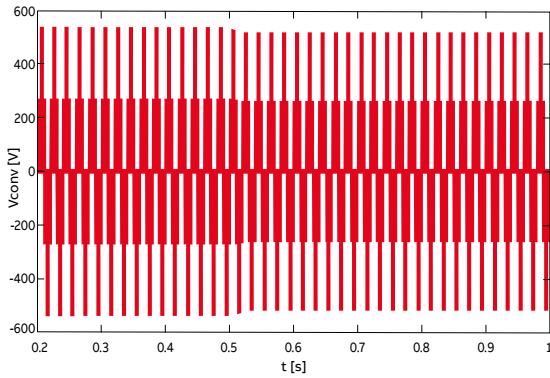


Figure 3.15 – Trend of phase-to-ground voltage at AC front-end converter terminals during a short circuit on DC side in Case 2a



Case 3a

For lower values of R_{sc} , V_{dc} becomes lower than $V_{dcl} = 2 \cdot \sqrt{2} \cdot V_1$ (where V_1 is the rms value of line to neutral voltage on the AC side), is and the converter works in over-modulation.

For an increasing fraction of time with decreasing R_{sc} , the electronic components are no longer PWM controlled and the FEC absorbs low frequency current harmonics: in this situation, the current is no longer limited, and it may exceed the limit value preset for switching components. In the system analyzed, since

$V_1 = 230V$, the minimum linear modulation voltage is equal to $V_{dcl} = 650V$. With $R_{sc} = 5 \Omega$, the DC-Bus voltage becomes $V_{dc} \approx 550V < V_{dcl}$ (Figure 3.16), so the FEC works in over-modulation (Figure 3.18).

Figure 3.16 – Trend of V_{dc} voltage during a short circuit on DC side in Case 3a

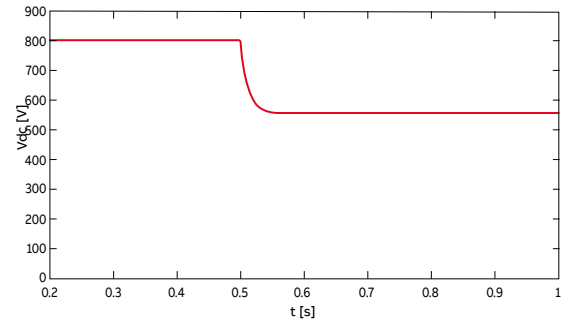


Figure 3.17 – Trend of I_{sc} current during a short circuit on DC side in Case 3a

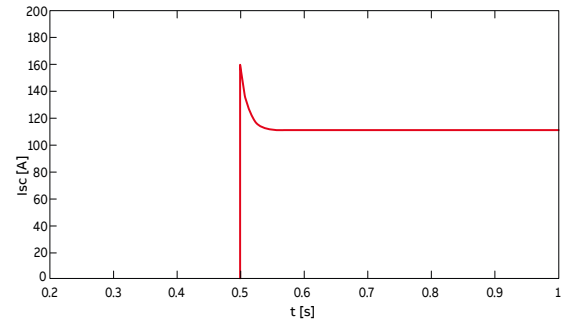
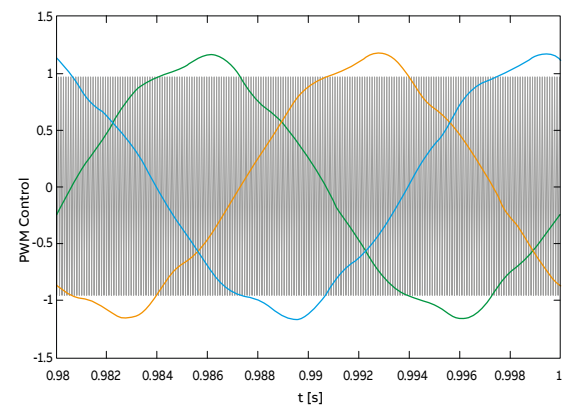


Figure 3.18 – PWM Control over-modulation during a short circuit on DC side in Case 3a



As we can see in Figures 3.19-3.20, with a fault at $t = 0.5s$, no-PWM control intervals appear in the electronic component currents when the linear modulation boundary is reached.

This causes an AC current distortion (Figure 3.21): the lower is R_{sc} , the higher is the distortion level.

Figure 3.19 – Trend of the current in the electronic component of the first leg of the cathodic star during a short circuit on DC side in Case 3a

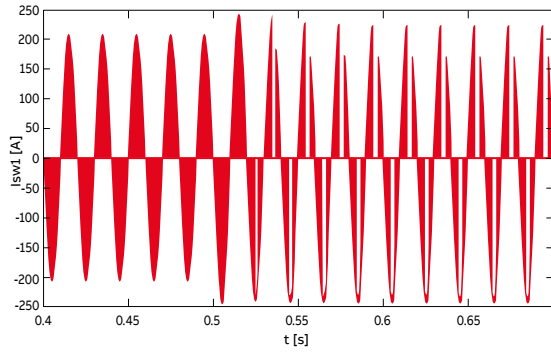


Figure 3.20 – Trend of the current in the electronic component of the first leg of the anodic star during a short circuit on DC side in Case 3a

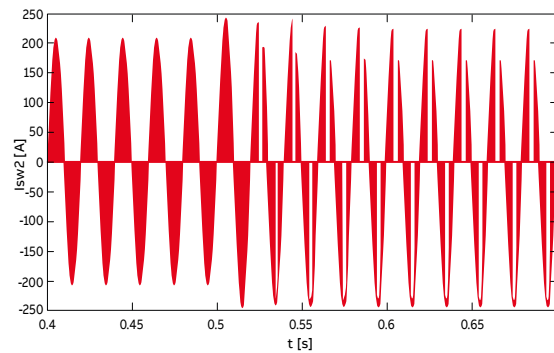
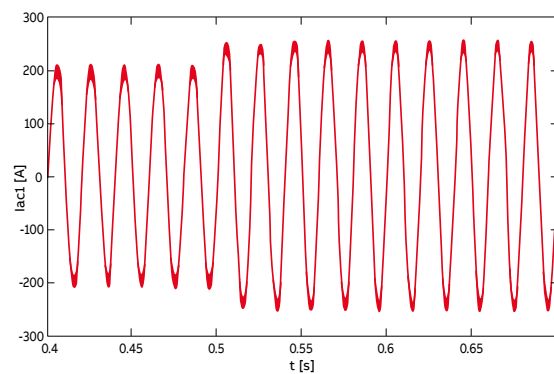


Figure 3.21 – Trend of I_{ac1} current during a short circuit on DC side in Case 3a



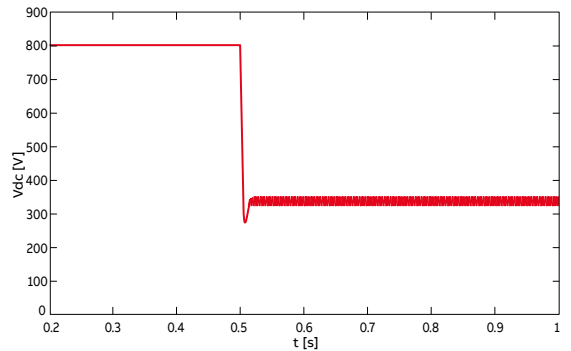
Case 4a

For even lower values of R_{sc} , DC voltage V_{dc} reaches the value $V_{dc2} = 1.35 \cdot \sqrt{3} \cdot V_1$, corresponding to that generated by the diode rectifier: with decreasing R_{sc} , the converter works for longer and longer fractions of time in an irregular way, i.e., bypassing the controlled semiconductors (fault current flows in freewheeling diodes).

In the case studied, since $V_1 = 230V$, the working boundary voltage as diode rectifier is equal to $V_{dc2} \approx 540V$.

With $R_{sc} = 0.5 \Omega$, the DC-Bus voltage becomes $V_{dc} \approx 340 V < V_{dc2}$ and it shows the typical trend of a rectified voltage of a diode bridge (Figure 3.22).

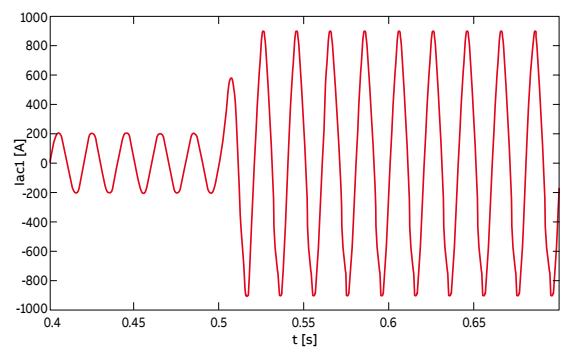
Figure 3.22 – Trend of V_{dc} voltage during a short circuit on DC side in Case 4a



The AC absorbed current (Figure 3.23), is no longer limited by the IGBTs control and then becomes so large that the semiconductor integrity may be prejudiced. Unlike the load current absorbed before the fault, where the low harmonic distortion is mainly due to harmonics at switching frequency and multiples of it, there is an increase of the harmonic distortion at low frequency during the fault (mainly the fifth, seventh and eleventh harmonic).

Moreover, as shown in Figure 3.23, there is not DC component, which demonstrates that a DC short circuit is “seen” by the FEC like an additional load with low resistance.

Figure 3.23 – Trend of I_{ac1} current during a short circuit on DC side in Case 4a



3. Fault analysis

Even the steady state component of short circuit current I_{sc} (Figure 3.24) becomes considerably higher than the FEC nominal current I_{dcn} , since it is not limited by the FEC. Besides, there is a big transient component due to the DC capacitors discharge (Figures 3.24-3.25).

Figure 3.24 – Trend of I_{sc} current during a short circuit on DC side in Case 4a

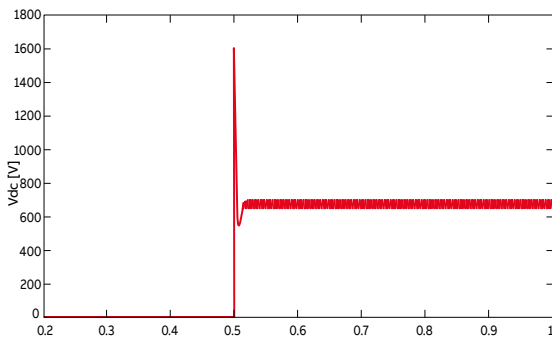
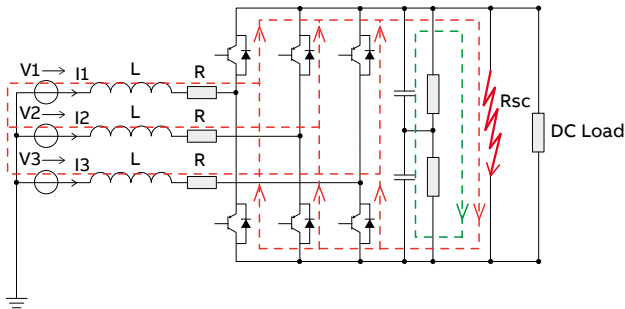


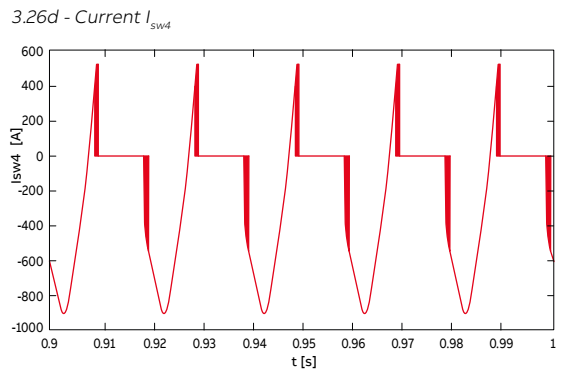
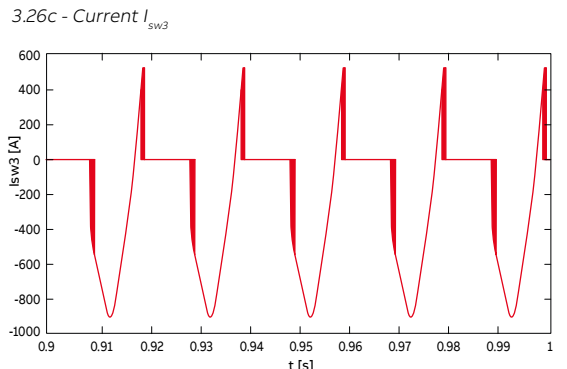
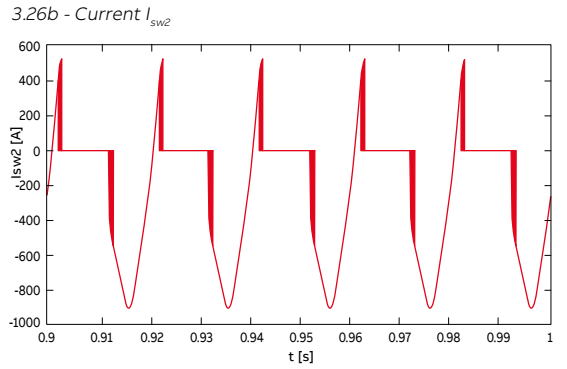
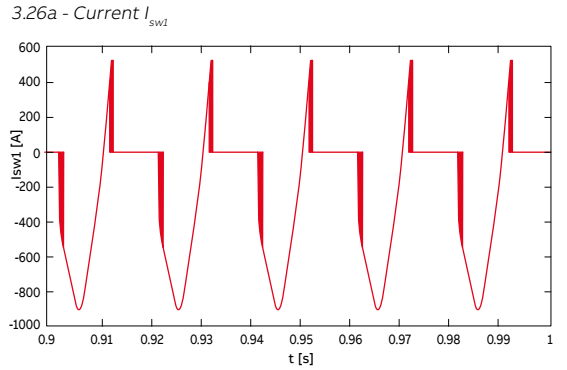
Figure 3.25 – I_{sc} current components during a short circuit on DC side



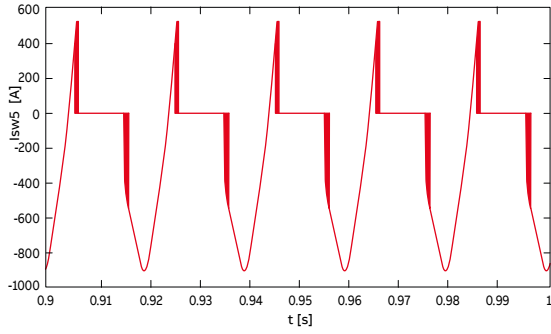
Under this operation condition there are always a diode of the cathodic star and one of the anodic star in the conduction state, as it can be seen in Figures 3.26a-f.

As a consequence, the fault current would pass through the FEC even if the IGBT command signals were switched off. Furthermore, Figures 3.26a-f show that a minimum PWM control still remains as long as the modulating wave is instant by instant lower than the carrier one in the control algorithm (even though in over-modulation situation).

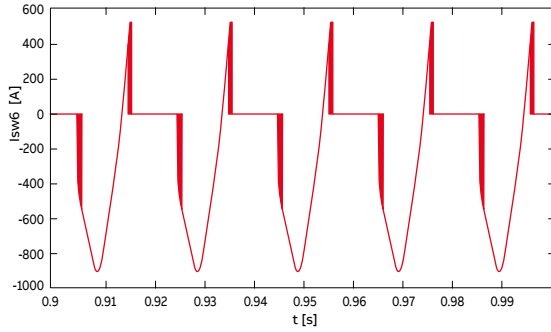
Figure 3.26 – Trend of the current in the electronic component during a short circuit on DC side in Case 4a



3.26e - Current i_{sw5}



3.26f - Current i_{sw6}



Before the fault, the current conduction inside every fundamental component period is divided equally between the IGBT and the correspondent freewheeling diode; on the contrary, after the fault, the conduction is strongly unbalanced towards both diodes of the cathodic and anodic star (Figures 3.27-3.28).

Figure 3.27 – Trend of the current in the electronic component of the first leg of the cathodic star during a short circuit on DC side in Case 4a

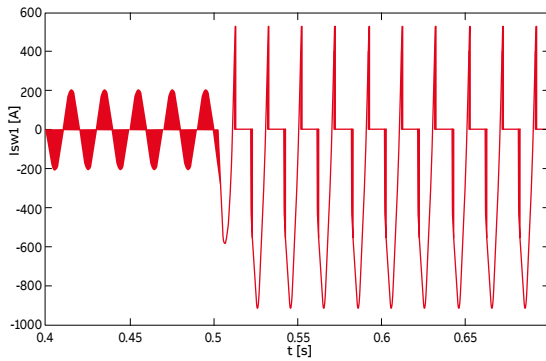


Figure 3.28 – Trend of the current in the electronic component of the first leg of the anodic star during a short circuit on DC side in Case 4a

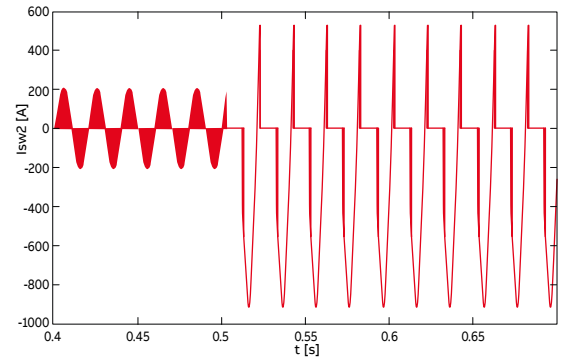
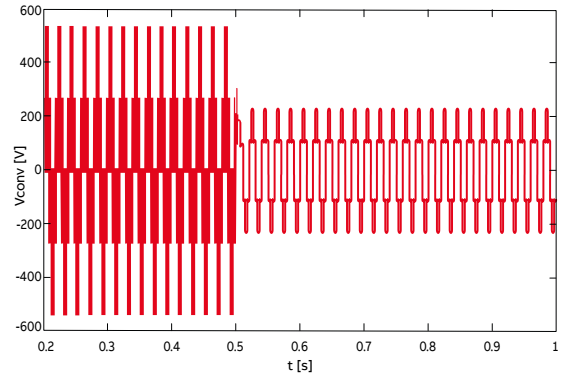


Figure 3.29 depicts the trend of the phase-to-ground voltage at AC front-end converter terminals: such trend involves the generation of low-frequencies voltage harmonics.

Figure 3.29 – Trend of phase-to-ground voltage at AC front-end converter terminals during a short circuit on DC side in Case 4a



3. Fault analysis

Case 5a

In the limit condition of zero fault resistance, the converter behaves like a diode rectifier in short circuit condition: fault current is only limited by the impedances of upstream network, MV/LV transformer, wirings, by the reactance of the incoming filter, and by the diode voltage drops. Resulting values of the fault current would likely bring to the breaking of the electronic components.

Considering $R_{sc} = 1m\Omega$, as it can be seen in Figures 3.30a-b, the fault current I_{sc} reaches considerable values, both in terms of DC capacitors' discharge peak and in terms of steady-state value, which is 10 times (more or less 1200A) the FEC nominal current on the DC side, without any possible limitation by the FEC control.

Moreover, if two or more MV/LV transformers were installed and in parallel and/or the connection cable size increased, the upstream AC grid equivalent impedance would decrease: as a result, the short circuit current would further increase.

Figure 3.30a – Trend of fault current I_{sc} during a short circuit on DC side in Case 5a (Cdc discharge component)

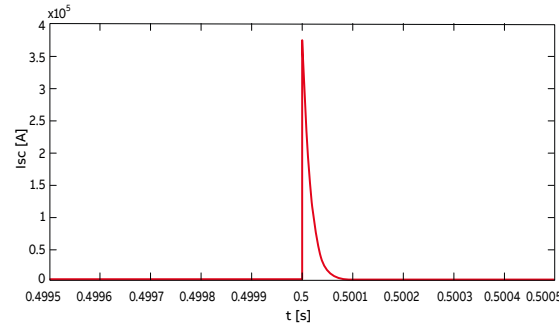
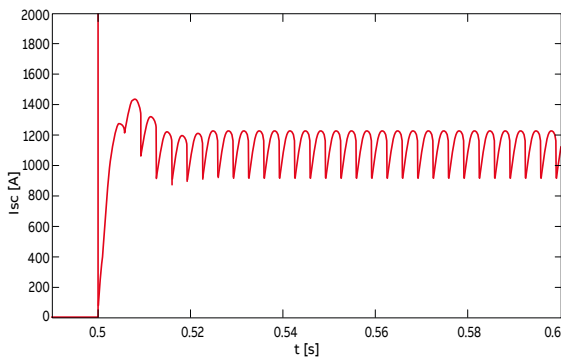


Figure 3.30b – Trend of fault current I_{sc} during a short circuit on DC side in Case 5a (steady state component)



Even with $R_{sc} = 1 m\Omega$, the DC FEC terminal currents still remain equal to each other (Figures 3.31a-b) and they respectively flow out of the upper terminal ($I_{convdc1}$) and into the lower terminal ($I_{convdc2}$) as a further confirmation that the short circuit is seen like a low resistance load in parallel.

Figure 3.31a – Trend of the current $I_{convdc1}$ during a short circuit on DC side in Case 5a

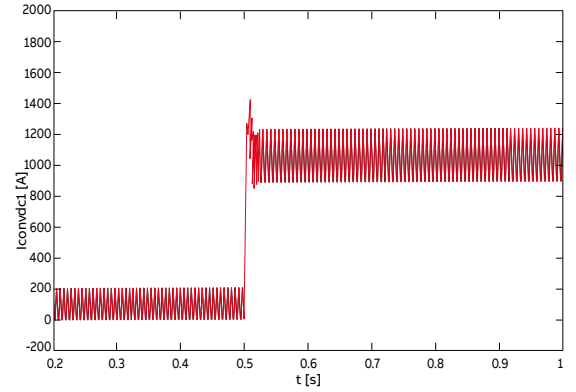


Figure 3.31b – Trend of the current $I_{convdc2}$ during a short circuit on DC side in Case 5a

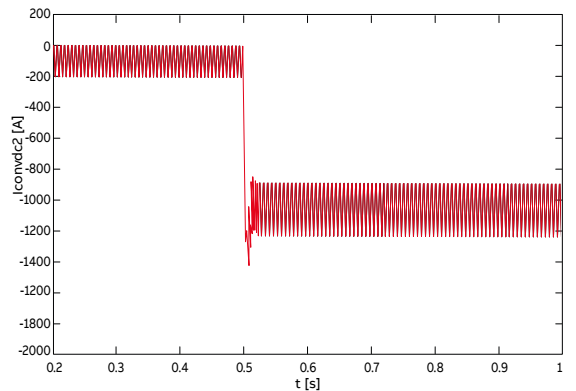
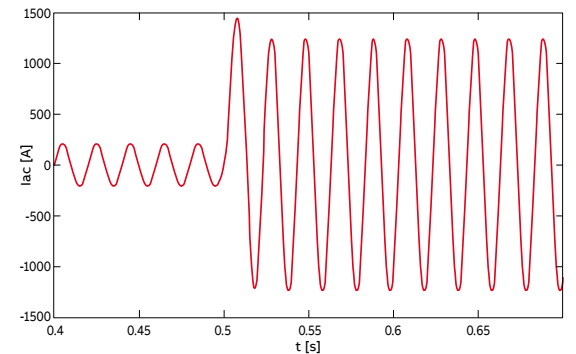


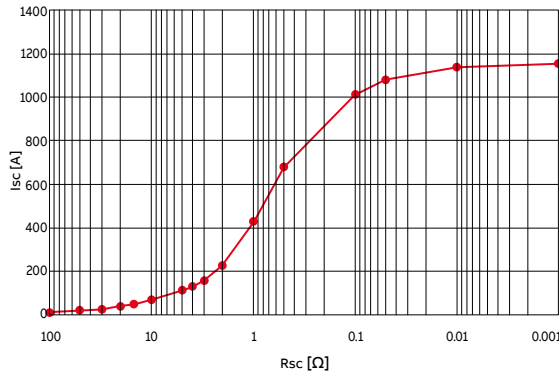
Figure 3.32 – Trend of I_{ac1} current during a short circuit on DC side in Case 5a



Even if we were considered the DESAT protection, it would be ineffective because the diode connected in anti-parallel to the IGBT makes the FEC works as three phase diode rectifier bypassing any possible control on IGBTs.

To sum up, Figure 3.33 depicts the DC short circuit current values I_{sc} as a function of the fault resistance R_{sc} . As we can see, with the decrease of R_{sc} , the short circuit current may reach values up to 10 times the FEC nominal current on the DC side I_{dcn} . As a result, protective devices are required.

Figure 3.33 - DC short circuit current values I_{sc} as a function of the fault resistance R_{sc} (FEC contribution, $I_{dcn} = 125$ A)



3.1.2 Behavior with ESS

The same cases of the previous section will be analyzed hereunder in order to see what changes during a short circuit adding the ESS, which is inserted in parallel to the DC-Bus at $t = 0.25s$, while the fault still occurs at $t = 0.5s^2$.

Case 1b

For R_{sc} values such that the FEC is able to maintain the V_{dc} at the nominal value V_{dcn} , the fault current $I_{sc} = V_{dcn}/R_{sc}$ remains at the same value of Case 1a.

Therefore, the presence of the ESS does not contribute to increase the short circuit current.

Nevertheless, since the power amounts delivered to the load R_L and to the fault R_{sc} are now shared between the FEC and the ESS, the current absorbed from the grid I_{ac1} decreases.

Since V_{dc} remains at its nominal value of 800V (Figure 3.34), assuming $R_{sc} = 100\Omega$, the fault current I_{sc} is still 8A like in Case 1a (Figure 3.35).

The ESS connection causes a transient DC-Bus voltage increase over the nominal value (Figure 3.34), but the FEC control intervenes to bring back the V_{dc} to the set value of 800V.

Moreover, since I_{ac1} is lower than in Case 1a (Figure 3.36), the ESS allows the FEC to reach its maximum AC current absorp

tion for lower R_{sc} values. This is better from the electronic component current point of view.

Figure 3.34 – Trend of V_{dc} voltage during a short circuit on DC side in Case 1b

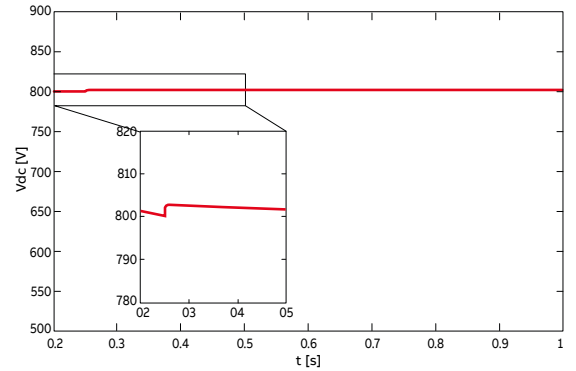


Figure 3.35 – Trend of I_{sc} current during a short circuit on DC side in Case 1b

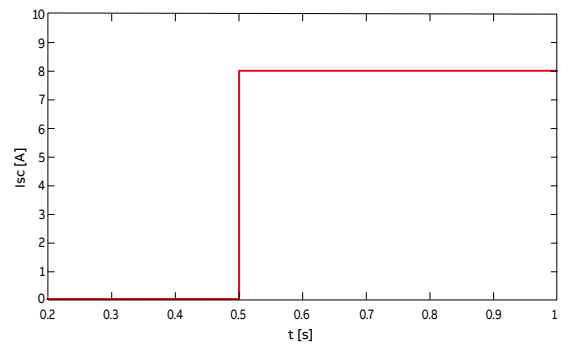
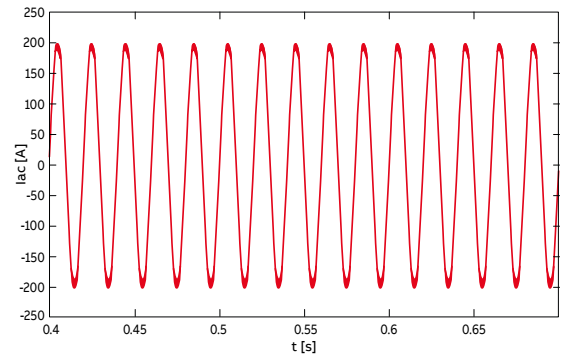


Figure 3.36 – Trend of I_{ac1} current during a short circuit on DC side in Case 1b



² See Annex B for the behavior in fault condition of the DC/DC converter that interfaces the ESS with the DC-Bus. In particular, the converter parallel capacitance can be added to C_{sc} series in order to have the total capacitance contribution.

3. Fault analysis

Case 2b

Unlike in Case 2a, assuming $R_{sc} = 30 \Omega$, V_{dc} is now maintained at its nominal value thanks to the ESS (Figure 3.37). As a consequence, the I_{ac1} no longer has to be limited by the FEC control at the maximum value of 240A.

In particular, I_{ac1} has a lower value (Figure 3.38) because now a portion of the load and fault power amounts are supplied by the ESS.

Indeed, the fault current has an higher value compared to the Case 2a due to the ESS contribution (Figure 3.39):

[3.3]

$$I_{sc} = \frac{V_{dc}}{R_{sc}} = \frac{800}{30} \approx 27A \quad (\text{Case 2b})$$

[3.4]

$$I_{sc} = \frac{V_{dc}}{R_{sc}} = \frac{774}{30} \approx 26A \quad (\text{Case 2a})$$

Figure 3.37 – Trend of V_{dc} voltage during a short circuit on DC side in Case 2b

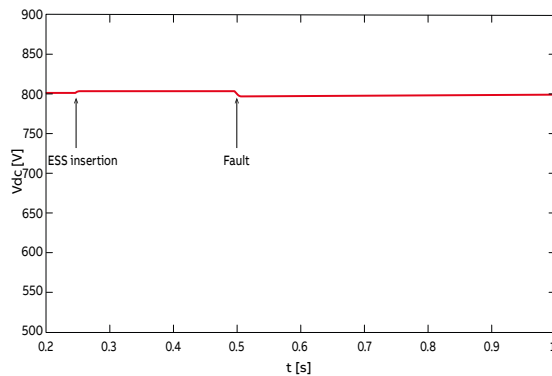


Figure 3.38 – Trend of I_{ac1} current during a short circuit on DC side in Case 2b

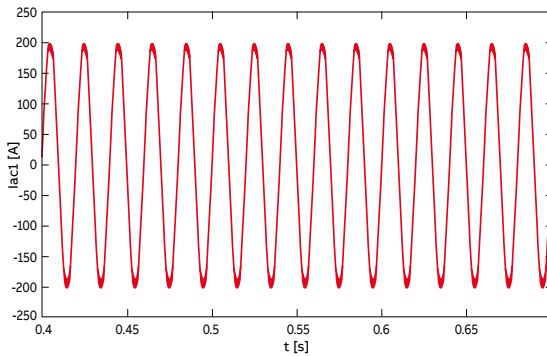
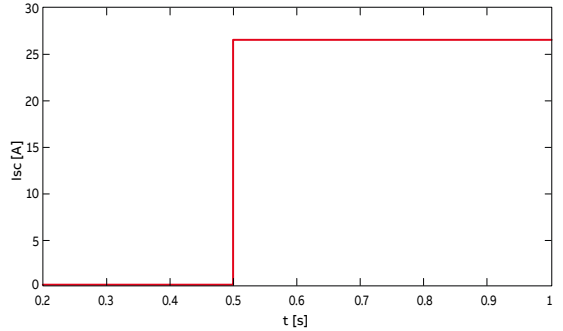


Figure 3.39 – Trend of I_{sc} current during a short circuit on DC side in Case 2b



The FEC still has a behavior like in the Case 2a, but for lower R_{sc} values.

Case 3b

Assuming $R_{sc} = 5 \Omega$, the DC-Bus voltage becomes now $V_{dc} \approx 777V > V_{dc1}$, which is higher than one of the Case 3a (Figure 3.40).

In particular, since V_{dc} is higher than V_{dc1} , the FEC still works in linear modulation condition (Figure 3.41), so the electronic component current is still regularly PWM controlled (Figure 3.42-3.43).

Moreover, since the V_{dc} is higher, the fault current I_{sc} increases (Figure 3.44).

Figure 3.40 – Trend of V_{dc} voltage during a short circuit on DC side in Case 3b

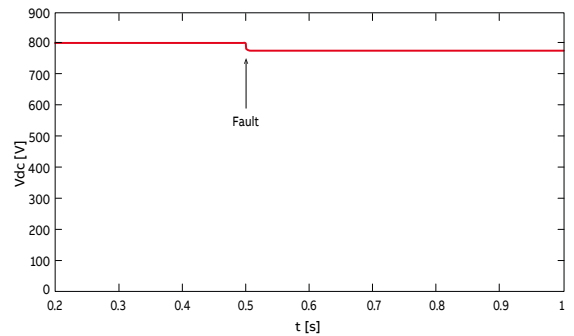


Figure 3.41 – PWM Control linear modulation during a short circuit on DC side in Case 3b

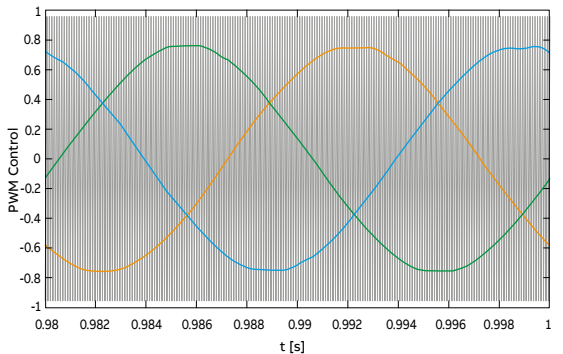


Figure 3.42 – Trend of the current in the electronic component of the first leg of the cathodic star during a short circuit on DC side in Case 3b

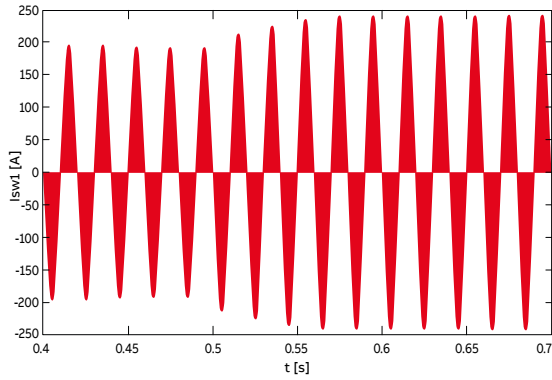


Figure 3.43 – Trend of the current in the electronic component of the first leg of the anodic star during a short circuit on DC side in Case 3b

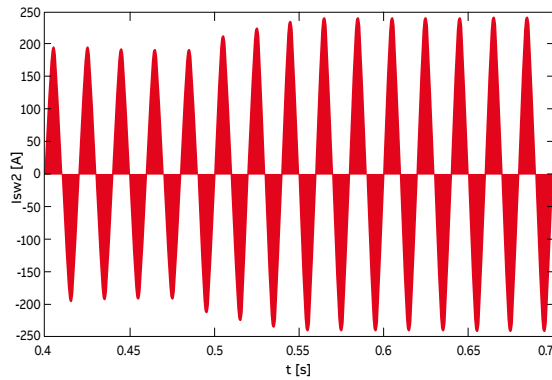
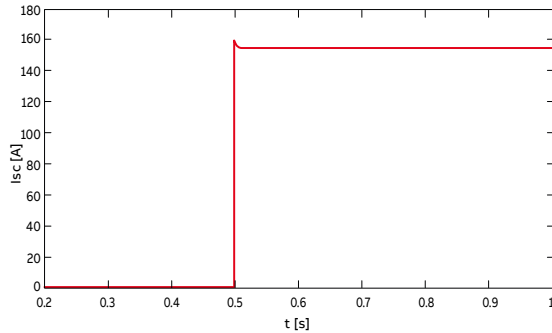


Figure 3.44 – Trend of I_sc current during a short circuit on DC side in Case 3b



Case 4b

Assuming $R_{sc} = 0.5 \Omega$, the DC-Bus voltage becomes $V_{dc} \approx 587 \text{ V} > V_{dc2}$ (Figure 3.45), so the FEC works in over-modulation, but not as a diode rectifier yet. As a consequence, the PWM control is not completely by-passed (Figure 3.46-3.47).

Figure 3.45 – Trend of V_{dc} voltage during a short circuit on DC side in Case 4b

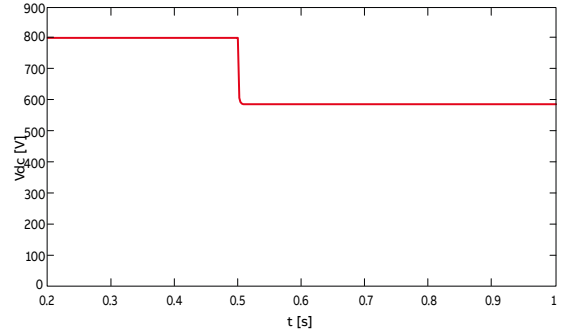


Figure 3.46 – Trend of the current in the electronic component of the first leg of the cathodic star during a short circuit on DC side in Case 4b

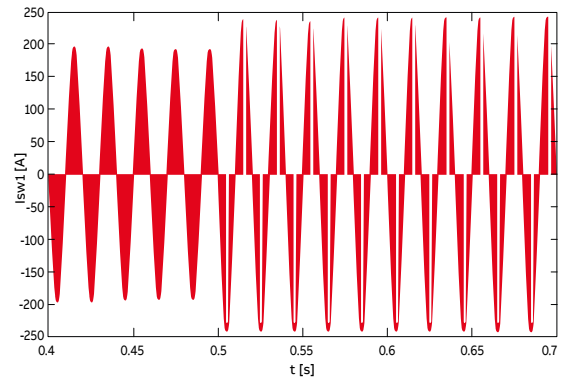
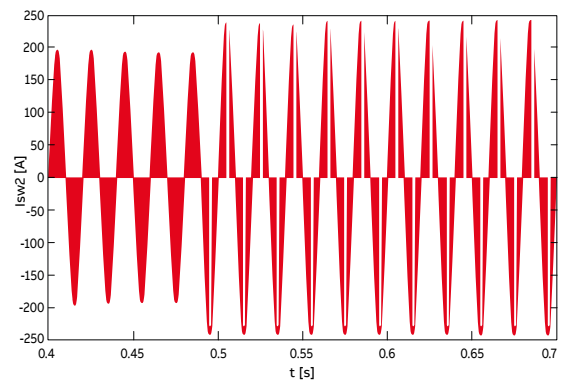


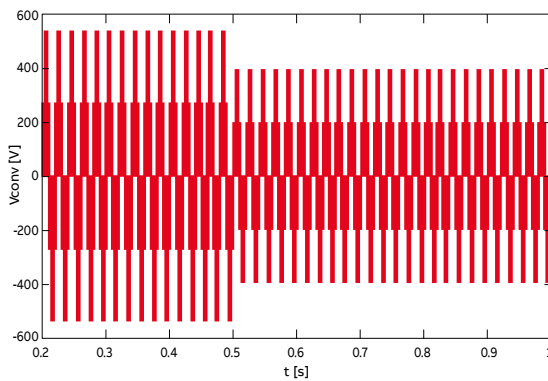
Figure 3.47 – Trend of the current in the electronic component of the first leg of the anodic star during a short circuit on DC side in Case 4b



3. Fault analysis

Figure 3.48 depicts the trend of the phase-to-ground voltage at the AC front-end converter terminals. We can see that, unlike in Case 4a, the FEC is able to maintain the same voltage waveform even during the fault, thanks to the ESS contribution.

Figure 3.48 – Trend of phase-to-ground voltage at AC front-end converter terminals during a short circuit on DC side in Case 4b



Case 5b

The fault current is the sum of the three components shown in Figure 3.49.

Assuming $R_{sc} = 1m\Omega$, the steady-state component of the fault current I_{sc} reaches a considerable value compared to the FEC nominal current and higher than in Case 5a (Figure 3.50a). Nevertheless, the peak value of the transient component remains equal to that one of Case 5a (Figure 3.50b), due to the DC capacitors C_{dc} discharge. This means that the peak is independent of the presence of the ESS. Even the FEC contribution remains the same (Figure 3.51). Furthermore, since the value of the ESS current contribution (Figure 3.52) is basically equal to the ratio between the ESS no-load voltage and the series of the ESS internal resistance and the fault resistance:

$$I_{dc1} = \frac{E_o}{R_i + R_{sc}} = \frac{803}{0.2 + 0.001} = 3995A \tag{3.5}$$

such fault current component does not affect the FEC.

Even in this case the DESAT protection is ineffective because the FEC works in the same manner of Case 5a. In particular the IGBT block is not able not only to limit the short circuit current from the AC grid but also the ESS fault contribution because it does not pass through the FEC (Figure 3.49).

Figure 3.49 – Isc current components with ESS

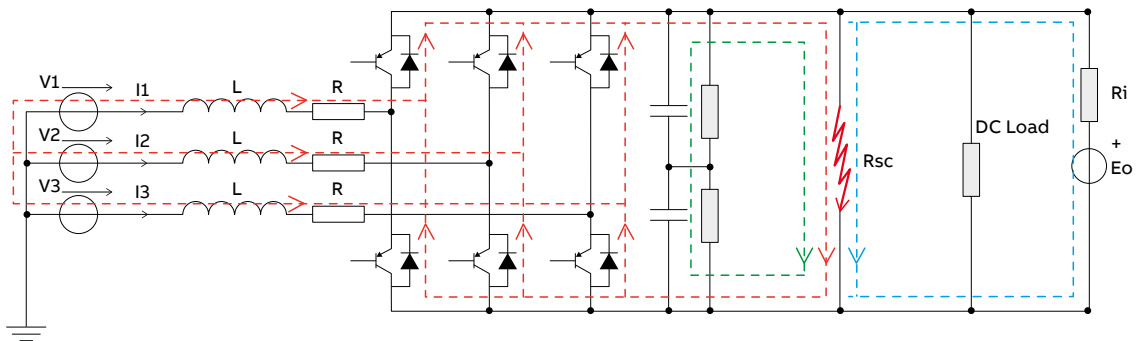


Figure 3.50a – Trend of fault current I_{sc} during a short circuit on DC side in Case 5b (steady state component)

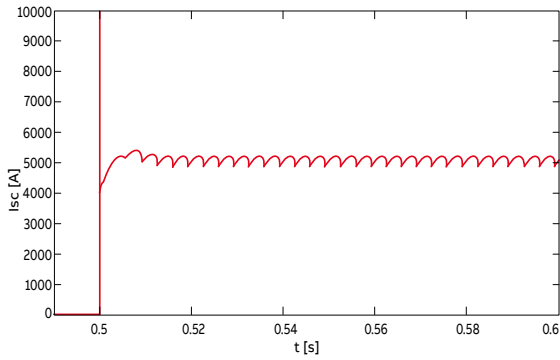


Figure 3.52 – Trend of fault current I_{dc1} during a short circuit on DC side in Case 5b

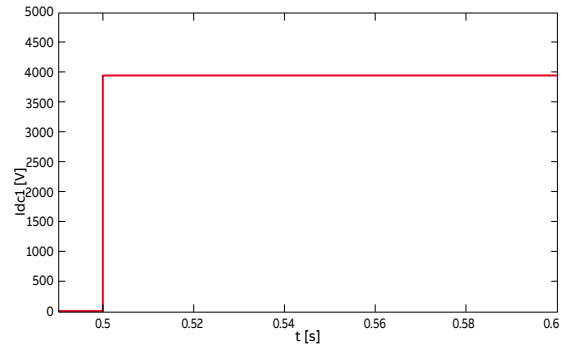


Figure 3.50b – Trend of fault current I_{sc} during a short circuit on DC side in Case 5b (C_{dc} discharge component)

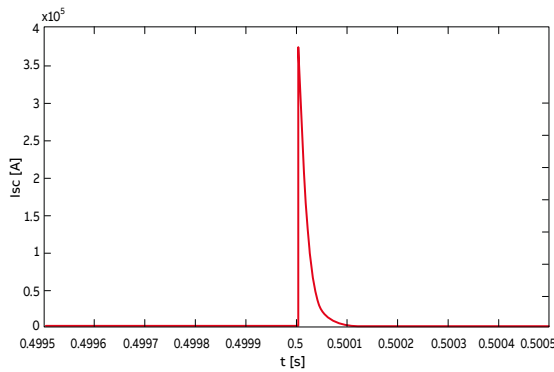
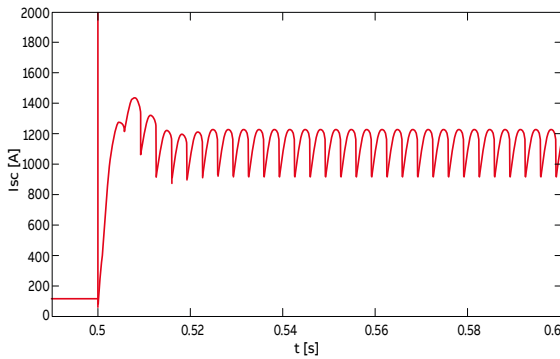


Figure 3.51 – Trend of current I^{dc} during a short circuit on DC side in Case 5b



To sum up, first of all the addition of an ESS is equivalent to the introduction of a source which is able to increase the fault current.

Moreover, the ESS contributes to maintaining the DC-Bus voltage at values higher than those in a passive DC microgrid.

As a result, the fault resistance for which the FEC starts to limit the AC grid absorbed current, the fault resistance for which the FEC works in over-modulation and the fault resistance for which the FEC works in an irregular way, (i.e., bypassing the controlled semiconductors) all result lower than those of a passive DC microgrid. Hence, the FEC current control capability improves.

Both the FEC and the ESS fault current depend on DC microgrid structure. Hence, it is not possible to consider the fault current equal to the sum of its value due to the FEC only without ESS, and of its value due to the ESS only without the FEC.

Although the presence of the ESS increases the short circuit current value, the AC current distortion decreases. For instance, with $R_{sc} = 0.5 \Omega$, the THD of I_{ac} decreases from 5% without ESS to 1.4% with ESS; indeed, maintaining the V_{dc} at a higher value (for every R_{sc} value), the ESS improves the FEC control capability, thus reducing in such manner the low frequency harmonic current absorption.

The lower the THD, the lower the impact on the MVAC grid in terms of upstream voltage distortion (better Power Quality).

3. Fault analysis

3.1.3 Behavior with PV plant

In the presence of a controlled current generator, which is connected at $t = 0.25s$ and simulates a PV plant connected to the LVDC microgrid, the same phenomena, which are explained in Cases 1b-5b, occur. Nevertheless, since the maximum PV plant current in short circuit condition I_{maxPV} is "limited", there is a lower V_{dc} support capability.

As a result, the R_{sc} values for which the FEC works in over-modulation, or like a diode rectifier, are between the case of absence and presence of the ESS³.

In the presence of both the ESS and the PV plant, their contribution sums to each other: the R_{sc} limit values become lower than the case of the presence of ESS only.

³ See Annex C for the behavior in fault condition of the DC/DC converter that interfaces the PV plant with the DC-Bus. In particular, the converter parallel capacitance can be added to C_{dc} series in order to have the total capacitances contribution.

3.2 Ground fault on DC side of the front-end converter

If a DC positive pole ground fault happens (but similar considerations are valid also for a DC negative pole ground fault), depending on the grounding configurations and on the ground fault resistance R_g , the same Cases of the previous section may occur. In systems where the transformer neutral point is grounded, the general purpose control of FECs cannot generally limit zero-sequence current due to a ground fault.

More specifically, two distinct behaviors are now possible if the fault resistance R_g is "high", i.e., large enough so that normal operation of the FEC is not altered, and if it is "low" otherwise.

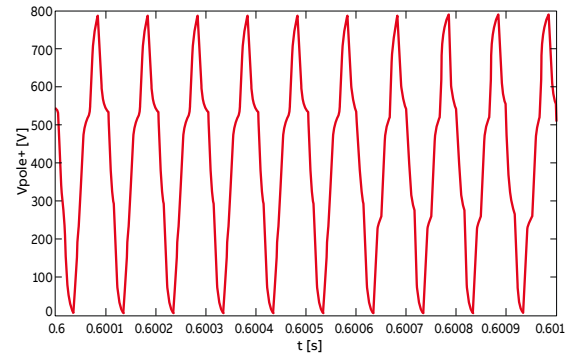
Moreover, it is still maintained the hypothesis that at first the IGBT self-protection is not considered so as to show ground fault current trend and path and to compare them to those in the presence of the self-protection.

3.2.1 System with the MV/LV transformer neutral point grounded

3.2.1-1 High fault resistance R_g without ESS and PV plant (S1=OFF, S2=ON)

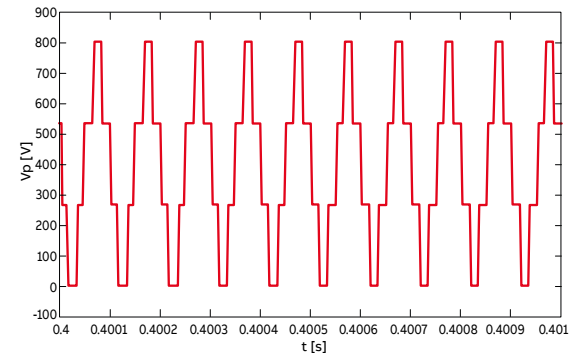
Figure 3.53a shows the trend of the voltage between the DC positive pole and the transformer neutral point in the presence of a ground fault ($R_g = 50\Omega$). If the star point of the transformer is grounded, the trend in Figure 3.53a corresponds also to the voltage between the poles and the ground.

Figure 3.53a - Trend of the potential of the DC positive pole with respect to the transformer neutral point during a ground fault on DC side without ESS and PV plant and with $R_g = 50 \Omega$



Hence, when a ground fault occurs on the DC positive pole (the same applies in the case of a ground fault on the negative pole), there is a change from step-like square wave (Figure 3.53b) to steps with exponential variation.

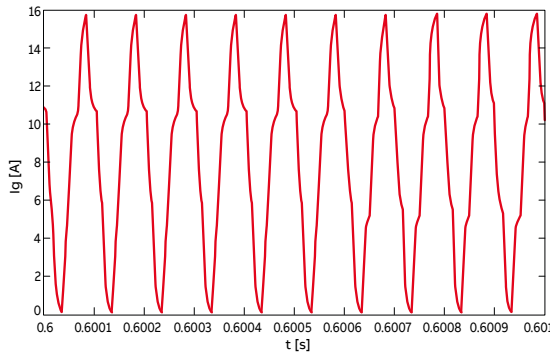
Figure 3.53b – Trend of the potential of the DC positive pole with respect to the transformer neutral point in the absence of fault



For high values of R_g (e.g. $R_g = 50 \Omega$), the ground fault current I_g (Figure 3.54) has the same waveform and frequency of the voltage in Figure 3.53.

In particular, the ratio between the DC component value and the value at the switching frequency remains constant and equal to 0.8-1.

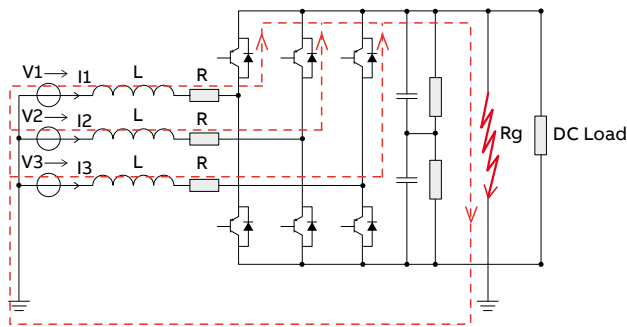
Figure 3.54 - Trend of I_g current during a ground fault on DC side in systems with the neutral point of the MV/LV transformer grounded without ESS and PV plant and with $R_g = 50 \Omega$



As it can be seen from the Figure 3.55, the DC component of I_g can flow only through the freewheeling diodes of the cathodic star⁴.

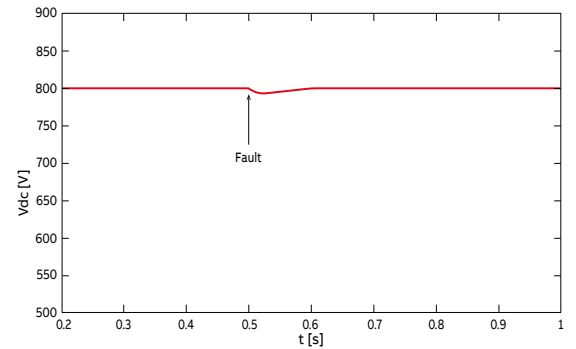
The component of the fault current that returns through the negative pole due to the distributed conductance of the DC cable is negligible if the leakage conductance is negligible.

Figure 3.55 – DC positive pole ground fault current path without ESS and PV plant in systems with the neutral point of the MV/LV transformer grounded



The DC-Bus voltage V_{dc} (Figure 3.56), after a transient sag when the fault occurs, is brought back to the nominal value by the FEC control.

Figure 3.56 – Trend of V_{dc} voltage during a ground fault on DC side in systems with the neutral point of the MV/LV transformer grounded without ESS and PV plant and with $R_g = 50 \Omega$



The electronic components work regularly as shown in Figures 3.57a-b, which depict respectively the current in the electronic component of the first leg of the cathodic star (I_{sw1}) and the current in the electronic component of the first leg of the anodic star (I_{sw2})⁵.

Figure 3.57a – Trend of I_{sw1} current during a ground fault on DC side in systems with the neutral point of the MV/LV transformer grounded without ESS and PV plant and with $R_g = 50 \Omega$

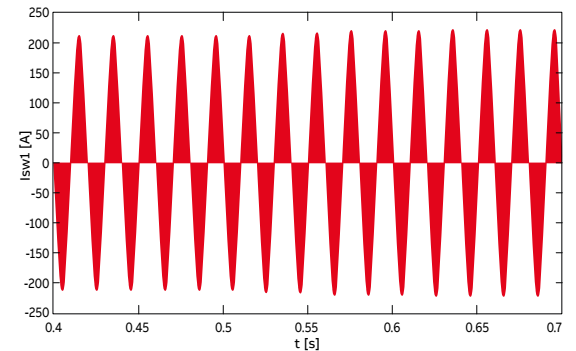
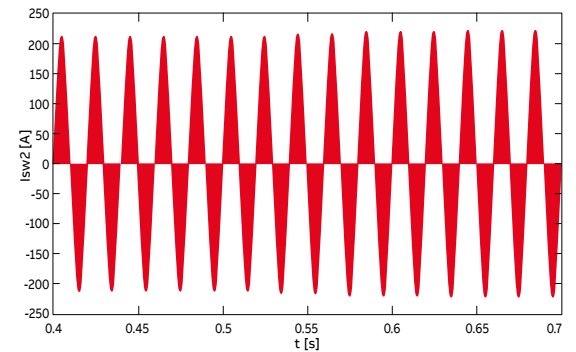


Figure 3.57b – Trend of I_{sw2} current during a ground fault on DC side in systems with the neutral point of the MV/LV transformer grounded without ESS and PV plant and with $R_g = 50 \Omega$



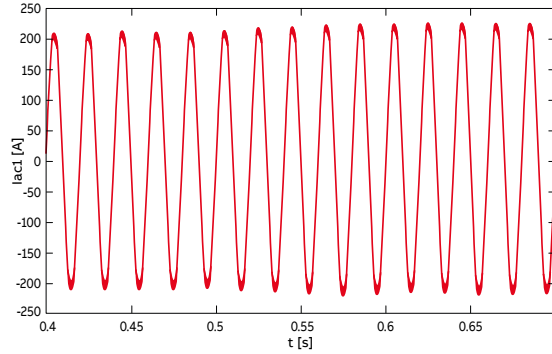
⁴ In dual manner, in case of a ground fault of the DC negative pole, the ground fault current would flow only in the freewheeling diodes of the anodic star.

⁵ Trends and values in the others FEC electronic components are equal.

3. Fault analysis

The waveform of the AC current I_{ac1} (Figure 3.58) does not change with respect to the no-fault condition (even if there is a DC component superimposed in each phase and equal to $I_g/3 = 8/3 = 2.7A$), since the FEC still works in linear modulation.

Figure 3.58 – Trend of I_{ac1} current during a ground fault on DC side in systems with the neutral point of the MV/LV transformer grounded without ESS and PV plant and with $R_g = 50 \Omega$



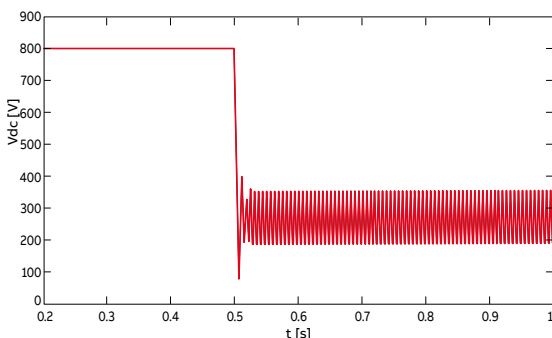
3.2.1.2 Low fault resistance R_g without ESS and PV plant (S1=ON, S2=ON/OFF)

The decreasing values of the fault resistance R_g cause voltage variations on the DC-Bus and give rise to a gradual loss of control by the converter. As the R_g decreases, the earth fault current I_g has a higher and higher DC component and I_g reaches such values that the use of protective devices is anyway required.

In particular, e.g. with $R_g = 50 \text{ m}\Omega$, the FEC behaves like a diode rectifier ($V_{dc} < 1.35 \cdot \sqrt{3} \cdot V_1$ as in Figure 3.59): it works for longer and longer fractions of time in an irregular way, i.e. bypassing the controlled semiconductors (fault current flows in freewheeling diodes).

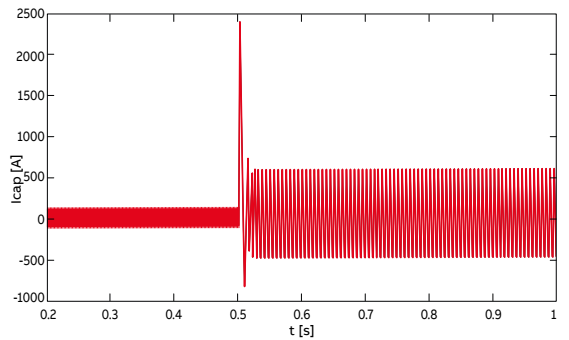
As we can see in Figure 3.59, as soon as the fault occurs ($t = 0.5 \text{ s}$), V_{dc} decreases discharging the DC capacitors (Figure 3.60) and reaching the steady state value, which guarantees a limited power delivery to the DC load.

Figure 3.59 – Trend of V_{dc} voltage during a ground fault on DC side in systems with the neutral point of the MV/LV transformer grounded without ESS and PV plant and with $R_g = 50 \text{ m}\Omega$



Since the steady state value of V_{dc} is not constant, there is a high current flowing through the DC capacitors.

Figure 3.60 – Trend of the DC capacitors current I_{cap} during a ground fault on DC side in systems with the neutral point of the MV/LV transformer grounded without ESS and PV plant and with $R_g = 50 \text{ m}\Omega$



The DC capacitor discharge current comes from the FEC lower terminal; as a result, the converter, during the fault transient, supplies a positive current flowing out of both terminals (Figures 3.61-3.62). This behavior corresponds to an abnormal FEC operation, since during normal operation current flows out of the upper terminal and into the lower one (Figures 3.61-3.62 before the fault).

The sum of the current from the upper terminal and of the current flowing through the capacitors makes the ground fault current I_g (minus the load current).

Figure 3.61 – Trend of the upper terminal current $I_{convdcl}$ during a ground fault on DC side in systems with the neutral point of the MV/LV transformer grounded without ESS and PV plant and with $R_g = 50 \text{ m}\Omega$

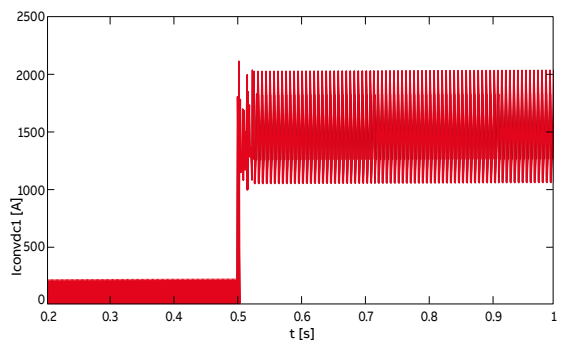
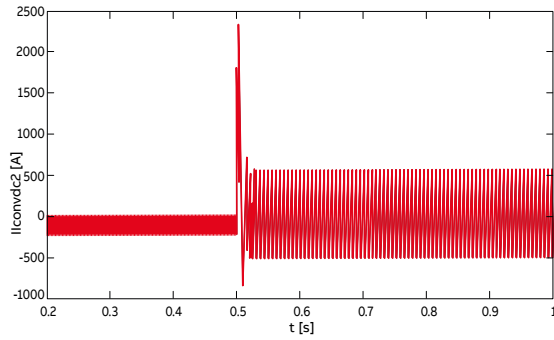
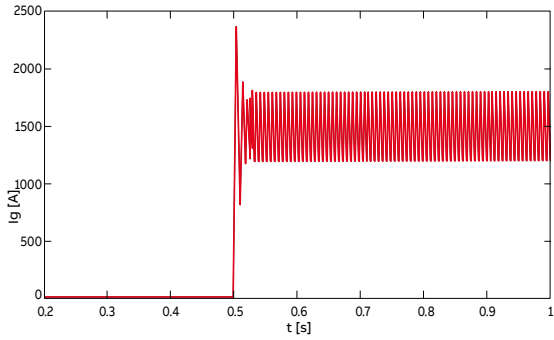


Figure 3.62 – Trend of the lower terminal current I_{convdc2} during a ground fault on DC side in systems with the neutral point of the MV/LV transformer grounded without ESS and PV plant and with $R_g = 50 \text{ m}\Omega$



I_g (Figure 3.63) has a large DC component and, unlike the cases with “high” R_g (Figure 3.54), low-frequency zero-sequence harmonics (mainly the 3rd, 6th and 9th).

Figure 3.63 – Trend of the ground fault current I_g during a ground fault on DC side in systems with the neutral point of the MV/LV transformer grounded without ESS and PV plant and with $R_g = 50 \text{ m}\Omega$



Moreover, I_g still follows the path of Figure 3.55, supplied by a zero-sequence voltage component, whose average value is equal to $V_{\text{dc}}/2$. Figures 3.64-3.65 depict respectively the trends of the DC pole voltage toward ground: during the fault I_g is supplied by the voltage in Figure 3.64 and limited by the total fault circuit resistance.

Figure 3.64 – Trend of the voltage of the DC positive pole $V_{\text{pole}+}$ during a ground fault on DC side in systems with the neutral point of the MV/LV transformer grounded without ESS and PV plant and with $R_g = 50 \text{ m}\Omega$

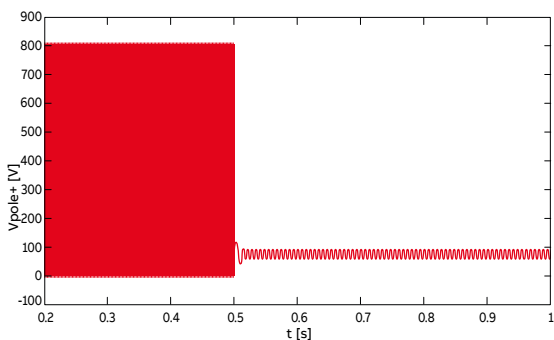
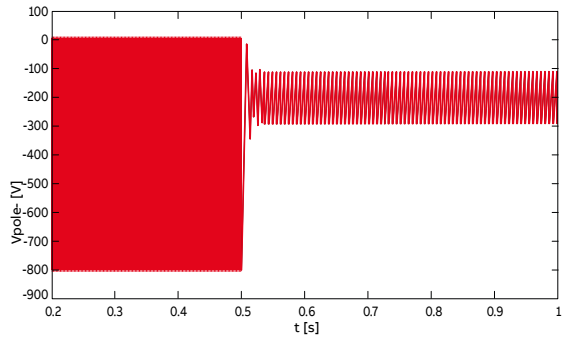


Figure 3.65 – Trend of the voltage of the DC negative pole $V_{\text{pole}-}$ during a ground fault on DC side in systems with the neutral point of the MV/LV transformer grounded without ESS and PV plant and with $R_g = 50 \text{ m}\Omega$



In steady-state conditions, the DC current component I_{convdc1} (Figure 3.61), which is the sum of the DC fault current component and of the load current V_{dc}/R , flows out from the FEC upper terminal, while only the DC load current I_{convdc2} (Figure 3.62) flows into the lower terminal, regardless of R_g low values. I_{ac1} not only has a large DC component, but also is no longer sinusoidal (Figure 3.66), due to over-modulation effect (Figure 3.67).

Figure 3.66 – Trend of I_{ac1} current during a ground fault on DC side in systems with the neutral point of the MV/LV transformer grounded without ESS and PV plant and with $R_g = 50 \text{ m}\Omega$

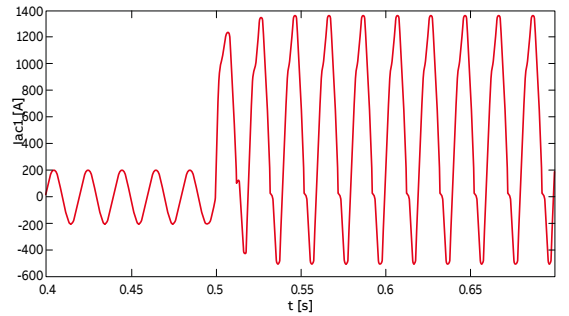
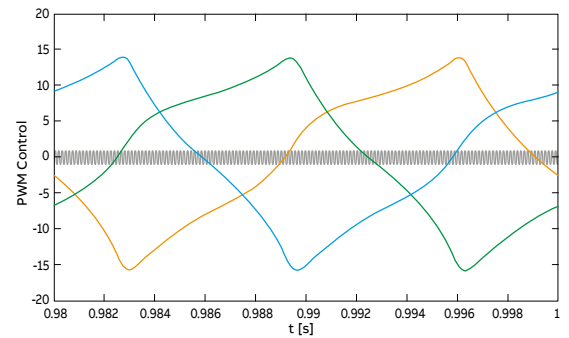


Figure 3.67 – PWM Control over-modulation during a ground fault on DC side in systems with the neutral point of the MV/LV transformer grounded without ESS and PV plant and with $R_g = 50 \text{ m}\Omega$



3. Fault analysis

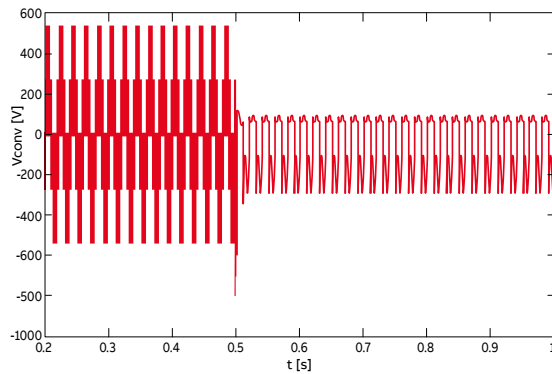
I_{ac1} is shifted by a value equal to one-third the fault current DC component.

Such component may cause several problems, such as the saturation of MV/LV transformer ferromagnetic core.

In steady-state conditions, I_{ac1} does not remain positive for all its period: this still involves the conduction of the anodic star freewheeling diodes.

Since the converter works like a diode rectifier, even the voltage at AC terminals trends to a square waveform due to over-modulation effect (Figure 3.68).

Figure 3.68 – Trend of the voltage at AC converter terminal V_{conv} during a ground fault on DC side in systems with the neutral point of the MV/LV transformer grounded without ESS and PV plant and with $R_g = 50\text{ m}\Omega$



If we look at the currents I_{sw1} (Figure 3.69a) and I_{sw2} (Figure 3.69b), we note that the DC component of the fault current flows through the freewheeling diodes of the cathodic star, while the DC component in the freewheeling diodes of the anodic star is only the DC load current.

Moreover, Figures 3.69a-b show clearly the non-PWM control for wide time intervals, due to over-modulation.

Figure 3.69a – Trend of I_{sw1} current during a ground fault on DC side in systems with the neutral point of the MV/LV transformer grounded without ESS and PV plant and with $R_g = 50\text{ m}\Omega$

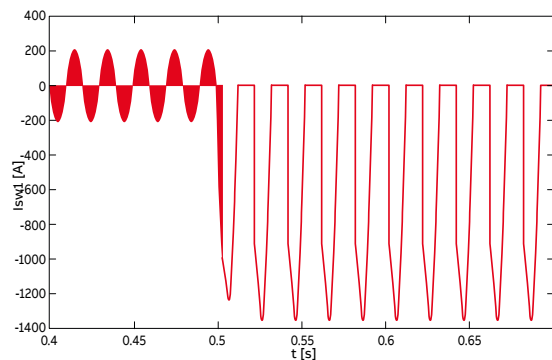
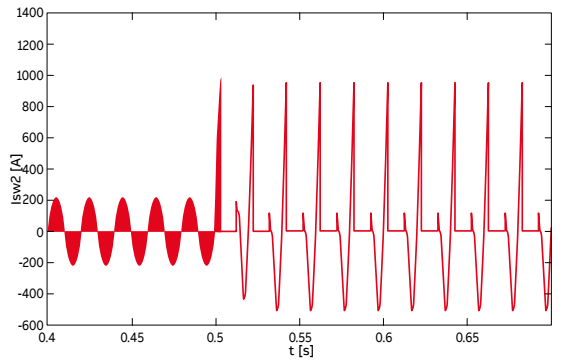


Figure 3.69b – Trend of I_{sw2} current during a ground fault on DC side in systems with the neutral point of the MV/LV transformer grounded without ESS and PV plant and with $R_g = 50\text{ m}\Omega$



In converters sold on the market, when the current in one of IGBTs tends to exceed the overload limits, a block command is sent to all converter IGBTs. Then, since all IGBTs are switched off, and only freewheeling diodes still remain in conduction, the converter works as a non-controlled diode rectifier. With the IGBT block the DC capacitor discharge contribution to the ground fault current is limited. Nevertheless, the ground fault current remains practically unchanged and equal to that in Figure 3.63, because, even without IGBT block, such current already flows only through the cathodic star freewheeling diodes (Figure 3.70a). On the contrary, I_{sw2} (Figure 3.70b) changes, since now the current can flow only through the freewheeling diodes and there is no longer any PWM control.

Even the trend of the AC absorbed current I_{ac1} is similar to that of a diode rectifier with a predominant DC component due to the fault (Figure 3.71).

Figure 3.70a – Trend of I_{sw1} current during a ground fault on DC side in systems with the neutral point of the MV/LV transformer grounded with IGBT block, without ESS and PV plant and with $R_g = 50\text{ m}\Omega$

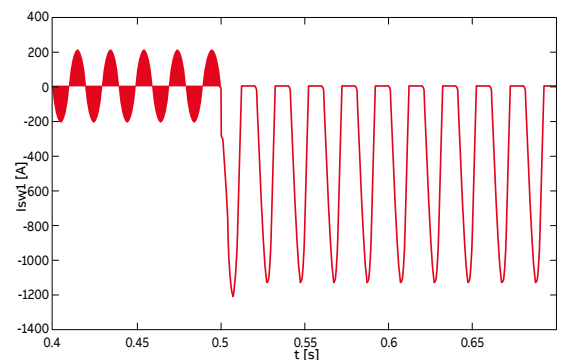


Figure 3.70b – Trend of I_{sw2} current during a ground fault on DC side in systems with the neutral point of the MV/LV transformer grounded with IGBT block, without ESS and PV plant and with $R_g = 50\text{ m}\Omega$

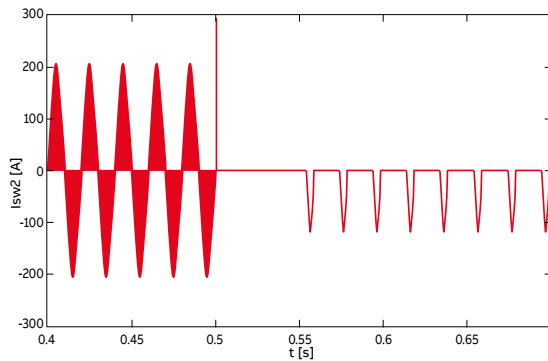


Figure 3.72 – Trend of I_g during a ground fault on DC side in systems with the neutral point of the MV/LV transformer grounded without ESS and PV plant and with $R_g = 1\text{ m}\Omega$

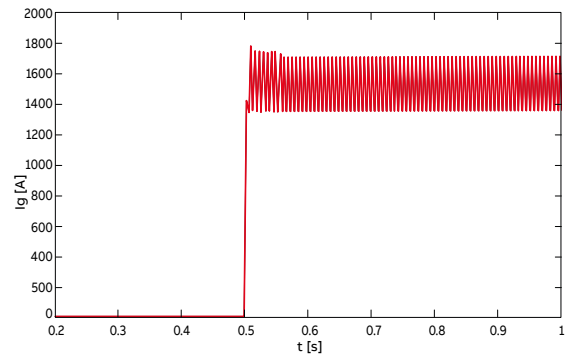
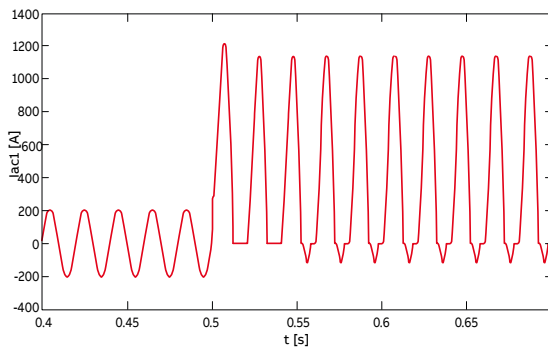


Figure 3.71 – Trend of I_{ac1} current during a ground fault on DC side in systems with the neutral point of the MV/LV transformer grounded with IGBT block, without ESS and PV plant and with $R_g = 50\text{ m}\Omega$



In particular, the loss of FEC control is more likely in the installations where the exposed conductive parts are connected to a protective grounding system that is the same as the operational grounding (e.g. industrial plants and large commercial users having their own transformation substation), since, in that case, impedance of the fault ring is usually very low (of mΩ order).

On the contrary, in low voltage installations where the protective grounding system is distinct from the operational, since the grounding system has been designed according to the relation:

[3.7]

$$R_t \leq \frac{120}{I_{diff}}$$

Considering a bolted ground fault with $R_g = 1\text{ m}\Omega$, we obtain a DC component of I_g (Figure 3.72) equal approximately to 1600A (≈ 13 times I_{dcn}), albeit IGBTs are blocked. Such fault current value may jeopardize the integrity of the freewheeling diodes.

Compared to the bolted short circuit between the DC poles, now the transient current peak due to the C_{dc} discharge is lower, because now the discharge impedance is not only R_{sc} , but it is equal to the sum $R_g + Z/3$ (where Z is the total AC grid equivalent impedance). Nevertheless, now, the steady-state value of the fault current is higher by more or less 30% than the steady-state value in bolted short circuit condition (≈ 10 times I_{dcn}): this is because the AC inductances do not create impedance to the DC component of the ground fault current flowing through the ground connection of the MV/LV transformer neutral point.

On the contrary, since a short circuit can be seen like an additional “low resistance load”, the I_{ac1} waveform does not change (Figure 3.32) and then the AC grid contribution is more limited by the inductive reactance.

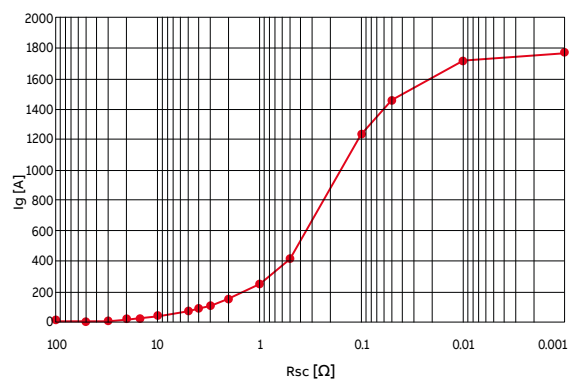
the grounding resistance can exceed the value for which the converter loses the control.

To sum up, Figure 3.73 depicts the DC ground fault current values I_g as a function of the fault resistance R_g .

As we can see, with the decrease of R_g , the fault current may reach values even higher than 14 times the FEC nominal current on the DC side I_{dcn} .

As a result, protective devices are required.

Figure 3.73 - DC component values of the ground fault current I_g as a function of the fault resistance R_g in systems with the neutral point of the MV/LV transformer grounded (FEC contribution, $I_{dcn} = 125\text{ A}$)



3. Fault analysis

3.2.1.3 High fault resistance R_g with ESS (S1=OFF, S2=ON)

For high values of R_g (e.g. $R_g = 50 \Omega$), direction of DC components of $I_{convdc1}$ (Figure 3.74) and $I_{convdc2}$ (Figure 3.75) is outwards for the upper terminal and inwards for the lower terminal of the converter.

This means there is no reclosing path for any possible contribution to fault by the storage system, which then feeds only the load, while the converter feeds both the load and the fault.

Indeed the DC component of $I_{convdc1}$ equal to 108 A, is the sum of the DC components of:

[3.8]

$$I_{convdc1} = I_{dc} = -I_{convdc2} + I_g = -(-100) + 8 = 108A$$

While the DC component of $I_{convdc2}$ is only equal to the load current FEC contribution.

Load current includes contributions by the storage system and by the FEC.

With reference directions as in Figure 2.2:

[3.9]

$$I_R = \frac{V_{dc}}{R_L} = \frac{800}{7.1} = 113A$$

[3.10]

$$I_R = I_{dc} - I_g + I_{dc1} = -I_{convdc2} + I_{dc1} = -(-100) + 13 = 113A$$

Figure 3.74 – Trend of $I_{convdc1}$ during a ground fault on DC side in systems with the neutral point of the MV/LV transformer grounded with ESS and $R_g = 50 \Omega$

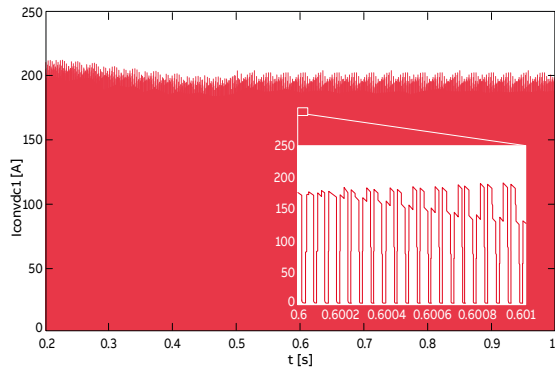
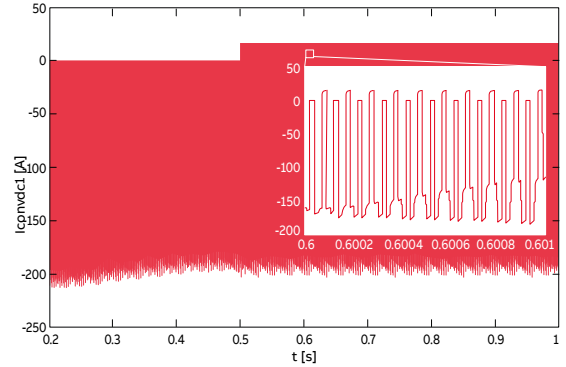


Figure 3.75 – Trend of $I_{convdc2}$ during a ground fault on DC side in systems with the neutral point of the MV/LV transformer grounded with ESS and $R_g = 50 \Omega$



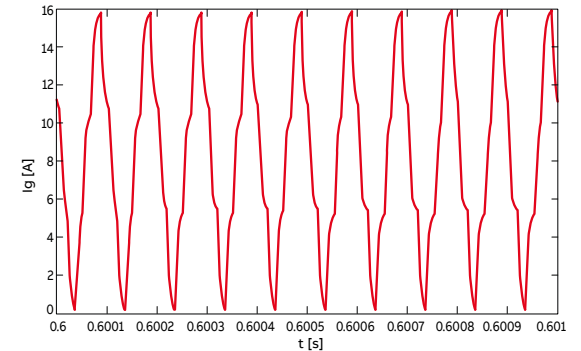
I_g (Figure 3.76) has the same amplitude and frequency as it would have without the ESS (Figure 3.54): this shows that for high values of R_g the ESS does not feed a ground fault. The DC component of I_g is:

[3.11]

$$I_g = I_{convdc1} + I_{convdc2} = 108 + (-100) = 8A$$

where the value of the DC component of $I_{convdc2}$ is negative, as shown in Figure 3.75

Figure 3.76 – Trend of I_g during a ground fault on DC side in systems with the neutral point of the MV/LV transformer grounded with ESS and $R_g = 50 \Omega$



3.2.1.4 Low fault resistance R_g with ESS (S1=ON, S2=ON/OFF)

The presence of the ESS keeps V_{dc} at a higher value than it would be without the storage system, like in the case of a short circuit.

Even if the ESS is present, the FEC does not operate correctly, because the lower the value of R_g , the more the DC components of $I_{convdc1}$ and $I_{convdc2}$ tend to be both directed outwards with respect to the upper and lower terminal of converter.

If R_g is even lower (e.g. $R_g = 50 \text{ m}\Omega$), not only the DC components, but the full waveforms of currents $I_{convdc1}$ (Figure 3.77) and $I_{convdc2}$ (Figure 3.78) are directed outwards of the DC terminals of the converter.

This means that there is a reclosing path for the fault current contribution supplied by the ESS (Figure 3.79)⁶ that in this condition feeds both the load and the fault, while the converter feeds only the fault.

The limit value of R_g below which this operation mode takes place, is the one for which $I_{convdc2} = 0$.

Figure 3.77 – Trend of $I_{convdc1}$ during a ground fault on DC side in systems with the neutral point of the MV/LV transformer grounded with ESS and $R_g = 50 \text{ m}\Omega$

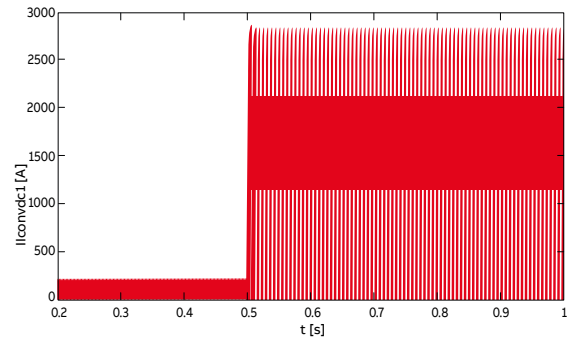
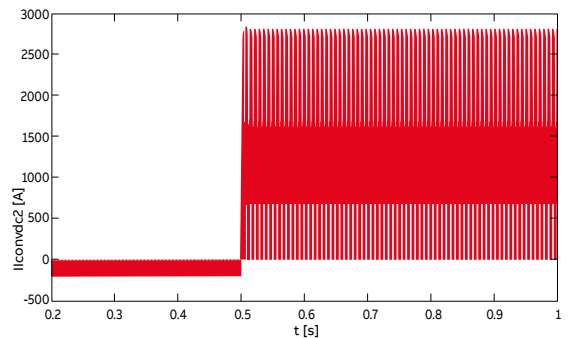
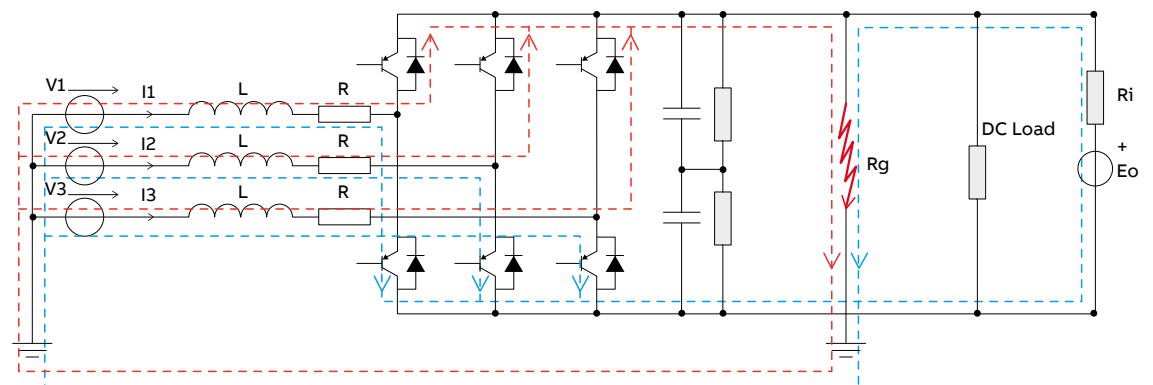


Figure 3.78 – Trend of $I_{convdc2}$ during a ground fault on DC side in systems with the neutral point of the MV/LV transformer grounded with ESS and $R_g = 50 \text{ m}\Omega$



⁶ In dual manner, in case of a ground fault on the DC negative pole, the ESS contribution to the ground fault current would flow only in the IGBTs of the cathodic star: as a consequence, both $I_{convdc1}$ and $I_{convdc2}$ would flow into the FEC terminals.

Figure 3.79 – DC positive pole ground fault current path with ESS and low fault resistance in systems with the neutral point of the MV/LV transformer grounded



3. Fault analysis

The ESS thus plays a key role in allowing reclosure of the DC component coming out of the negative terminal of the FEC.

This is an extremely important fact, because, due to the lack of grounding of the storage system, its presence is usually neglected in a first approximation calculation of I_g in case of a ground fault of a single pole.

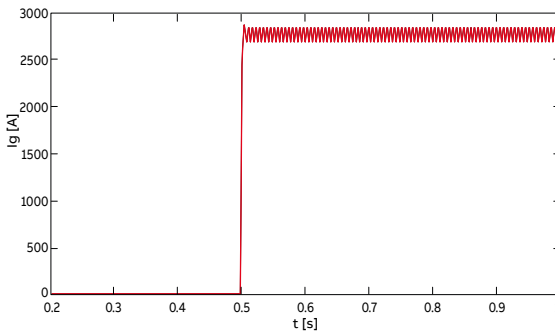
With reference to the path of I_g as shown in Figure 3.79 and $R_g = 50 \text{ m}\Omega$, the DC component of I_g (Figure 3.80) is still given by:

[3.12]

$$I_g = I_{convdc1} + I_{convdc2} = 1572 + 1193 = 2765A$$

but now the DC component of $I_{convdc2}$ is positive, as shown in Figure 3.78.

Figure 3.80 – Trend of I_g during a ground fault on DC side in systems with the neutral point of the MV/LV transformer grounded with ESS and $R_g = 50 \text{ m}\Omega$



The DC component of current fed by the ESS I_{dc1} (Figure 3.81) now results from the sum of fault contribution $I_{convdc2}$ and the DC load current, which shows that all load current is generated by the ESS, while current from the converter flows into the ground fault:

[3.13]

$$I_{dc1} = \frac{V_{dc}}{R_L} + I_{convdc2} = \frac{548}{7.1} + 1193 = 1270A$$

Figure 3.81 – Trend of I_{dc1} during a ground fault on DC side in systems with the neutral point of the MV/LV transformer grounded with ESS and $R_g = 50 \text{ m}\Omega$

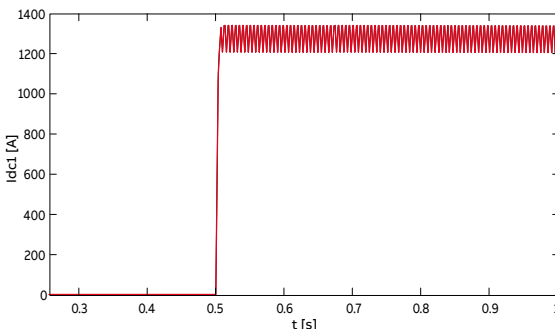
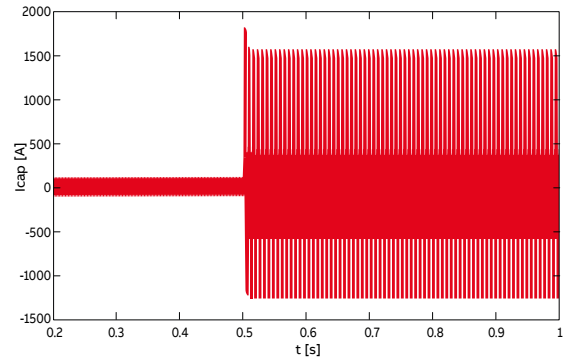


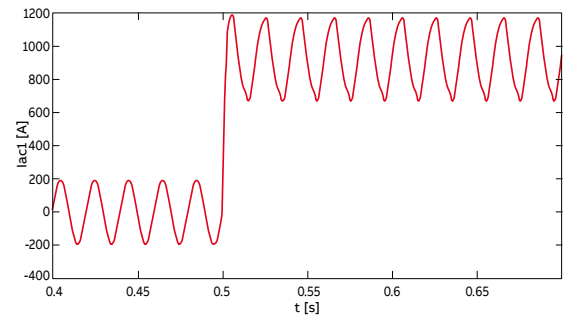
Figure 3.82 shows the current flowing in the filter capacitance C_{dc} : it can be noted that, even if the ESS keeps V_{dc} high, a considerable ripple current flows in the capacitors, which may then be damaged⁷.

Figure 3.82 – Trend of the DC capacitor current I_{cap} during a ground fault on DC side in systems with the neutral point of the MV/LV transformer grounded with ESS and $R_g = 50 \text{ m}\Omega$



As shown in Figure 3.83, depending on the value of R_g , I_{ac1} may be completely positive, and all the AC component absorbed by the converter feeds the fault.

Figure 3.83 – Trend of I_{ac1} current during a ground fault on DC side in systems with the neutral point of the MV/LV transformer grounded with ESS and $R_g = 50 \text{ m}\Omega$



If current I_{ac1} is always positive, it flows only in the freewheeling diodes of cathodic star (Figure 3.84a) and in the IGBTs of the anodic star (Figure 3.84b).

Figure 3.84a – Trend of I_{sw1} current during a ground fault on DC side in systems with the neutral point of the MV/LV transformer grounded with ESS and $R_g = 50\text{ m}\Omega$

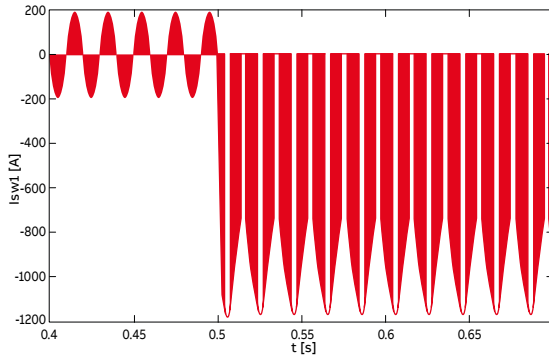
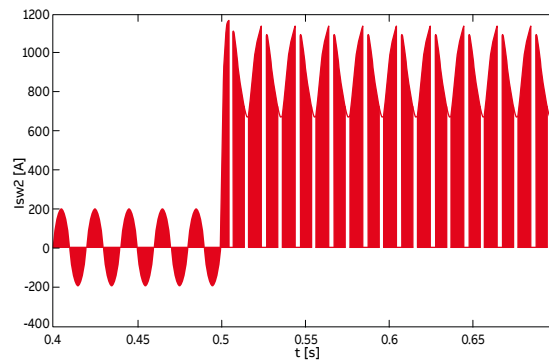


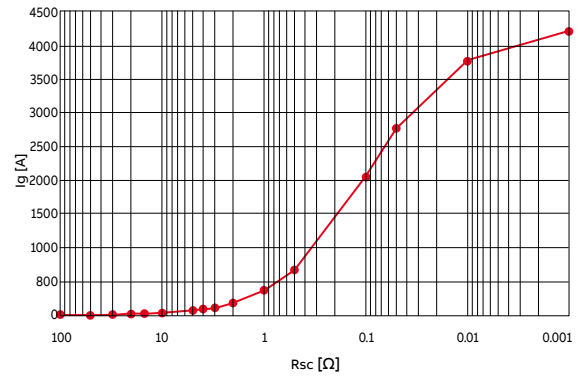
Figure 3.84b – Trend of I_{sw2} current during a ground fault on DC side in systems with the neutral point of the MV/LV transformer grounded with ESS and $R_g = 50\text{ m}\Omega$



To sum up, Figure 3.85 depicts the DC ground fault current values I_g as a function of the fault resistance R_g with the ESS.

As we can see, with the decrease of R_g , the fault current may reach values even higher than 33 times the FEC nominal current on the DC side I_{dcn} . As a result, protective devices are required.

Figure 3.85 - DC component values of the ground fault current I_g as a function of the fault resistance R_g in systems with the neutral point of the MV/LV transformer grounded with ESS ($I_{dcn} = 125\text{ A}$)

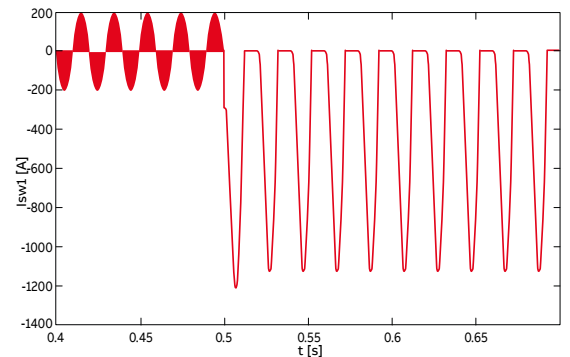


If the IGBT block is considered, the currents I_{sw1} and I_{sw2} change as shown in Figures 3.86a-b.

As it can be seen, unlike in Figures 3.84a-b, there is no longer the PWM control and in particular, since I_{sw2} flowed only in the IGBT, now it is cancelled.

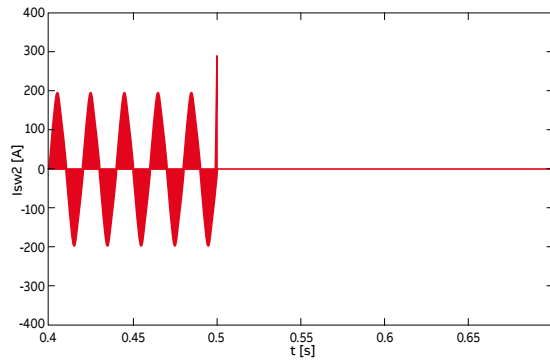
As a result, the ESS contribution to the ground fault current is interrupted.

Figure 3.86a – Trend of I_{sw1} current during a ground fault on DC side in systems with the neutral point of the MV/LV transformer grounded with ESS, IGBT block and $R_g = 50\text{ m}\Omega$



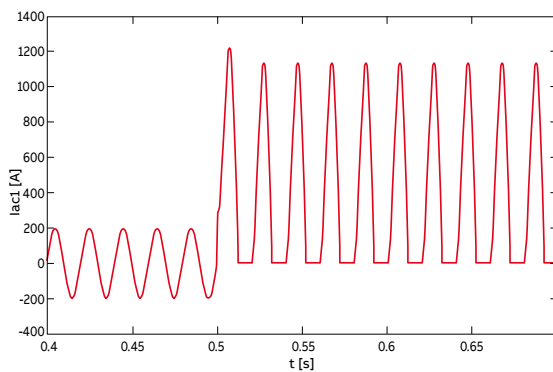
3. Fault analysis

Figure 3.86b – Trend of I_{sw2} current during a ground fault on DC side in systems with the neutral point of the MV/LV transformer grounded with ESS, IGBT block and $R_g = 50 \text{ m}\Omega$



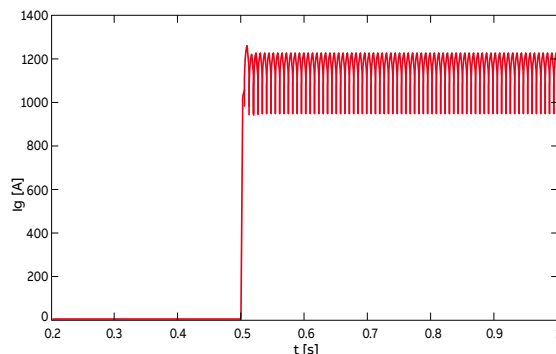
Even blocking the IGBTs and interrupting the ESS contribution, the I_{ac1} (with $R_g = 50 \text{ m}\Omega$) still remains always positive (Figure 3.87), but with a DC component lower than the I_{ac1} of Figure 3.83.

Figure 3.87 – Trend of I_{ac1} current during a ground fault on DC side in systems with the neutral point of the MV/LV transformer grounded with ESS, IGBT block and $R_g = 50 \text{ m}\Omega$



Even removing the ESS contribution, the ground fault current I_g still remains high (Figure 3.88), so it has to be interrupted by suitable protective devices.

Figure 3.88 – Trend of I_g during a ground fault on DC side in systems with the neutral point of the MV/LV transformer grounded with ESS, IGBT block and $R_g = 50 \text{ m}\Omega$



To sum up, first of all the ESS connection corresponds to the introduction of a source that is able to feed the ground fault for low fault resistance values. Nevertheless, FECs sold on the market usually avoid such contribution by blocking their IGBTs. The ESS maintains the V_{dc} at a higher value than one of a passive LVDC microgrid, improving the power quality of the DC loads. Moreover, R_g values for which the FEC starts to limit the AC current absorption, for which the FEC control turns to over-modulation and for which the FEC works like a diode rectifier are lower than those of a passive LVDC microgrid, improving the FEC current control capability. Even for the ground fault, both the FEC and the ESS fault contributions depend on the LVDC microgrid structure: hence, it is not possible to consider the fault current equal to the sum of its value due to the FEC without ESS only and of its value due to only the ESS without the FEC only, like in DC short circuit condition.

3.2.1.5 Behavior with PV plant

In the presence of a controlled current generator, which is connected at $t = 0.25\text{s}$ and simulates a PV plant connected to the LVDC microgrid, the same phenomena, which are explained in Cases 1b-5b, occur.

Nevertheless, since the maximum PV plant current in short circuit condition I_{maxPV} is “limited”, there is a lower V_{dc} support capability.

As a result, the R_g values for which the FEC works in over-modulation or like a diode rectifier are between the case of absence and presence of the ESS⁸.

In the presence of both the ESS and the PV plant, their contributions sum to each other: the R_g limit values become lower than the case of the only ESS presence. Also in presence of PV plant, as R_g decreases, the PV generator provides the same reclosing path for unidirectional current component $I_{conVdc2}$ shown in Figure 3.79 and it theoretically forces in semiconductors of the anodic star a current that can be larger than the load current. Furthermore, as for the scenario with the ESS, for high values of R_g , the converter feeds both the DC load and the earth fault, while the PV plant only supplies the load.

On the other hand, for low R_g values, the converter only feeds the fault, while the PV plant supplies both

⁸ See Annex C for the behavior in fault condition of the DC/DC converter that interfaces the PV plant with the DC-Bus. In particular, the converter parallel capacitance can be added to C_{dc} series in order to have the total capacitances contribution.

the DC load and the fault by $I_{dc1} = V_{dc/R} + I_{convdc2}$. However, because the PV plant can provide a maximum possible fault current I_{pvmax} , fault current does not increase more.

The DC component of I_{ac1} current is also limited and currents I_{ac1} and I_{sw2} may span both polarities (Figures 3.89, 3.91).

Figure 3.89 – Trend of I_{ac1} during a ground fault on DC side in systems with the neutral point of the MV/LV transformer grounded with PV plant and $R_g = 50\text{ m}\Omega$

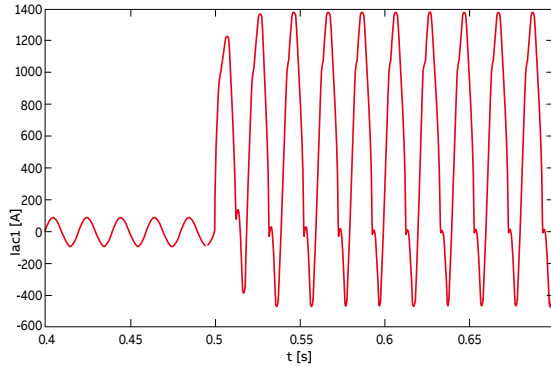


Figure 3.90 – Trends of I_{sw1} during a ground fault on DC side in systems with the neutral point of the MV/LV transformer grounded with PV plant and $R_g = 50\text{ m}\Omega$

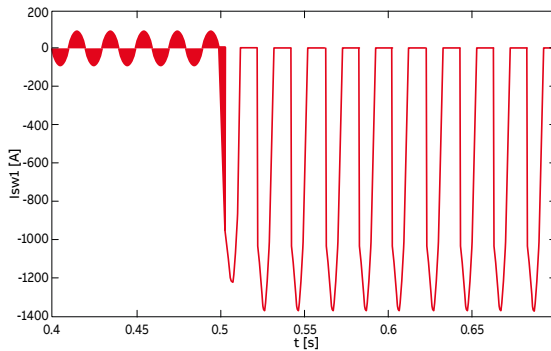
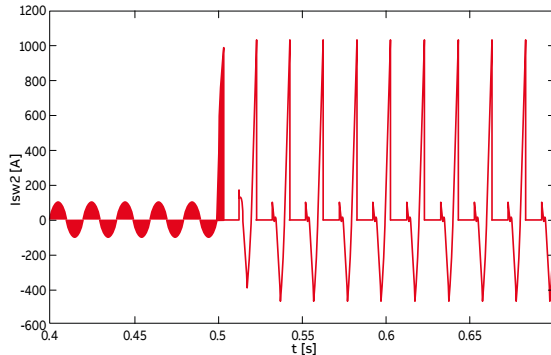


Figure 3.91 – Trends of I_{sw2} during a ground fault on DC side in systems with the neutral point of the MV/LV transformer grounded with PV plant and $R_g = 50\text{ m}\Omega$



3.2.2 Systems with the DC negative pole grounded

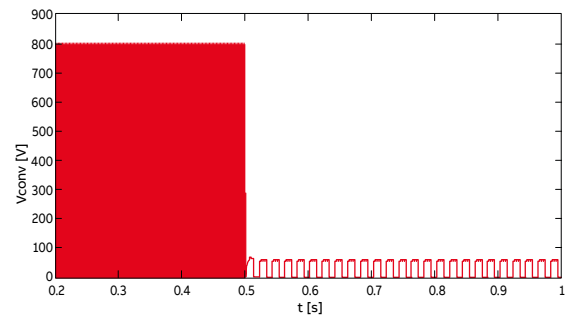
In these systems, because the DC negative pole is grounded while the transformer neutral point is isolated, a ground fault of the DC positive pole is equivalent to a short circuit between the DC poles. Then, the analysis is the same as for a short circuit on DC side, both for active and passive networks (as discussed in Section 3.1).

Since the negative pole is solidly grounded, an accidental contact of it to ground would cause no harm: the situation is similar to an earth contact when neutral is solidly grounded at the source (transformer station). Since a ground fault is equivalent to a short circuit on the DC side, no DC component is present in the current absorbed from the AC side (independent of R_g value). Hence, such a fault is seen by the FEC as an additional, "low impedance load".

In particular, (in the LVDC microgrid analyzed) the R_g value for which the FEC starts to limit V_{dc} is equal to $R_g = 13\ \Omega$, whereas with the DC negative pole grounded, this condition occurs for $R_g = R_{sc} = 45\ \Omega$: this means that the limit between "high fault resistance" and "low fault resistance" changes. This is because in systems with the transformer neutral point grounded, the total zero-sequence impedance "seen" by the fault current is $3R_g + Z$, while in the systems with the DC negative pole grounded, the fault current only "sees" R_g . Moreover, now the DC voltage feeding the fault is equal to the whole DC-Bus voltage V_{dc} , while in systems with the transformer neutral point grounded the fault is fed by a DC voltage equal to $V_{dc}/2$. As a consequence, the R_g value for which the FEC starts to limit the power transfer is higher than in the systems analyzed previously. Moreover, we can observe the AC converter terminal voltage variation compared to the previous systems. For example, assuming $R_g = 50\text{ m}\Omega$, V_{conv} (Figure 3.92) decreases and tends to a square waveform, but always positive, unlike V_{conv} in Figure 3.68.

If ESS and PV plant were present, the waveform would be the same, but the maximum value of V_{conv} during the fault would be higher, since V_{dc} would be higher.

Figure 3.92 – Trend of the voltage at AC converter terminal V_{conv} in systems with the DC negative pole grounded during a ground fault on DC side without ESS and PV plant and with $R_g = 50\text{ m}\Omega$



3. Fault analysis

3.2.3 Systems with the DC mid-point grounded

DC mid-point grounding offers some engineering advantages, e.g. availability of two different voltage levels, dimensioning of insulation system for only half the full rated voltage, at the expenses of some additional installation complexity.

Nevertheless, DC mid-point grounding has the drawback that, in case of ground fault on one pole, depending on the fault resistance, even if the converter is able to control the DC-Bus voltage, the voltage between the positive pole and the ground V_{pole+} tends to zero, while the voltage of the healthy pole with respect to ground V_{pole-} may float and reach the full rated DC voltage ($-V_{dc}$), which may cause problems to the isolation system. (Figure 3.93-3.94).

Figure 3.93 – Trend of the voltage of the DC positive pole V_{pole+} in systems with the DC mid-point grounded during a ground fault on DC side without ESS and PV plant and with $R_g = 50 \Omega$ (S1=OFF, S2=ON), $50 \text{ m}\Omega$ (S1=ON, S2=ON/OFF)

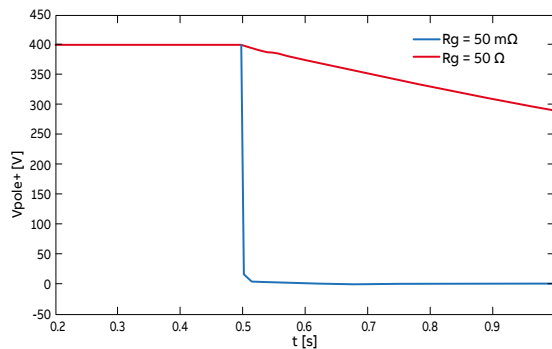
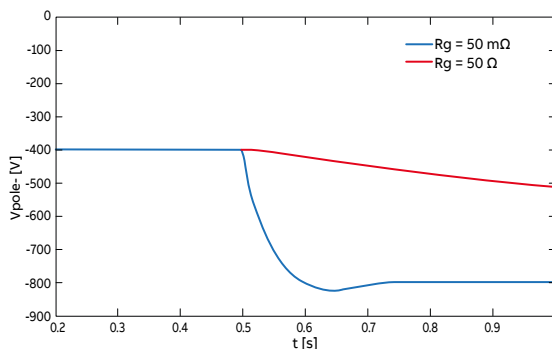
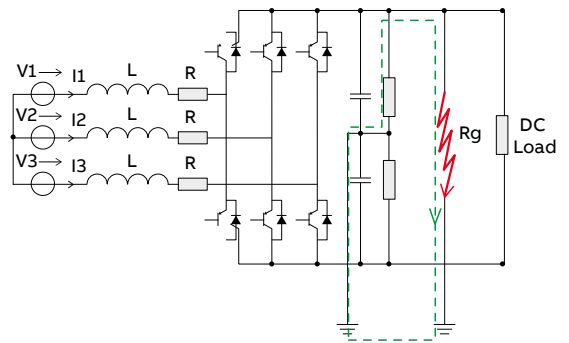


Figure 3.94 – Trend of the voltage of the DC negative pole V_{pole-} in systems with the DC mid-point grounded during a ground fault on DC side without ESS and PV plant and with $R_g = 50 \Omega$ (S1=OFF, S2=ON), $50 \text{ m}\Omega$ (S1=ON, S2=ON/OFF)



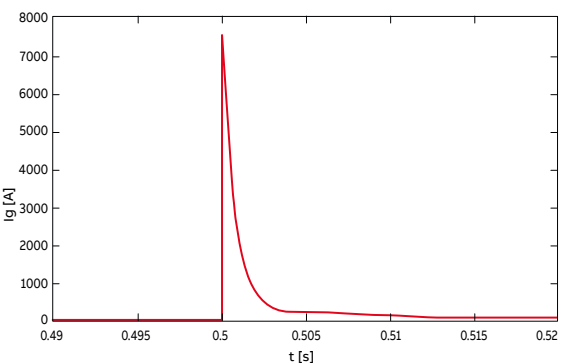
Unlike transformer neutral point grounded systems, in which the fault current I_g flows in the connection between the transformer neutral to ground, in systems with the mid-point grounded, the I_g flows through the ground connection of the DC mid-point. If no ESS and PV plant are present, the converter does not feed the fault, because there is no reclosing path for the DC component of I_g (Figure 3.95): so, it can keep the V_{dc} at the rated value, independent of the R_g value. As a consequence, the 5 different possible cases of Section 3.1 do not apply, and the converter keeps feeding the load.

Figure 3.95 – DC positive pole ground fault current path in systems with the DC mid-point grounded without ESS and PV plant



Thus, the I_g value is only due to the discharge of the capacitance C_{dc} on the DC positive pole, and it decays to zero as shown in Figure 3.96.

Figure 3.96 – Trend of I_g during a ground fault on DC side in systems with the DC mid-point grounded without ESS and PV plant and with $R_g = 50 \text{ m}\Omega$ (S1=ON, S2=ON/OFF)



If ESS or PV plant are present, the steady state behavior is the same: these source, similarly to the converter, feed only the load, because there is no reclosing path for the DC component of the fault current. So, similar results are obtained for the variation of V_{pole+} and V_{pole-} with varying values of the values of R_g (Figures 3.97-3.98).

Figure 3.97 – Trend of the voltage of the DC positive pole V_{pole+} in systems with the DC mid-point grounded during a ground fault on DC side with ESS and $R_g = 50 \Omega$ ($S1=OFF$, $S2=ON$), $50 \text{ m}\Omega$ ($S1=ON$, $S2=ON/OFF$)

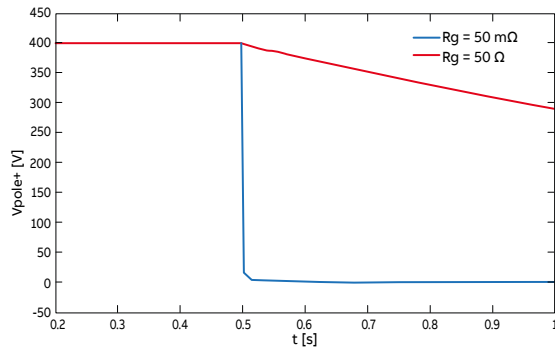
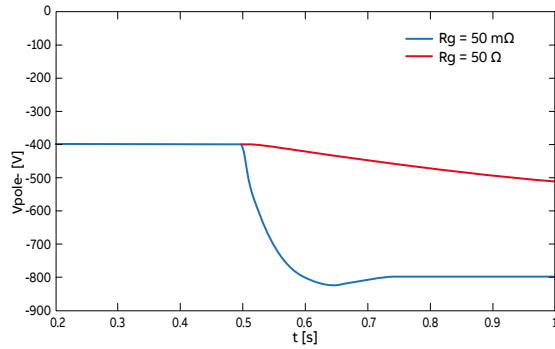


Figure 3.98 – Trend of the voltage of the DC negative pole V_{pole-} in systems with the DC mid-point grounded during a ground fault on DC side with ESS and $R_g = 50 \Omega$ ($S1=OFF$, $S2=ON$), $50 \text{ m}\Omega$ ($S1=ON$, $S2=ON/OFF$)



If ESS is present, the steady state value of the I_g (Figure 3.99) is still zero. However, a transient current I_{dcl} is generated by the ESS at the moment of the fault (Figure 3.100): this

transient contribution to fault current recloses in the negative pole capacitance C_{dc} (Figure 3.101): the I_g peak value is not affected, but the duration of the initial phase of transient is increased.

Figure 3.99 – Trend of I_g during a ground fault on DC side in systems with the DC mid-point grounded with ESS and $R_g = 50 \text{ m}\Omega$ ($S1=ON$, $S2=ON/OFF$)

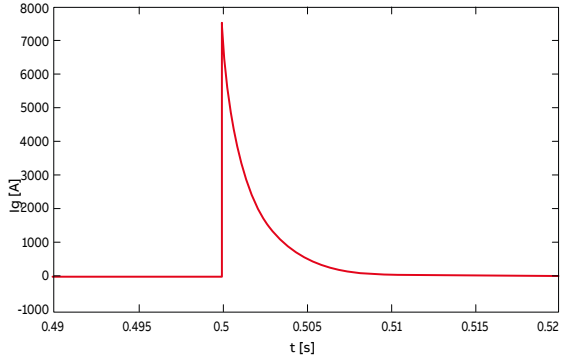


Figure 3.100 – Trend of I_{dcl} during a ground fault on DC side in systems with the DC mid-point grounded with ESS and $R_g = 50 \text{ m}\Omega$ ($S1=ON$, $S2=ON/OFF$)

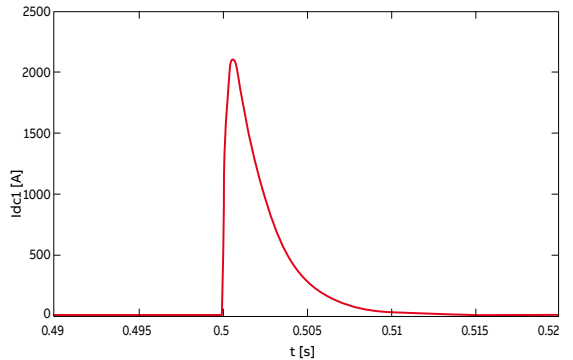
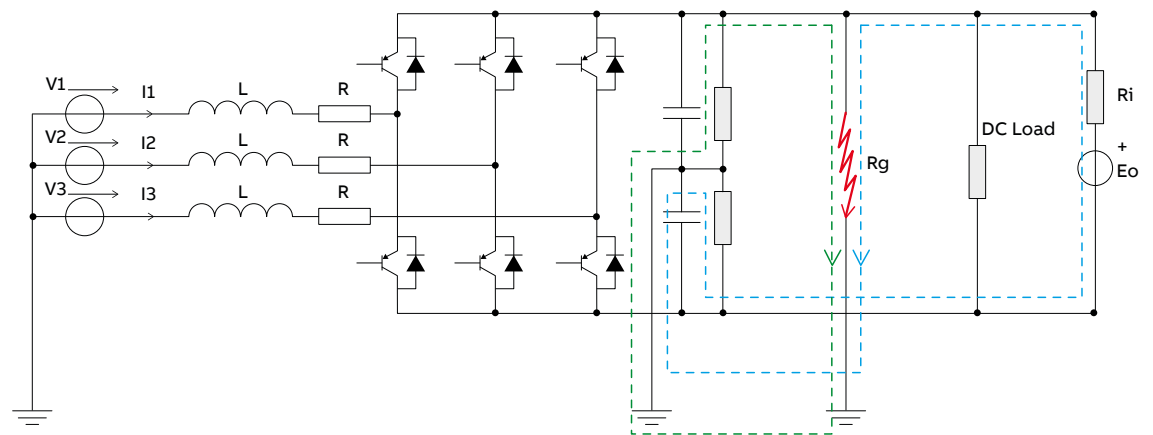


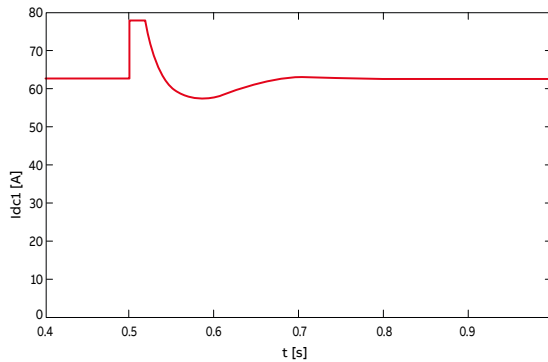
Figure 3.101 – DC positive pole ground fault current path in systems with the DC mid-point grounded with ESS



3. Fault analysis

If a PV plant is present, the same phenomena occur as seen for ESS, but the value of the current I_{dc1} is limited to the maximum current I_{PVmax} : Figure 3.102 shows the transient current, which flows in the negative-side capacitance C_{dc} superimposed to the steady state load current. If both ESS and PV are present, fault current includes the sum of their contributions.

Figure 3.102 – Trend of I_{dc1} during a ground fault on DC side in systems with the DC mid-point grounded with PV plant and $R_g = 50\text{ m}\Omega$ (S1=ON, S2=ON/OFF)



3.3 Short circuit on AC side of the front-end converter

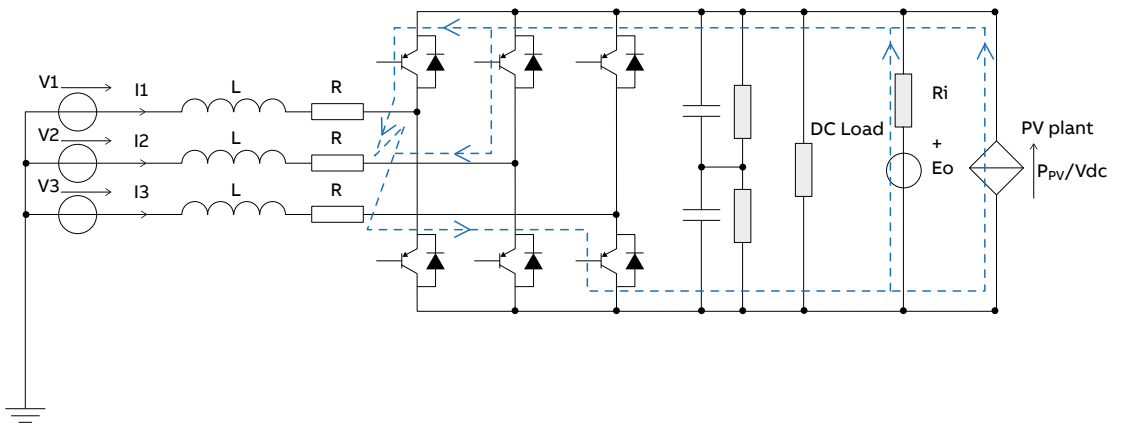
For voltages on the AC side lower than -15% of the nominal value, the converter usually disconnects from the grid.

Instead, when there is a need to deliver to the grid all the currents available in the case of a strong decrease in the voltage (Figure 3.103) to meet LVFRT (Low Voltage Fault Ride Through) requirements, e.g. in order to increase the short-circuit current of the plant, the peak value (without distortion) of the current exchanged with the grid, is given by:

$$[3.14] \quad \hat{I}_{conv_{max}} = \sqrt{2} \cdot \frac{I_{conv_{nom}}}{0.85} = \sqrt{2} \cdot I_{conv_{max}} \approx 1.7 \cdot I_{conv_{nom}}$$

assuming there is constant power.

Figure 3.103 – AC three phase short circuit current path



To preserve the integrity of the semiconductors, all converters limit the instantaneous value of the current, which is usually set at a higher value than the value given by (3.14).

As a consequence, as the grid voltage falls below the prescribed minimum values, the current passes first from a sinusoidal to a trapezoidal shape, then to a squared one as shown in Figures. 3.104-3.105-3.106.

Figure 3.104 – AC current waveform when the power supplied is equal to the maximum value and $V_1 > 85\% V_{1n}$

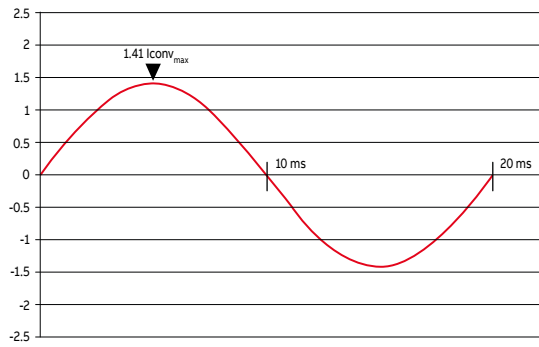


Figure 3.105 - AC current waveform when the power supplied is equal to the maximum value and $V_1 < 85\% V_{1n}$

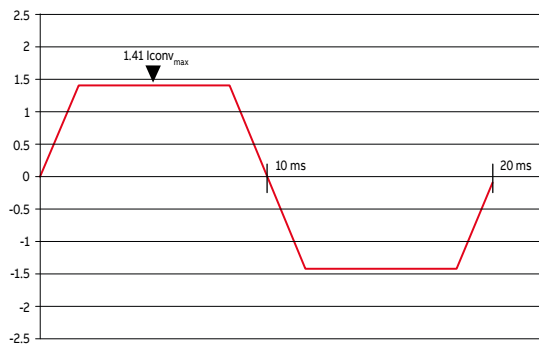
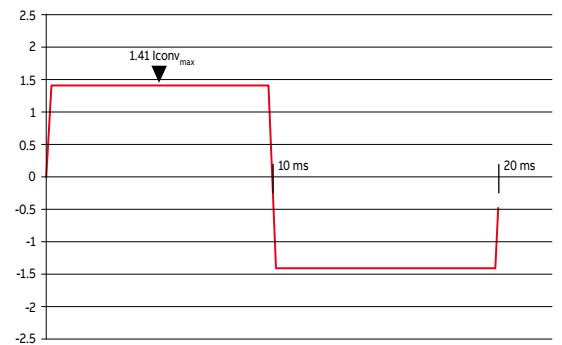


Figure 3.106 - AC current waveform when the power supplied is equal to the maximum value and with a bolted short circuit



Hence, in case of an AC short circuit, the converter supplies a current of 50%-100% more than the rated value. Considering the FEC used in this study, the maximum current supplied during an AC short circuit is:

[3.15]

$$I_{sc_conv} = I_{conv_max} = 1.7 \cdot I_{conv_nom} = 1.7 \cdot 144 = 245A$$

This consideration does not take into account of the presence of capacitors possibly installed on the converter AC side: such capacitors would increase the short circuit current peak due to their discharge. Besides, in the particular case of n-converters installed in parallel, if an AC side short-circuit occurred on the paralleling bar, the fault current would be about n-times the value of in (3.14) and consequently the protective device should have an adequate breaking capacity.

3. Fault analysis

3.4 Ground fault on AC side of the front-end converter

Considering the system shown in Figure 1.5, if a ground fault occurs on AC side of the FEC, the same cases of Section 3.1 may happen, depending on the value of the fault resistance R_g' , both with passive and active LVDC microgrids. In particular, even in this condition, we can distinguish between operation in presence of an “high fault resistance” and a “low fault resistance”.

Moreover, we keep the hypothesis that at first the IGBT self-protection is not considered in order to show ground fault current trend and path and compare them to those in the presence of the self-protection.

3.4.1 High fault resistance R_g' without ESS and PV plant (S1=OFF, S2=ON)

Assuming “high fault resistances” (e.g. $R_g = 50 \Omega$), V_{dc} is maintained at the rated value: thus, the ground fault is “seen” by the FEC as an “additional DC load”. Indeed, even the FEC control still works in linear modulation with a current increase during the fault (Figures 3.107a-b).

Nevertheless, unlike the DC load R_L (whose applied voltage remains constant at V_{dc} value), the “additional DC load” R_g' has an applied voltage that varies between V_{dc} value and zero, as shown in Figure (3.108), due to the switching effect of the IGBT of the first leg of the cathodic star.

Figure 3.107a – Trend of I_{sw1} current during a ground fault on AC side in systems with the DC negative pole grounded without ESS and PV plant and with $R_g' = 50 \Omega$

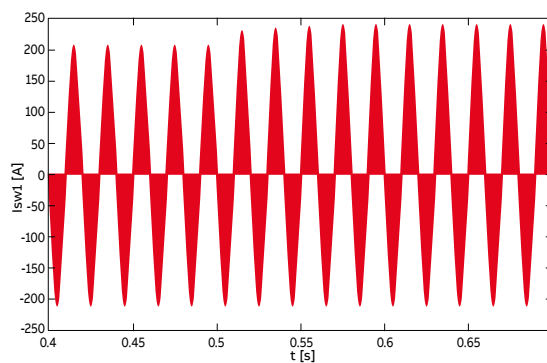


Figure 3.107b – Trend of I_{sw2} current during a ground fault on AC side in systems with the DC negative pole grounded without ESS and PV plant and with $R_g' = 50 \Omega$

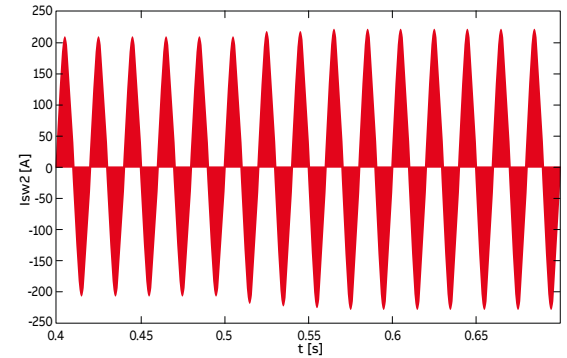
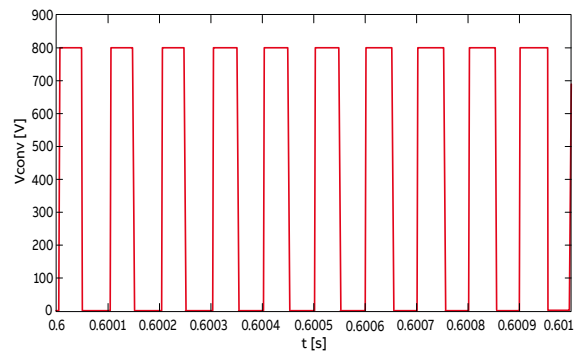


Figure 3.108 – Trend of the voltage at AC converter terminal V_{conv} in systems with the DC negative pole grounded without ESS and PV plant and with $R_g' = 50 \Omega$



The ground fault power is supplied by the AC grid by means of an AC current increase (Figure 3.109), which is transformed into a zero-sequence current by the converter and injected into the fault.

In particular, the DC component of I_g' recloses through the FEC lower terminal and the electronic components as shown in Figure 3.110.

Figure 3.109 - Trend of I_{ac1} current during a ground fault on AC in systems with the DC negative pole grounded without ESS and PV plant and with $R_g' = 50 \Omega$

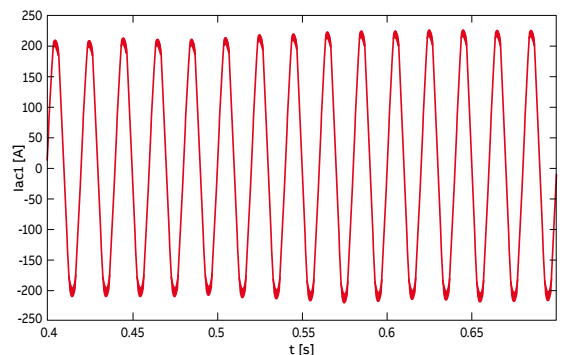
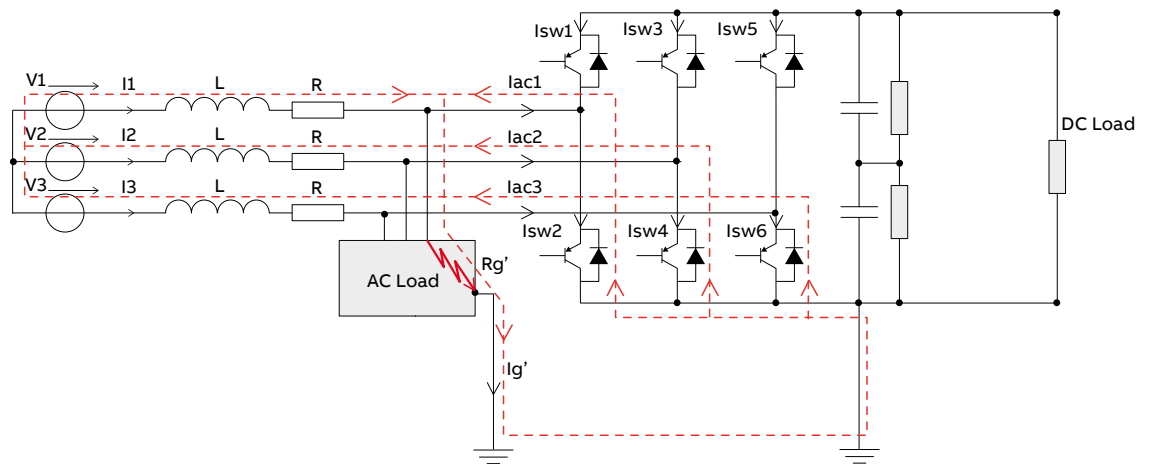


Figure 3.110 – AC ground fault current path without ESS and PV plant in systems with the DC negative pole grounded with $R_g' = 50 \Omega$



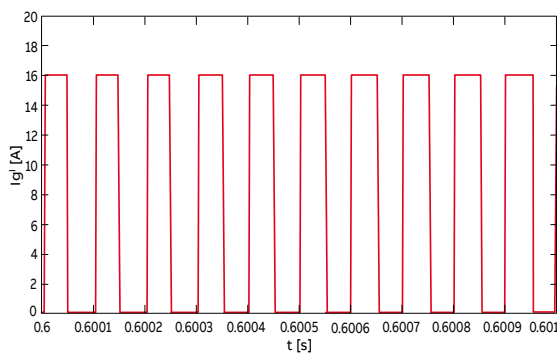
Because of the voltage trend (Figure 3.108) applied to the fault resistance, the fault current (Figure 3.111) has a DC component (8A) and the harmonics at switching and multiple switching frequency. In particular, unlike the DC load current whose values is equal to V_{dc}/R_L , the DC component of the fault current is equal to:

[3.16]

$$I'_{gdc} = \frac{V_{dc}}{2 \cdot R_g'} = \frac{800}{2 \cdot 50} = 8A$$

where $V_{dc}/2$ is also the average value of V_{conv} (Figure 3.108).

Figure 3.111 – Trend of I_g' during a ground fault on AC side in systems with the DC negative pole grounded without ESS and PV plant and $R_g' = 50 \Omega$



As it can be seen in Figure 3.110, in the “additional load” $R_{g'}$ there are the sum of the three DC current components that flows in all the AC phases:

[3.17]

$$I'_{gdc} = -I_{ac1_dc} - I_{ac2_dc} - I_{ac3_dc} = 3 + 2 + 3 = 8A$$

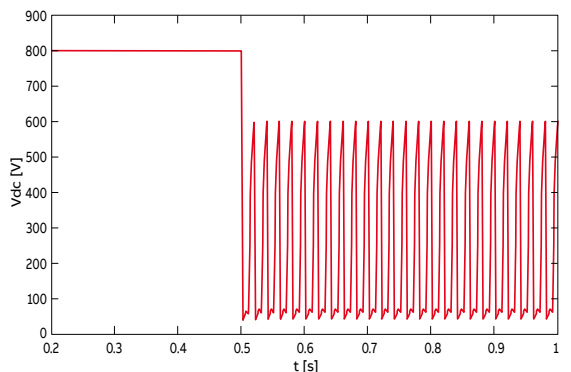
As a result, the fault current DC component on AC side flows not only in the faulty phase, but also in the healthy ones through the transformer windings:

this may create further problems, for example the transformer core saturation. With high faults resistances, since the FEC control is able to maintain the DC-Bus voltage V_{dc} at its rated value, the DC capacitors discharge current is zero. Even considering the IGBT block, since the ground fault current flows through the freewheeling diodes of the anodic star, such current cannot be eliminated. Hence, a suitable residual current device, able to detect ground fault currents with DC components, has to be installed on AC side to interrupt such currents.

3.4.2 Low fault resistance R_g' without ESS and PV plant (S1=ON, S2=ON/OFF)

Considering “low fault resistances” (e.g. $R_g = 50 m\Omega$), the FEC control is no longer able to maintain the V_{dc} at the rated value (Figure 3.112).

Figure 3.112 - Trend of V_{dc} voltage during a ground fault on AC in systems with the DC negative pole grounded without ESS and PV plant and with $R_g' = 50 m\Omega$



With reference to Figure 3.112, as soon as the AC ground fault occurs ($t = 0.5s$), there is a sudden discharge of DC capacitors (Figure 3.113)⁹.

⁹ The DC component is zero, since the areas under the positive I_{cap} values are equal to the areas under the negative values.

3. Fault analysis

As a result the V_{dc} drops. The C_{dc} discharge current flows into the fault passing through the IGBT of the first leg of the cathodic star (Figure 3.114).

When the discharge is over, the FEC works as a diode rectifier and the V_{dc} raises again reaching the value corresponding to the power delivered to the DC load. Then, a new capacitor discharge happens and the previous FEC behavior occurs.

The discharge current appears in the fault current I_g' (Figure 3.115) and in the current I_{act} at the FEC terminal of faulty phase (Figure 3.116).

Figure 3.113 – Trend of the DC capacitor current I_{cap} during a ground fault on AC side in systems with the DC negative pole grounded without ESS and PV plant and with $R_g' = 50\text{ m}\Omega$

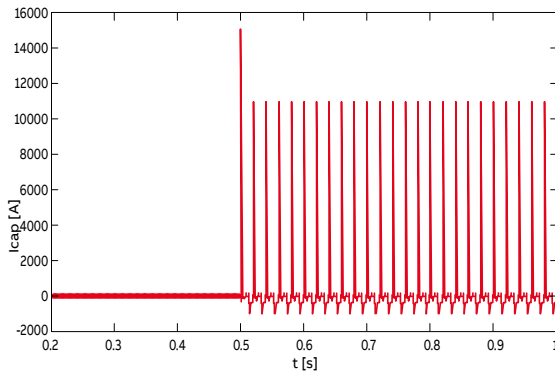


Figure 3.114 – Trend of I_{sw1} current during a ground fault on AC side in systems with the DC negative pole grounded without ESS and PV plant and with $R_g' = 50\text{ m}\Omega$

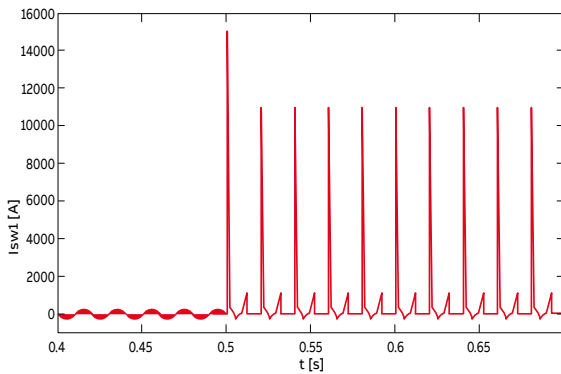


Figure 3.115 – Trend of I_g' during a ground fault on AC side in systems with the DC negative pole grounded without ESS and PV plant and $R_g' = 50\text{ m}\Omega$

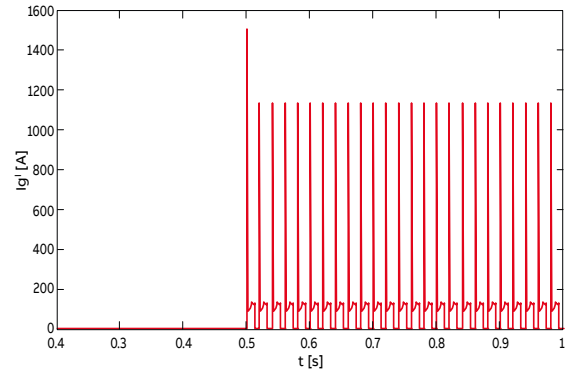
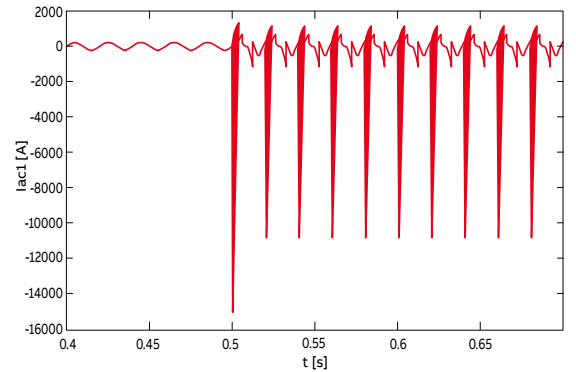


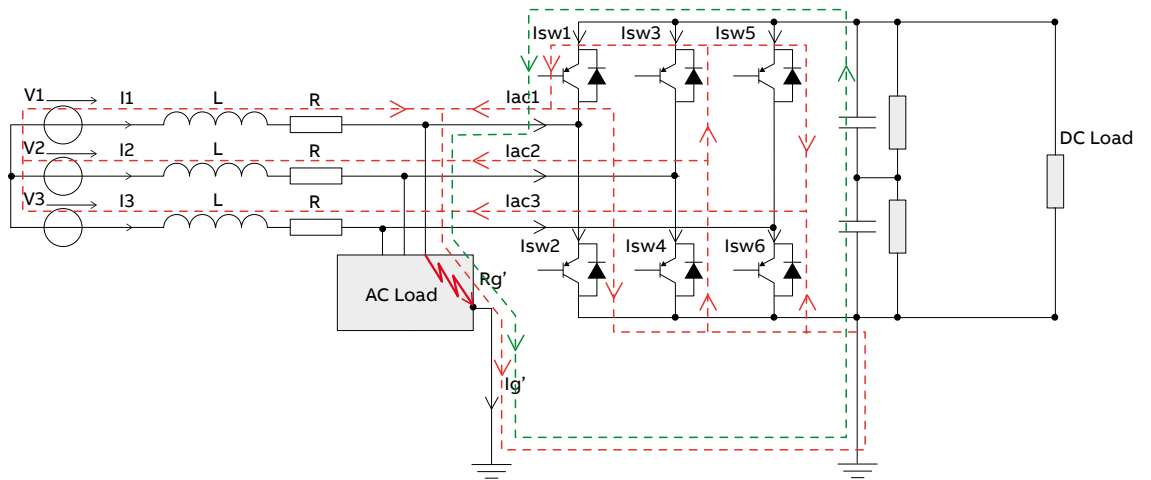
Figure 3.116 – Trend of I_{act} during a ground fault on AC side in systems with the DC negative pole grounded without ESS and PV plant and with $R_g' = 50\text{ m}\Omega$



As Figure 3.115 shows, I_g' still has a DC component (756A) equal to the ratio between the V_{conv} average value and R_g' , but now the average value of V_{conv} is no longer equal to $V_{dc}/2$.

In particular, such DC component of I_g' still flows into the converter through the lower terminal and the electronic components as shown in Figure 3.117.

Figure 3.117 – AC ground fault current path in systems with the DC negative pole grounded without ESS and PV plant with $R_g' = 50 \text{ m}\Omega$



As Figure 3.117 shows, the fault current DC component on AC side still flows not only in the faulty phase, but also in the healthy ones through the transformer windings. The DC component of the ground fault current is still the sum of the DC component of AC currents. With $R_g' = 50 \text{ m}\Omega$, such sum is equal to:
As a result, AC currents (Figures 3.118a-c) have high distortion (not only with DC component, but also with low-frequency harmonics).

[3.18]

$$I'_{g_dc} = -(I_{ac1_dc} + I_{ac2_dc} + I_{ac3_dc}) = -(-170 - 68 - 518) = 756 \text{ A}$$

AC currents (Figures 3.118a-c) have high distortion (not only with DC component, but also with low-frequency harmonics).

Figure 3.118 - Trend of AC side currents without AC load currents during a ground fault on AC side in systems with the DC negative pole grounded without ESS and PV plant and with $R_g' = 50 \text{ m}\Omega$

Figure 3.118a

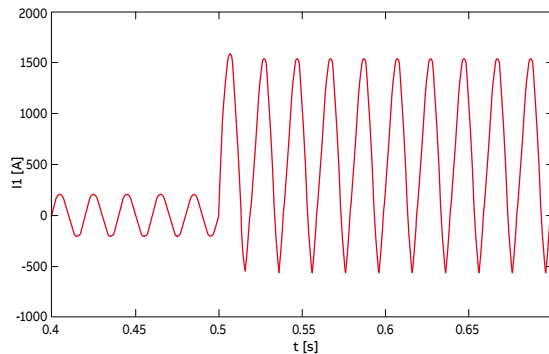


Figure 3.118b

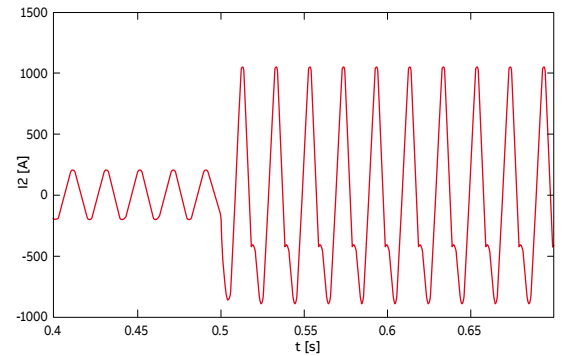
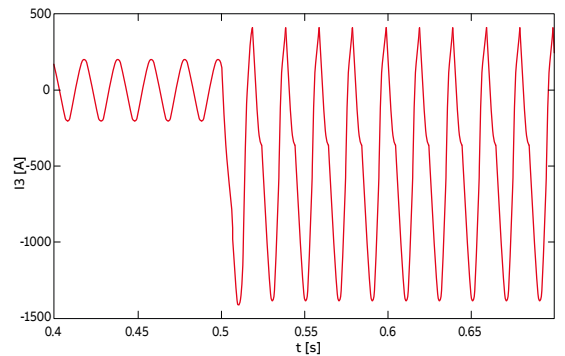


Figure 3.118c



Even considering the embedded IGBT block, the fault current I_g' remains high since, despite the current in the IGBT of the first leg of the chatodic star is interrupted, the fault current still flows through the freewheeling diodes of the anodic star towards the transformer windings (Figure 3.117).

3. Fault analysis

3.4.3 High fault resistance R_g' with ESS and PV plant (S1=OFF, S2=ON)

ESS and PV plant don't feed the fault for high fault resistances, as it can be seen by the trend of I_g' in Figure 3.119: such trend is equal to the one in Figure 3.111. Therefore, the ground fault power is still supplied by the AC grid.

Nevertheless, now, the AC current at FEC terminals decreases (Figure 3.120), since the DC load and the "additional DC load" are partially fed by ESS and PV plant.

Figure 3.119 – Trend of I_g' during a ground fault on AC side in systems with the DC negative pole grounded with ESS, PV plant and $R_g' = 50 \Omega$

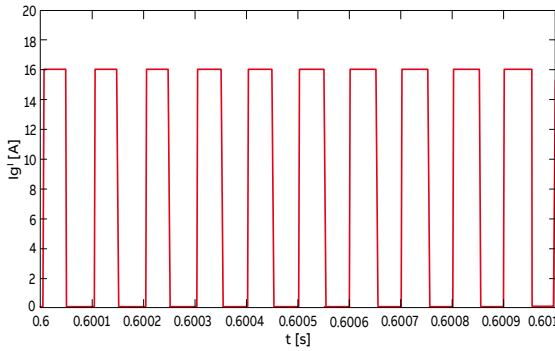
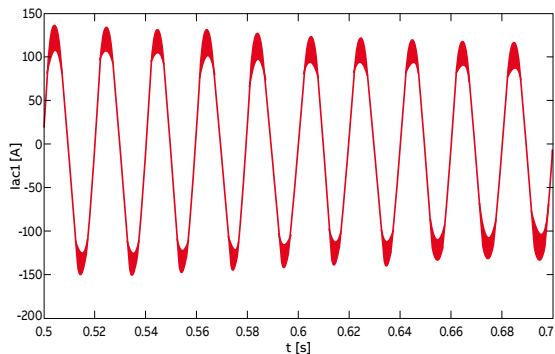


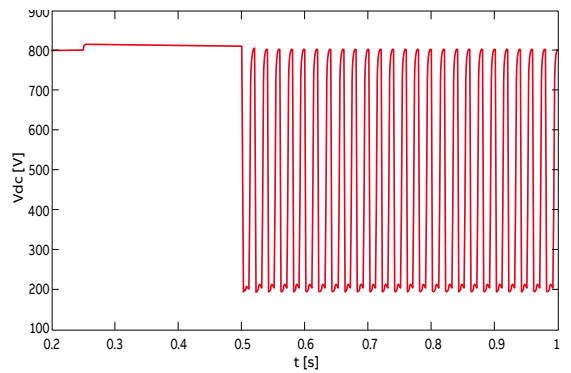
Figure 3.120 - Trend of I_{ac1} current during a ground fault on AC in systems with the DC negative pole grounded with ESS, PV plant and with $R_g' = 50 \Omega$



3.4.4 Low fault resistance R_g' with ESS and PV plant (S1=ON, S2=ON/OFF)

ESS and PV plant maintain the V_{dc} at a higher value (Figure 3.121).

Figure 3.121 - Trend of V_{dc} voltage during a ground fault on AC in systems with the DC negative pole grounded with ESS, PV plant and $R_g' = 50 \text{ m}\Omega$



In particular, like in DC fault condition with low fault resistance, ESS and PV plant feed both the fault and the load, while the FEC feeds only the fault. With reference to Figure 3.122, assuming $R_g' = 50 \text{ m}\Omega$, for the DC component:

[3.19]

$$I_{dc1} = \frac{V_{dc}}{R_L} - (-I_{convdc1}) = \frac{384}{7.1} - (-2104) = 2158A$$

[3.20]

$$I_g' = -I_{convdc1} - I_{convdc2} = -(-2104) - (-578) = 2682A$$

As it can be seen from Figure 3.122 for low fault resistances, the DC component of $I_{convdc1}$ (Figure 3.123) flows into the upper terminal (instead of flowing out as in the normal operation) in a dual manner compared to what happens in the systems with the transformer neutral point grounded where the DC component of $I_{convdc2}$ flows out of the lower terminal (instead of flowing into as in normal operation).

Figure 3.122 – AC ground fault current path in systems with the DC negative pole grounded with ESS, PV plant and low fault resistance

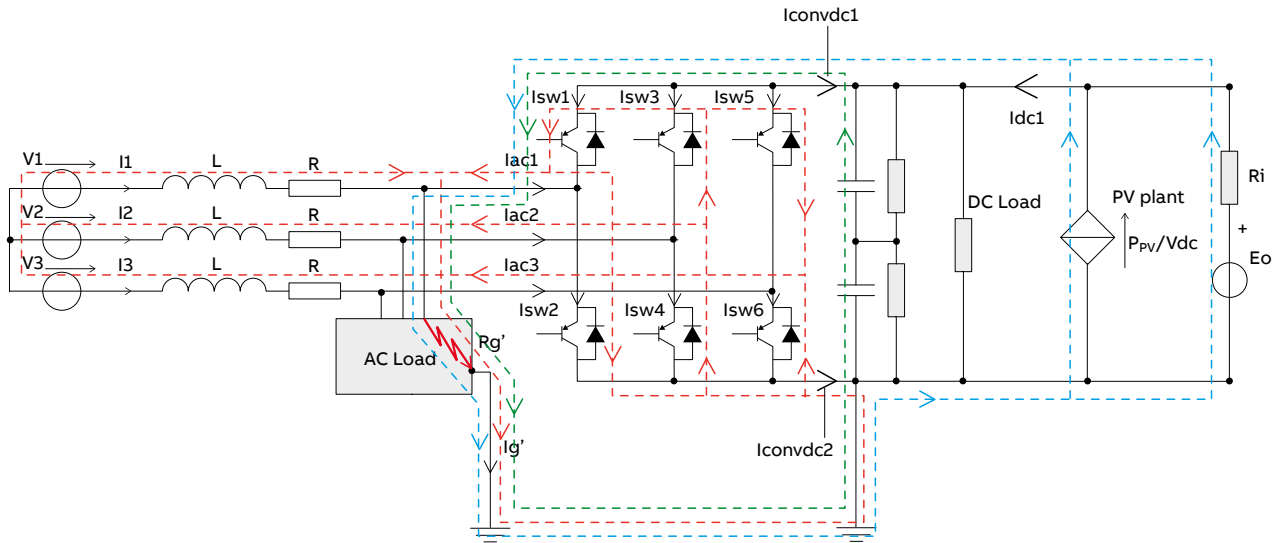


Figure 3.123 – Trend of $I_{convdc1}$ during a ground fault on AC side in systems with the DC negative pole grounded with ESS, PV plant and $R_g' = 50\text{ m}\Omega$

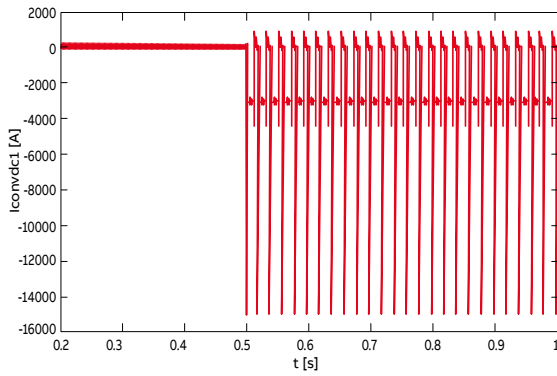


Figure 3.125 – Trend of I_{dc1} during a ground fault on AC side in systems with the DC negative pole grounded with ESS, PV plant and $R_g' = 50\text{ m}\Omega$

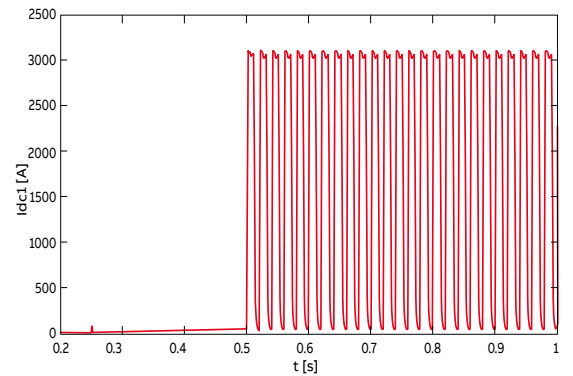


Figure 3.124 – Trend of $I_{convdc2}$ during a ground fault on AC side in systems with the DC negative pole grounded with ESS, PV plant and $R_g' = 50\text{ m}\Omega$

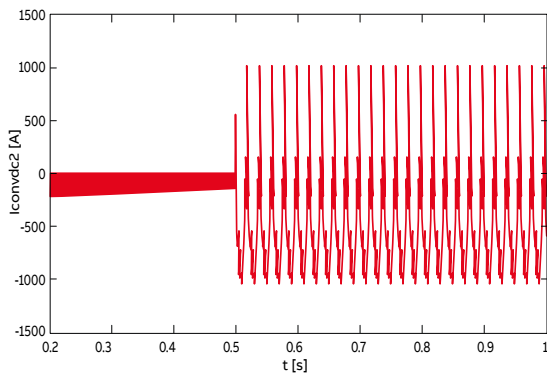
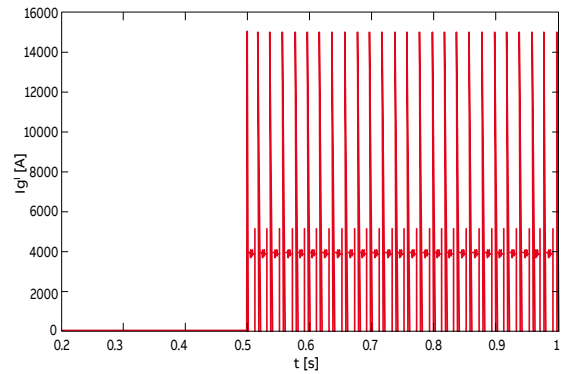


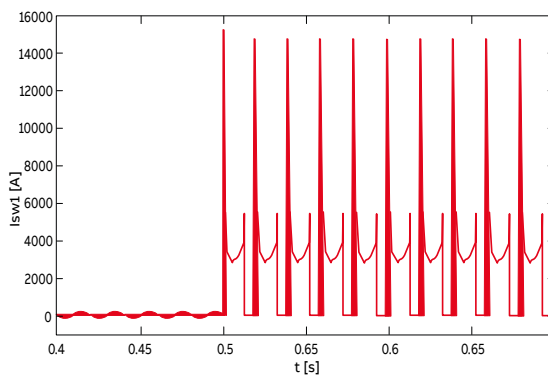
Figure 3.126 – Trend of $I_{g'}$ during a ground fault on AC side in systems with the DC negative pole grounded with ESS, PV plant and $R_g' = 50\text{ m}\Omega$



3. Fault analysis

ESS and PV plant force a current which is always positive in the IGBT of the first leg of the cathodic star (Figure 3.127). This current has such a value that jeopardizes the electronic component integrity.

Figure 3.127 – Trend of I_{sw1} during a ground fault on AC side in systems with the DC negative pole grounded with ESS, PV plant and $R_g' = 50 \text{ m}\Omega$



Taking into account the IGBT block, the I_{sw1} is interrupted preventing the ESS contribution to the ground fault current. However, such current still has a high value due to the fault power supplied by the AC grid, similarly to what happens when considering a passive LVDC microgrid.

To sum up, even in case of a ground fault on AC side, the high fault resistance is “seen” by the FEC as an “additional DC load” to which a voltage with $V_{dc}/2$ average value is applied. For low fault resistance value, since the V_{dc} is no longer maintained fixed at its nominal value, there are repetitive charge-discharge cycles of the DC capacitors that create high fault current peaks. Like in faults on DC side, ESS and PV plant start to feed the fault when the V_{dc} becomes lower than a particular value depending on the fault resistance. Nevertheless, in dual manner compared to faults on DC side, now the generators start to feed the fault when the current of the FEC upper terminal becomes negative, which means that such current flows into the terminal instead of flowing out like in normal operation.

4. DC fault protection – The ABB offer

The preferred method for DC fault protection is the use of circuit breakers: ABB offers the following types of air circuit breakers, molded-case circuit breakers, and miniature circuit breakers for the DC overcurrent protection of active LVDC microgrids¹⁰.

The minimum operational voltage (supplied by the dedicated low voltage measuring module PR120/LV) is 24V DC.

Thanks to their unique technology, the trip units type PR122/DC-PR123/DC allow the protection functions already available in alternating current to be carried out. The Emax DC range maintains the same electrical and mechanical accessories in common with the Emax range for alternating current applications.

4.1 Air circuit breakers

Air circuit breakers of Emax series comply with the Std. IEC 60947-2 and equipped with DC electronic trip units type PR122/DC and PR123/DC.

They have an application field ranging from 800A (with E2) to 5000A (with E6) and breaking capacities from 35kA to 100kA (at 500V DC).

By connecting three breaking poles in series, it is possible to achieve the rated voltage of 750V DC, while with four poles in series the limit raises to 1000V DC.



¹⁰ As regards the modality of pole connection according to the network type and to the service voltage, please refer to the tables shown in the QT5 "ABB circuit breakers for direct current applications"-1SDC007104G0202.

| | | E2 | | E3 | | E4 | | E6 |
|--|----------------------|------|------|------|------|------|------|------|
| Rated service voltage Ue | [V] | 1000 | | 1000 | | 1000 | | 1000 |
| Rated impulse withstand voltage Uimp | [kV] | 12 | | 12 | | 12 | | 12 |
| Rated insulation voltage Ui | [V] | 1000 | | 1000 | | 1000 | | 1000 |
| Poles | [Nr.] | 3/4 | | 3/4 | | 3/4 | | 3/4 |
| Rated uninterrupted current Iu | | B | N | N | H | S | H | H |
| | [A] | 800 | | 800 | | | | |
| | [A] | 1000 | | 1000 | | | | |
| | [A] | 1250 | | 1250 | | | | |
| | [A] | 1600 | 1600 | 1600 | 1600 | 1600 | | |
| | [A] | | | 2000 | 2000 | 2000 | | |
| | [A] | | | 2500 | 2500 | 2500 | | |
| | [A] | | | | | 3200 | 3200 | 3200 |
| | [A] | | | | | | | 4000 |
| | [A] | | | | | | | 5000 |
| Rated short-time withstand current for (0.5s) Icw | [kA] | | | | | | | |
| | 500V DC (III) | 35 | 50 | 60 | 65 | 75 | 100 | 100 |
| | 750V DC (III) | 25 | 25 | 40 | 40 | 65 | 65 | 65 |
| | 750V DC (III) | 25 | 40 | 50 | 50 | 65 | 65 | 65 |
| | 1000V DC (IV) | 25 | 25 | 35 | 40 | 50 | 65 | 65 |
| Utilization category (IEC 60947-2) | | B | B | B | B | B | B | B |
| Isolation behaviour | | ■ | | ■ | | ■ | | ■ |
| Versions | | F-W | | F-W | | F-W | | F-W |

4. DC fault protection – The ABB offer

4.2 Molded-case circuit breakers

4.2.1 SACE Tmax XT molded-case circuit breakers for direct current applications

ABB offers the new series of molded-case circuit breakers SACE Tmax XT up to 800A for the protection of the DC installations in accordance with both IEC (up to 750Vdc) and UL (up to 600Vdc) Standards. The following circuit breakers are available:

- XT1 160 and XT3 250 IEC equipped with thermomagnetic trip units TMD with adjustable thermal threshold ($I_1 = 0.7..1 \times I_n$) and fixed magnetic threshold ($I_3 = 10 \times I_n$);
- XT1 125 and XT3 225 UL equipped with thermomagnetic trip units TMF with both fixed thermal and fixed magnetic thresholds ($I_3 = 10 \times I_n$);
- XT2 160 and XT4 160/250 IEC equipped with thermomagnetic trip units TMD and TMA with adjustable thermal threshold ($I_1 = 0.7..1 \times I_n$) and magnetic threshold I_3 adjustable in the range $8..10 \times I_n$ for 40A, $6..10 \times I_n$ for 50A and $5..10 \times I_n$ for $I_n \geq 63A$.

- XT2 125 and XT4 250 UL equipped with thermomagnetic trip units TMF and TMA with adjustable thermal threshold ($I_1 = 0.7..1 \times I_n$) and magnetic threshold I_3 adjustable in the range $5..10 \times I_n$ for $I_n \geq 80A$.
- XT5 400/630 and XT6 800 IEC equipped with thermomagnetic trip units TMA with adjustable thermal threshold ($I_1 = 0.7..1 \times I_n$) and magnetic threshold I_3 adjustable in the range $5..10 \times I_n$.
- XT5 400/600 and XT6 800 UL equipped with thermomagnetic trip units TMA with adjustable thermal threshold ($I_1 = 0.7..1 \times I_n$) and magnetic threshold I_3 adjustable in the range $5..10 \times I_n$.



IEC

| Size | | XT1 | | | | | XT2 | | | | | XT3 | |
|--|----------|-------------------------------|----------|----------|----------|----------|------------------------------|----------|----------|----------|----------|----------------|----------|
| Rated uninterrupted current | [A] | 160 | | | | | 160 | | | | | 250 | |
| Poles | [No.] | 3, 4 | | | | | 3, 4 | | | | | 3, 4 | |
| Rated service voltage, Ue | (DC) [V] | 500 | | | | | 500 | | | | | 500 | |
| Rated insulation voltage, Ui | (DC) [V] | 800 | | | | | 1000 | | | | | 800 | |
| Rated impulse withstand voltage Uimp | [kV] | 8 | | | | | 8 | | | | | 8 | |
| Versions | | Fixed, Plug-in ⁽²⁾ | | | | | Fixed, Withdrawable, Plug-in | | | | | Fixed, Plug-in | |
| Breaking capacities according to IEC 60947-2 | | B | C | N | S | N | N | S | H | L | V | N | S |
| Rated ultimate short-circuit breaking capacity, Icu | | | | | | | | | | | | | |
| Icu @ 250V (DC) 2-pole in series | [kA] | 18 | 25 | 36 | 50 | 70 | 36 | 50 | 70 | 85 | 100 | 36 | 50 |
| Icu @ 500V (DC) 2-pole in series | [kA] | - | - | - | - | - | - | - | - | - | - | - | - |
| Icu @ 500V (DC) 3-pole in series ⁽¹⁾ | [kA] | 18 | 25 | 36 | 50 | 70 | 36 | 50 | 70 | 85 | 100 | 36 | 50 |
| Icu @ 750V (DC) 3-pole in series | [kA] | - | - | - | - | - | - | - | - | - | - | - | - |
| Rated service short-circuit breaking capacity, Ics | | | | | | | | | | | | | |
| Ics @ 250V (DC) 2-pole in series | [kA] | 100% | 100% | 100% | 100% | 75% | 100% | 100% | 100% | 100% | 100% | 100% | 75% |
| Ics @ 500V (DC) 2-pole in series | [kA] | - | - | - | - | - | - | - | - | - | - | - | - |
| Ics @ 500V (DC) 3-pole in series ⁽¹⁾ | [kA] | 100% | 100% | 100% | 100% | 75% | 100% | 100% | 100% | 100% | 100% | 100% | 75% |
| Ics @ 750V (DC) 3-pole in series | [kA] | - | - | - | - | - | - | - | - | - | - | - | - |

⁽¹⁾ XT1: a 4 poles in series connection is required to be used in 500 V DC installations.

⁽²⁾ XT1 plug-in $I_n \max = 125A$



IEC

| Size | | XT4 | | | | | | XT5 | | | | | | XT6 | | |
|--|----------|------------------------------|------|------|------|------|------|------------------------------|------|------|------|-------------------|--------------------|---------------------|------|-----|
| Rated uninterrupted current | [A] | 160/250 | | | | | | 400 / 630 | | | | | | 800 | | |
| Poles | [No.] | 3, 4 | | | | | | 3, 4 | | | | | | 3, 4 | | |
| Rated service voltage, Ue | (DC) [V] | 750 | | | | | | 750 | | | | | | 750 | | |
| Rated insulation voltage, Ui | (DC) [V] | 1000 | | | | | | 1,000 | | | | | | 1,000 | | |
| Rated impulse withstand voltage Uimp | [kV] | 8 | | | | | | 8 | | | | | | 8 | | |
| Versions | | Fixed, Withdrawable, Plug-in | | | | | | Fixed, Withdrawable, Plug-in | | | | | | Fixed, Withdrawable | | |
| Breaking capacities according to IEC 60947-2 | | | | | | | | | | | | | | | | |
| Rated ultimate short-circuit breaking capacity, Icu | | | | | | | | | | | | | | | | |
| Icu @ 250V (DC) 2-pole in series | [kA] | 36 | 50 | 70 | 85 | 100 | 100 | 25 | 35 | 50 | 70 | 85 | 100 | 35 | 50 | 70 |
| Icu @ 500V (DC) 2-pole in series | [kA] | 36 | 50 | 70 | 85 | 100 | 100 | 25 | 35 | 50 | 70 | 85 | 100 | 20 | 35 | 50 |
| Icu @ 500V (DC) 3-pole in series ⁽¹⁾ | [kA] | 36 | 50 | 70 | 85 | 100 | 100 | - | - | - | - | - | - | - | - | - |
| Icu @ 750V (DC) 3-pole in series | [kA] | - | - | - | - | 50 | 70 | - | - | - | - | 85 ⁽¹⁾ | 100 ⁽¹⁾ | 18 | 24 | 36 |
| Rated service short-circuit breaking capacity, Ics | | | | | | | | | | | | | | | | |
| Ics @ 250V (DC) 2-pole in series | [kA] | 100% | 100% | 100% | 100% | 100% | 100% | 100% | 100% | 100% | 100% | 100% | 100% | 100% | 100% | 50% |
| Ics @ 500V (DC) 2-pole in series | [kA] | 100% | 100% | 100% | 100% | 100% | 100% | 100% | 100% | 100% | 100% | 100% | 100% | 100% | 100% | 50% |
| Ics @ 500V (DC) 3-pole in series ⁽¹⁾ | [kA] | 100% | 100% | 100% | 100% | 100% | 100% | - | - | - | - | - | - | - | - | - |
| Ics @ 750V (DC) 3-pole in series | [kA] | - | - | - | - | 100% | 100% | - | - | - | - | 100% | 100% | 100% | 100% | 75% |

⁽¹⁾ Power supply only from the top



UL

| Molded case circuit-breakers (MCCB) | | XT1 | | | | | XT2 | | | | | XT3 | | | | |
|--|-----------------------------|------------------------------|----|----|--|----|---------------------------------|----|----|----|----|-------------------------------|----|--|--|--|
| Frame Size | [A] | 125 | | | | | 125 | | | | | 225 | | | | |
| Poles | [No.] | 3, 4 | | | | | 3, 4 | | | | | 3, 4 | | | | |
| Rated voltage | (DC) [V] | 500 | | | | | 500 | | | | | 500 | | | | |
| Versions | | Fixed, Plug-in | | | | | Fixed, Withdrawable, Plug-in | | | | | Fixed, Plug-in | | | | |
| Interrupting ratings | | | | | | | | | | | | | | | | |
| | | N | S | H | | N | S | H | L | V | X | N | S | | | |
| 250 V (DC) 2 poles in series | [kA] | 35 | 42 | 50 | | 35 | 50 | 65 | 75 | 85 | 85 | 25 | 35 | | | |
| 500 V (DC) 2 poles in series | [kA] | - | - | - | | - | - | - | - | - | - | - | - | | | |
| 500 V (DC) 3 poles in series | [kA] | - | - | - | | 35 | 50 | 65 | 75 | 85 | 85 | 25 | 35 | | | |
| 500 V (DC) 4 poles in series | [kA] | 35 | 50 | 50 | | - | - | - | - | - | - | - | - | | | |
| 600 V (DC) 3 poles in series | [kA] | - | - | - | | - | - | - | - | - | - | - | - | | | |
| Mechanical life | [No. Operations] | 25000 | | | | | 25000 | | | | | 25000 | | | | |
| | [No. Hourly operations] | 240 | | | | | 240 | | | | | 240 | | | | |
| Dimensions | Fixed 3 poles | [76.2x70x130]/[3x2.75x5.12] | | | | | [90x82.5x130]/[3.54x3.25x5.12] | | | | | [105x70x150]/[4.13x2.75x5.90] | | | | |
| (Width x Depth x Height) | 4 poles | [101.6x70x130]/[4x2.75x5.12] | | | | | [120x82.5x130]/[4.72x3.25x5.12] | | | | | [140x70x150]/[5.51x2.75x5.90] | | | | |
| Weight | Fixed 3/4 poles | [1.1-2.43]/[1.4-3.07] | | | | | [1.2-2.65]/[1.6-3.53] | | | | | [1.7-3.37]/[2.1-4.63] | | | | |
| | Plug-in (EF) 3/4 poles | [2.21-4.87]/[2.82-6.22] | | | | | [2.54-5.60]/[3.27-7.21] | | | | | [3.24-7.14]/[4.1-9.04] | | | | |
| | Withdrawable (EF) 3/4 poles | - | | | | | [3.32-7.32]/[4.04-8.91] | | | | | - | | | | |
| Trip units for power distribution | | | | | | | | | | | | | | | | |
| TMF | | ■ | | | | | ■ | | | | | ■ | | | | |
| TMA | | - | | | | | ■ | | | | | - | | | | |
| TMG | | - | | | | | - | | | | | - | | | | |



UL

| Molded case circuit-breakers (MCCB) | | XT4 | | | | | | XT5 | | | | | | XT6 | | |
|--|-----------------------------|--------------------------------|----|----|----|-----|-----|--------------------------------|----|----|-----|-----|-----|------------------------------------|----|----|
| Frame Size | [A] | 250 | | | | | | 400-600 | | | | | | 800 | | |
| Poles | [No.] | 3, 4 | | | | | | 3, 4 | | | | | | 3, 4 | | |
| Rated voltage | (DC) [V] | 600 | | | | | | 600 | | | | | | 600 | | |
| Versions | | Fixed, Withdrawable, Plug-in | | | | | | Fixed, Withdrawable, Plug-in | | | | | | Fixed, Withdrawable | | |
| Interrupting ratings | | | | | | | | | | | | | | | | |
| | | N | S | H | L | V | X | N | S | H | L | V | X | N | S | H |
| 250 V (DC) 2 poles in series | [kA] | 35 | 42 | 50 | 85 | 100 | 100 | 35 | 50 | 70 | 100 | 100 | 100 | 35 | 50 | 70 |
| 500 V (DC) 2 poles in series | [kA] | - | - | - | - | - | - | 25 | 35 | 50 | 70 | 100 | 100 | 35 | 35 | 50 |
| 500 V (DC) 3 poles in series | [kA] | - | - | - | - | - | - | - | - | - | - | - | - | - | - | - |
| 500 V (DC) 4 poles in series | [kA] | - | - | - | - | - | - | - | - | - | - | - | - | - | - | - |
| 600 V (DC) 3 poles in series | [kA] | 35 | 50 | 65 | 75 | 85 | 85 | 16 | 25 | 35 | 50 | 70 | 70 | 20 | 20 | 35 |
| Mechanical life | [No. Operations] | 25000 | | | | | | 20000 | | | | | | 20000 | | |
| | [No. Hourly operations] | 240 | | | | | | 60 | | | | | | 60 | | |
| Dimensions | Fixed 3 poles | [105x82.5x160]/[4.13x3.25x6.3] | | | | | | [140x103x205]/[5.51x4.05x8.07] | | | | | | [210x103.5x268]/[8.27x4.07x10.55] | | |
| (Width x Depth x Height) | 4 poles | [140x82.5x160]/[5.51x3.25x6.3] | | | | | | [186x103x205]/[7.32x4.05x8.07] | | | | | | [280x103.5x268]/[11.02x4.07x10.55] | | |
| Weight | Fixed 3/4 poles | [2.5-5.51]/[3.5-7.72] | | | | | | [2.5-5.51]/[3.5-7.72] | | | | | | - | | |
| | Plug-in (EF) 3/4 poles | [4.19-9.24]/[5.52-12.17] | | | | | | - | | | | | | - | | |
| | Withdrawable (EF) 3/4 poles | [5-11.02]/[6.76-14.90] | | | | | | - | | | | | | - | | |
| Trip units for power distribution | | | | | | | | | | | | | | | | |
| TMF | | ■ | | | | | | - | | | | | | - | | |
| TMA | | ■ | | | | | | ■ | | | | | | ■ | | |
| TMG | | - | | | | | | ■ | | | | | | - | | |

4. DC fault protection – The ABB offer

4.2.2 Tmax T molded-case circuit breakers for applications up to 1000V DC

Tmax T solutions provides the circuit breakers T4, T5 and T6 for direct current applications up to 1000V.

These circuit breakers are available in four-pole version with TMD or TMA thermomagnetic trip units. These circuit breakers are available in fixed version and comply with all accessories except for the residual current release.

| | | T4 | T5 | T6 |
|---|------|------------------|------------------------------------|------------------|
| Rated uninterrupted current I _u | [A] | 250 | 400/630 | 630/800 |
| Poles | | 4 | 4 | 4 |
| Rated service voltage U _e | [V] | 1000 | 1000 | 1000 |
| Rated impulse withstand voltage U _{imp} | [kV] | 8 | 8 | 8 |
| Rated insulation voltage U _i | [V] | 1150 | 1150 | 1000 |
| Test voltage at industrial frequency for 1 min. | [V] | 3500 | 3500 | 3500 |
| Rated ultimate short-circuit breaking capacity I _{cu} (DC) 4 poles in series | [kA] | V ⁽¹⁾ | V ⁽¹⁾ | L ⁽¹⁾ |
| Utilization category (IEC 60947-2) | | A | B (400A) ⁽²⁾ - A (630A) | B ⁽³⁾ |
| Isolation behaviour | | ■ | ■ | ■ |
| Trip units: thermomagnetic | | | | |
| T adjustable, M fixed | TMD | ■ | - | - |
| T adjustable, M adjustable (5..10 x I _n) | TMA | ■ | ■ | ■ |
| Versions | | F | F | F ⁽⁴⁾ |

⁽¹⁾ Power supply only from the top

⁽²⁾ I_{cw} = 5kA

⁽³⁾ I_{cw} = 7.6 kA (630A) - 10kA (800A)

⁽⁴⁾ For T6 in the withdrawable version, please ask ABB SACE

There is also the solution with jumpers for connection of poles in series.

| | | T4 | T5 | T6 |
|--|------|-------------|---------------------|-------------|
| Rated uninterrupted current | [A] | 80...250 | 400/630 | 630/800 |
| Poles | | 4 | 4 | 4 |
| Rated service voltage U _e (DC) 2 poles + 2 poles in series | [V] | 1000 | 1000 | 1000 |
| Rated impulse withstand voltage U _{imp} | [kV] | 8 | 8 | 8 |
| Rated insulation voltage U _i (AC) 50-60 Hz | [V] | 1150 | 1150 | 1000 |
| Test voltage at power frequency for 1 min. | [V] | 3500 | 3500 | 3500 |
| Rated ultimate short-circuit breaking capacity in Dc, I _{CU} (DC) 2 poles + 2 poles in series | [kA] | 20 | 20 | 20 |
| Rated ultimate short-circuit breaking capacity in Dc, I _{CS} (DC) 2 poles + 2 poles in series | [kA] | 10 | 10 | 10 |
| Category of use (IEC 60947-2) | | A | B (400A) - A (630A) | B |
| Behaviour on isolation | | ■ | ■ | ■ |
| Reference Standards | | IEC 60947-2 | IEC 60947-2 | IEC 60947-2 |
| Thermomagnetic releases | TMD | ■ | - | - |
| | TMA | ■ | ■ | ■ |
| Terminals | | F | F | F |
| Version | | F | F | F |

4.2.3 Tmax PV molded case circuit breakers

Tmax PV is a series of T generation.

They are both switch-disconnector and circuit breakers for direct current applications with high values, suitable to be installed in photovoltaic plants and they comply with both IEC as well as UL.

The connection ensure simplicity and ease of use³.

In particular, regarding the Tmax PV circuit breakers, there are T4, T5 and T6 in compliance with Standard UL 489B and T4 in compliance with IEC 60947-2.



²² For wiring configurations and for further technical information please refer to the catalogue and to the installation instructions. If a polarity on the inverter side is connected to ground, ask ABB the proper size of the fuse and the configuration of the CB poles.

Electrical characteristics

| Tmax PV circuit breaker in compliance with UL 489B | | T4N/PV | T5N/PV | T6N/PV |
|---|------------------|----------|----------------|-----------|
| Frame size | (A) | 200 | 400 | 600-800 |
| Rated service current | (A) | 40-200 | 225-400 | 600-800 |
| Number of poles | (No.) | 3 | 3 | 4 |
| Rated service voltage | (V) | 1000V DC | 1000V DC | 1000V DC |
| Short-circuit interrupting rating @ 1000V DC | (kA) | 7.5 | 5 | 10 |
| Trip Unit | | TMD/TMA | TMD/TMA | TMA |
| Versions | | F | F | F |
| Standard terminals | | F | F | F |
| Connections* | | Jumpers | Jumpers | Jumpers |
| Terminals provided with jumper kit (see ordering codes for details) | | FCCuAl | FCCuAl-FCCU-ES | FCCuAl-EF |
| Mechanical life | (No. Operations) | 7500 | 7500 | 7500 |
| Electrical life (operations @ 1000V DC) | (No. Operations) | 1000** | 500** | 500** |

* Selection of one of the jumper connection options is mandatory; ** Opening with SOR or UVR

Electrical characteristics

| Tmax PV circuit breaker in compliance with UL 489B | | T4N-PV/E |
|--|------------------|--|
| Frame size | (A) | 250 |
| Rated service current | (A) | 100-250 |
| Number of poles | (No.) | 4 |
| Rated service voltage, Ue | (V) | 1500 |
| Rated impulse withstand voltage, Uimp | (kV) | 8 |
| Rated insulation voltage, Ui | (V) | 1500 |
| Rated ultimate short-circuit breaking capacity @ 1500V DC, Icu | (kA) | 25 according to IEC 60947-2 Edition 5.0 Annex P (τ = 1 ms) |
| Rated service short-circuit breaking capacity @ 1500V DC, Ics | (kA) | 10 according to IEC 60947-2 Edition 4.2 and GB 14048.2 (τ = 5 ms) |
| Rated service short-circuit breaking capacity @ 1500V DC, Ics | (kA) | 20 according to IEC 60947-2 Edition 5.0 Annex P (τ = 1 ms) |
| Rated service short-circuit breaking capacity @ 1500V DC, Ics | (kA) | 7.5 according to IEC 60947-2 Edition 4.2 and GB 14048.2 (τ = 5 ms) |
| Trip Unit | | TMF |
| Versions | | F |
| Standard terminals | | FCCu |
| Connections* | | Jumpers |
| Mechanical life | (No. Operations) | 7500 |
| Electrical life (operations @ 1500V DC) | (No. Operations) | 1000** |

* Selection of one of the jumper connection options is mandatory; ** Opening with SOR or UVR

4. DC fault protection – The ABB offer

4.3 Miniature circuit breakers

For the use in direct current, both miniature circuit breakers series S200M UC as well as series S800S UC and S800 PV are available.

4.3.1 S200M UC

Miniature circuit breakers series S200M UC comply with Standard CEI EN 60947-2 and differ from the standard versions in that they are equipped with permanent magnetic elements on the internal arcing chambers. Such elements allow the electric arc to be broken up to voltages equal to 440Vd.c. (for 2-pole circuit breakers).

The presence of these permanent magnetic elements establishes the circuit-breaker polarity (positive or negative); as a consequence, their connection shall be carried out in compliance with the polarity indicated on the circuit breakers.

An incorrect connection of the polarities could damage the circuit-breaker. Circuit breakers series S200M UC, special version for d.c. applications, are available with characteristics B, C, K and Z.



| General Data | |
|--|---|
| Standards | IEC/EN 60898-2 UL1077, CSA 22.2 No. 235 |
| Poles | 1P, 2P, 3P, 4P |
| Rated current In | 0.2-63 A |
| Rated frequency f | 0/50/60 Hz |
| Rated insulation voltage Ui | 253 V AC (phase to ground), 440 V AC (phase to phase) |
| Overvoltage Category | III |
| Pollution Degree | 3 |
| IEC/EN 60898-2 | |
| Tripping Characteristics | B, C |
| Rated operational voltage Un | 1P: 230 V AC, 220 V DC 2P: 400 V AC, 440 V DC 3...4P: 400 V AC* |
| Max. power frequency recovery voltage Umax | 1P: 253 V AC, 250 V DC 2P: 440 V AC, 500 V DC 3...4P: 440 V AC* |
| Min. operating voltage | 12 V AC, 12 V DC |
| Rated short-circuit capacity Icn | 10 kA |
| Energy limiting class | 3 |
| Rated impulse withstand voltage Uimp (1.2/50 µs) | 4 kV (test voltage 6.2 kV at sea level, 5 kV at 2,000 m) |
| Dielectric test voltage | 2.0 kV (50/60 Hz, 1 min) |
| Reference temperature for tripping characteristics | 30 °C |
| Electrical endurance | In ≤ 25 A: 20,000 ops. (AC), In > 25 A: 10,000 ops. (AC), 1,000 ops. (DC) |

* only acc. to IEC/EN 60898-1

| IEC/EN 60947-2 | |
|--|--|
| Tripping Characteristics | B, C, K, Z |
| Rated operational voltage Un | 1P: 253 V AC, 220 V DC 2...4P: 440 V AC, 440 V DC |
| Max. power frequency recovery voltage Umax | 1P: 266 V AC, 250 V DC 2...4P: 462 V AC, 500 V DC |
| Min. operating voltage | 12 V AC, 12 V DC |
| Rated ultimate short-circuit breaking capacity Icu | ≤40 A: 10 kA (AC); 10 kA (DC) >40 A: 6 kA (AC); 10 kA (DC) |
| Rated service short-circuit breaking capacity Ics | ≤40 A: 7.5 kA (AC); 10 kA (DC) >40 A: 6 kA (AC); 10 kA (DC) |
| Rated impulse withstand voltage Uimp (1.2/50 µs) | 4 kV (test voltage 6.2 kV at sea level, 5 kV at 2,000 m) |
| Dielectric test voltage | 2.0 kV (50/60 Hz, 1 min) |
| Reference temperature for tripping characteristics | B, C 55 °C K, Z 20 °C |
| Electrical endurance | In < 25 A: 20,000 ops. (AC), 10,000 ops. (AC); 1,500 ops. (DC) |
| UL 1077 / CSA 22.2 No. 235 | |
| Tripping Characteristics | C, K, Z |
| Rated voltage | 1P: 277 V AC, 250 V DC 2...4P: 480 Y/277 V AC, 500 V DC |
| Rated interrupting capacity | 6 kA (AC), 10 kA (DC) |
| Application | 6 kA (AC), 10 kA (DC) |
| Reference temperature for tripping characteristic | 25 °C |
| Electrical endurance | 6,000 ops. 1 cycle (1 s - ON, 9 s - OFF) |
| Mechanical data | |
| Housing | Insulation group I, RAL 7035 |
| Toggle | Insulation group II, black, sealable |
| Contact position indication | Real CPI (green OFF / red ON) |
| Protection degree acc. to DIN EN 60529 | IP20, IP40 in enclosure with cover |
| Mechanical endurance | 20,000 ops. |
| Shock resistance acc. to IEC/EN 60068-2-27 | 25 g, 2 shocks, 13 ms |
| Vibration resistance acc. to IEC/EN 60068-2-6 | 5 g, 20 cycles at 5...150...5 Hz with load 0.8 In |
| Environmental conditions acc. to IEC/EN 60068-2-30 | 28 cycles with 55 °C/90-96 % and 25 °C/95-100 % |
| Ambient temperature | -25 ... +55 °C |
| Storage temperature | -40 ... +70 °C |

4.3.2 S800S UC

The miniature circuit breakers series S800S UC can be connected without respect of the polarity (+/-). For the circuit breakers series S800S UC the available characteristic curves are B and K and both typologies have rated currents up to 125A and breaking capacity of 50kA.



The following table shows the electrical characteristics of the MCBs type S800S UC:

| | | | S800S UC |
|--|---|------|-----------------|
| Reference Standard | | | IEC 60947-2 |
| Rated current I_n | [A] | | 10...125 |
| Poles | | | 1, 2, 3, 4 |
| Rated voltage U_e | d.c./poles | [V] | 250 |
| Max. operating voltage U_b max | d.c./poles | | 250 |
| Insulation voltage U_i | d.c./poles | [V] | 250 |
| Rated impulse voltage U_{imp} | d.c./poles | [kV] | 8 |
| Rated ultimate short-circuit breaking capacity I_{cu} IEC 60947-2 | [kA] | | 50 |
| Rated service short-circuit breaking capacity I_{cs} IEC 60947-2 | [kA] | | 50 |
| Suitable for isolation in compliance with CEI EN 60947-2 | [kA] | | 3 |
| Characteristics of the thermomagnetic release | B: 4I_n < I_m < 7 I_n | | ■ |
| | K: 7I_n < I_m < 14 I_n | | ■ |

4. DC fault protection – The ABB offer

4.3.3 S800 PV

The series of products S800 PV includes devices suitable to be used in DC circuits with high voltages, typical of photovoltaic plants (in the connection section between panels and inverter).

The S800PV-S providing maximum safety even in the event of reverse polarisation, the S800PV-S series offers high performance in a compact design. The interchangeable terminals (ring lugs or cage terminals) make the system even more convenient. In addition, busbar are available for fast and easy serial pole connection.



The following table shows the electrical characteristics of the MCBs and switch-disconnectors of the series S800 PV

| | | | | S800 PV-S | S800 PV-M |
|---|--------------|------------|------|--|---------------------------------|
| Reference standard | | | | IEC / EN 60947-2 | IEC / EN 60947-3 |
| Rated current, I _n | | [A] | | 10 ... 125 | 32, 63, 125 |
| Poles | | | | 2 ... 4 | 2 ... 4 |
| Rated operational voltage, U _e | 2 poles (dc) | [V] | | 800 (I _n =10...80A); 600 (I _n =100...125A) | 800 (I _n =32...125A) |
| | 4 poles (dc) | [V] | | | |
| Rated insulation voltage, U _i | | [V] | | 1500 | 1500 |
| Rated impulse withstand voltage, U _{imp} | | [kV] | | 8 | 8 |
| Rated ultimate short-circuit current, I _{cu} | 800 Vd.c. | (2 poles)* | [kA] | 5 | - |
| | 1200 Vd.c. | (4 poles)* | [kA] | 5 | - |
| Rated service breaking capacity, I _{cs} | 800 Vd.c. | (2 poles)* | [kA] | 5 | - |
| | 1200 Vd.c. | (4 poles)* | [kA] | 5 | - |
| Rated short-time withstand current, I _{cw} | 800 Vd.c. | (2 poles)* | [kA] | - | 1.5 |
| | 1200 Vd.c. | (4 poles)* | [kA] | - | 1.5 |
| Rated short-circuit making capacity, I _{cm} | 800 Vd.c. | (2 poles)* | [kA] | - | 0.5 |
| | 1200 Vd.c. | (4 poles)* | [kA] | - | 0.5 |
| Utilization category | | | | A | DC-21A |

* Please refer to the connection diagrams.

4.4 Fuse-disconnectors

E 90 PV series fuse disconnectors, designed for operating voltages of 1000 V DC with utilization category DC-20B, are particularly suited for protection against overcurrents of photovoltaic systems.

The single-pole or two-pole E 90 PV disconnectors for 10.3 x 38 mm cylindrical fuse links offer a reliable, compact and affordable solution for photovoltaic installations.

Versions with blown fuse indicator allow to check whether the fuse is still working correctly or not.



Technical features

| Type | | E 90/32 PV | E 90/32 PV according to UL |
|--|--------------------|---|----------------------------|
| Rated current | [A] | 30 | |
| Type of current | | DC | |
| Fuse | [mm] | 10 x 38 | |
| Max power dissipation accepted | [W] | 3 | |
| Rated frequency | [Hz] | - | |
| Tightening torque | | PZ2 2-2.5 Nm | PZ2 18-22 lb-in |
| Protection degree | | IP20 | |
| Terminals cross-section | [mm ²] | 25 | |
| Rated insulation voltage | [kV] | 1 | |
| Cross-section rigid copper conductors | | 1.5 - 25 mm ² | n..a. |
| Cross-section stranded copper conductors | | 1.5 - 16 mm ² | 8÷3 AWG |
| Operating temperature | [°C] | -5/+40 ⁽¹⁾ | |
| Storage temperature | [°C] | -25/+70 ⁽²⁾ | |
| Altitude | [m] | 2000 | |
| Degree of relative humidity at temperature | [°C] | max.90% with temp.+20°C 50% with max. temp.+40°C | |
| Voltage range for LED indicator light | | 24-1000 AC/DC (only s version) | |
| Can be padlocked (open) | | ■ | |
| Can be sealed (closed) | | ■ | |
| IEC 60947-3 | | | |
| Utilization category | | DC-20B | |
| Rated voltage | [V] | 1000 | |

⁽¹⁾ for lower temperature verify fuse technical characteristics, for higher temperature refer to derating table in Chapter 5 of Electrical installation solutions for buildings - Technical details

⁽²⁾ for more than 24h max temperature is +55 °C

4. DC fault protection – The ABB offer

4.5 Fuse-holder

E 90 PV fuse holder

The E 90 PV 1500 series of fuse holders has been designed for applications up to 1500 V DC.

Thanks to their rated voltage up to 1500 V DC they are the ideal solution for protecting cells and inverters. In case of maintenance, they ensure isolation of circuits and strings up to 1500 V in direct current, in total safety. The main features of E 90 PV 1500 fuse holders include venting grooves and cooling chambers which improved heat dissipation.



Technical features

| Type | E90/32 PV1500 | |
|---|--------------------|---|
| Reference standards | - | IEC 60269-1,-2,-6 UL 4248-19 |
| Rated current | [A] | 32 (acc. IEC) / 30 (acc. UL) |
| Rated operational voltage | [V] | 1500 V DC |
| Fuse size | [mm] | 10×85 and 10/14×85 |
| Max. power dissipation accepted | [W] | 6 |
| Tightening torque | [Nm] | PZ2 2-2.5 Nm (PZ2 18-22 lb-in) |
| Protection degree | - | IP20 |
| Rated insulation voltage | [kV] | 1 |
| Cross section rigid copper conductors (1 wire) | [mm ²] | 16-10 AWG |
| Cross section stranded copper conductors (1 wire) | [mm ²] | 0.75 – 25 (18-4 AWG) |
| Cable temperature | [°C] | max 90 (acc. UL) |
| Operating temperature | [°C] | > -5 |
| Storage temperature | [°C] | > -25 |
| Degree of relative humidity at temperature | [°C] | max.90% with temp.+20°C 50% with max. temp.+40°C |

4.6 GE Rapid

The Gerapid line of high speed DC circuit breakers is designed for protection of main DC circuits at Traction Power Substations. In addition, Gerapid is widely used for protection of DC drives, as field discharge breakers or commutation switches in DC shunt excitation systems of synchronous generators, as protection for super-conducting coils and in many specialized DC power distribution systems, whenever high speed opening and efficient energy dissipation is required.

All breakers are type tested as per EN 50123-2, IEC 60947-2 or IEEE C37.14 standards and are certified by UL, CCC, CESI and GOST organizations.



| EN 50123-2 / IEC 61992-2 "Railway applications. Fixed installations. D.C. switchgear. D.C. circuit breakers." | | | | |
|---|--------------------------------|---------|-------------------|---------|
| GERapid Type | 2607 | 4207 | 6007 | 8007 |
| Rated current | 2 600A | 4 200 A | 6 000 A | 8 000 A |
| Rated voltage | 1 000 V - 3 600 V | | 1 000 V - 3 000 V | |
| Rated insulation voltage | 2 000 V - 4 000 V | | 2 000 V - 3 600 V | |
| Rated withstand voltage | 10 kW - 15 kW / 50 Hz / 60 sec | | | |
| Rated inpulse voltage | 18 kW - 30 kW | | | |
| Rated breaking capacity | 30 - 125 kA | | | |

| IEEE/ANSI C37.14 "IEEE Standard for Low-Voltage DC Power Circuit Breakers Used in Enclosures." UL certified types are 2508, 4008, 5008 and 6008. | | | | | | |
|---|--------------------|--------------------|---------|-----------------|---------|---------|
| GERapid Type | 2607 2508 UL | 4207 4008 UL | 5008 UL | 8007 6008 UL | 8007R* | 10007R* |
| Rated current | 2 600 A 2 500 A | 2 600 A 2 500 A | 5 000 A | 6 000 A | 6 000 A | 8 000 A |
| Rated voltage | 800 V | | | 800 V - 1 200 V | | |
| Rated withstand voltage | 3 700 V | | | 10 000 V | | |
| Rated inpulse voltage | 200 kA | | | | | |
| Rated breaking capacity | 25 kA - 35 kA | | | 150 kA | | |

* Rectifier Circuit Breaker

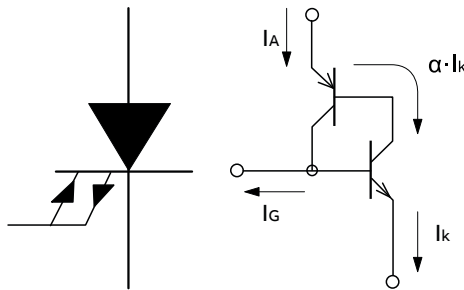
For further information about the complete ABB offer for DC applications, please have a look at the DC brochure at the following link:
<http://search.abb.com/library/Download.aspx?DocumentID=9AKK107991A7820&LanguageCode=en&DocumentPartId=&Action=Launch>

Annex A: Description of the main power-electronic-switches

A.1 GTO (Gate Turn-Off thyristor)

A GTO is a special type of thyristor, which is a high-power semiconductor device. GTOs, as opposed to normal thyristors, are fully controllable switches which can be turned on and off by their gate (Figure A.1).

Figure A.1 – Circuit symbol and equivalent circuit of a GTO



Normal thyristors (silicon-controlled rectifiers) are not fully controllable switches (a "fully controllable switch" can be turned on and off at will).

Thyristors can only be turned ON and cannot be turned OFF. Thyristors are switched ON by a gate signal, but even after the gate signal has been de-asserted (removed), the thyristor remains in the ON-state until any turn off condition occurs (which can be the application of a reverse voltage to the terminals, or when the current flowing through (forward current) falls below a certain threshold value known as the "holding current"). Thus, a thyristor behaves like a normal semiconductor diode after it has been turned on or "fired".

The GTO can be turned-on by a gate signal, and can also be turned-off by a gate signal of negative polarity.

The main feature that differentiates the GTO from a normal thyristor is a special gate arrangement, which enables the interruption of the load current at any desired time by applying a negative current to the gate. Hence, in contrast to the thyristor, the GTO can be operated as a true on/off switch [2].

Turning on in the GTO is accomplished by a "positive current" pulse between the gate and cathode terminals. As the gate-cathode behaves like a PN junction, there will be some relatively small voltage between the terminals.

The turning on phenomenon in a GTO however is, not as reliable as in an SCR (thyristor) and small positive gate current must be maintained even after turn on to improve reliability.

Turning off is accomplished by a "negative voltage" pulse between the gate and cathode terminals. Some of the forward current (about one-third to one-fifth) is "stolen" and used to induce a cathodegate voltage that in turn, induces the forward current to fall and the GTO will switch off (transitioning to the 'blocking' state).

The main design goal for GTOs has always been to achieve a maximum current turn off capability with a minimum gate current requirement.

The ratio of the two currents is referred to as the turn off gain.

Unfortunately, a higher turn off gain generally results in a poor scaling of the maximum turn off current with the area of the GTO, thereby setting certain economic limits to the device size.

GTO thyristors suffer from long switch off times, whereby, after the forward current falls, there is a long tail time where residual current continues to flow until all remaining charges from the device are taken away.

This restricts the maximum switching frequency to approx. 1 kHz: this limitation has very unfavorable consequences in DC/AC converters, since a low switching frequency leads to an high content of undesired harmonics in the AC signal. It may be noted however, that the turn off time of a GTO is approximately ten times faster than of a comparable SCR.

A further disadvantage of the GTO is the fact that the device must always be equipped with expensive and bulky protection circuit.

GTO thyristors usually consist of a large number (hundreds or thousands) of small thyristor cells connected in parallel.

A distributed buffer gate turn-off thyristor (DB-GTO) is a thyristor with additional PN layers in the drift region to reshape the field profile and increase the voltage blocked in the off state. Compared to a typical PN-PN structure of a conventional thyristor, this thyristor would be a PN-PN-PN type structure.

GTO thyristors are available with or without reverse blocking capability. Reverse blocking capability adds to the forward voltage drop because of the need to have a long, low doped P1 region. GTO thyristors capable of blocking reverse voltage are known as Symmetrical GTO thyristors (abbreviated S-GTO).

Usually, the reverse blocking voltage rating and forward blocking voltage rating are the same. The typical application for symmetrical GTO thyristors is in current source inverters.

GTO thyristors incapable of blocking reverse voltage are known as Asymmetrical GTO thyristors (abbreviated A-GTO), and are generally more common than Symmetrical GTO thyristors.

They typically have a reverse breakdown rating in the tens of volts.

A-GTO thyristors are used where either a reverse conducting diode is applied in parallel (for example, in voltage source inverters) or where reverse voltage would never occur (for example, in switching power supplies or DC traction choppers).

GTO thyristors can be fabricated with a reverse conducting diode in the same package.

These are known as RC-GTO, for Reverse Conducting GTO.

Unlike insulated gate bipolar transistors (IGBT), GTO thyristors require external devices ("snubber circuits") to shape the turn on and turn off currents to prevent device damages.

During turning on, the device has a maximum di/dt rating limiting the rise of current.

This is to allow the entire bulk of the device to reach turn on status before the full current is reached.

If this rating is exceeded, the area of the device nearest the gate contacts will overheat and melt because of overcurrent.

The rate of di/dt is usually controlled by adding a saturable reactor (turn-on snubber), although turn-on di/dt is a less serious constraint with GTO thyristors than it is with normal thyristors, because of the way the GTO is constructed from many small thyristor cells in parallel. Reset of the saturable reactor usually places a minimum off time requirement on GTO based circuits.

During turn off, the forward voltage of the device must be limited until the current tails off.

The limit is usually around 20% of the forward blocking voltage rating. If the voltage rises too fast at turning off, not all of the device will turn off and the GTO will fail, often explosively, due to the high voltage and current focused on a small portion of the device. Substantial snubber circuits are added around the device to limit the rise of voltage at turning off. Resetting the snubber circuit usually places a minimum on time requirement on GTO based circuits.

The minimum on and off time is handled in DC motor chopper circuits by using a variable switching frequency at the lowest and highest duty cycle.

This is observable in traction applications where the frequency will ramp up as the motor starts, then the frequency stays constant over most of the speed ranges, then the frequency drops back down to zero at full speed.

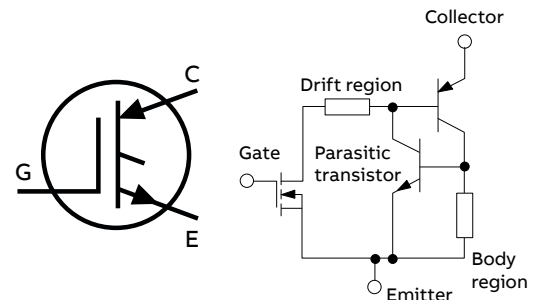
A.2 IGBT (Insulated Gate Bipolar Transistor)

The IGBT is a three-terminal power semiconductor device primarily used as an electronic switch and in newer devices it is noted for combining high efficiency and fast switching.

It switches electric power in many modern appliances: Variable-Frequency Drives (VFDs), electric cars, trains, variable speed refrigerators, airconditioners and even stereo systems with switching amplifiers. The IGBT combines the simple gate-drive characteristics of MOSFETs (Metal Oxide Semiconductor Field Effect Transistor) with the high-current and low-saturation-voltage capability of bipolar tran-

sistors (Figure A.2). The IGBT combines an isolated gate FET for the control input, and a bipolar power transistor as a switch, in a single device. The IGBT is used in medium- to high-power applications such as switched-mode power supplies, traction motor control and induction heating. Large IGBT modules typically consist of many devices in parallel and can have very high current handling capabilities in the order of hundreds of amperes with blocking voltages of 6000 V, equating to hundreds of kilowatts.

Figure A.2 – Circuit symbol and equivalent circuit of an IGBT



IGBT is a fairly recent invention. The first-generation devices of the 1980s and early 1990s were relatively slow in switching, and prone to failure through such modes as latchup (in which the device will not turn off as long as the current is flowing) and secondary breakdown (in which a localized hotspot in the device goes into thermal runaway and burns the device out at high currents).

Second-generation devices were much improved, and the current third-generation ones are even better, with speed rivaling MOSFETs, and excellent ruggedness and tolerance of overloads.

The extremely high pulse ratings of second- and third-generation devices also make them useful for generating large power pulses in areas like particle and plasma physics, where they are starting to supersede older devices like thyratrons and triggered spark gaps.

The success of the IGBT is due to several features:

- high input impedance, resulting in small and inexpensive gate driver circuits;
- no need to employ snubber circuits as with GTOs;
- capability of surviving a short circuit for a certain limited period of time;
- advantageous balance between conduction losses and switching losses, which allows the IGBT to be used economically over a wide range of switching frequencies;
- good scalability, such as a proportional relationship between the useful current and the area of the component.

The IGBT is a semiconductor device with four alternating layers (P-N-P-N) that are controlled by a metal-oxide-semiconductor (MOS) gate structure without regenerative action.

An IGBT cell is constructed similarly to a n-channel vertical construction power MOSFET except the n+ drain is replaced with a p+ collector layer, thus forming a vertical PNP bipolar junction transistor.

Annex A: Description of the main power-electronic-switches

This additional p+ region creates a cascade connection of a PNP bipolar junction transistor with the surface n-channel MOSFET.

An IGBT has a significantly lower forward voltage drop compared to a conventional MOSFET in higher blocking voltage rated devices. As the blocking voltage rating of both MOSFET and IGBT devices increases, the depth of the n- drift region must increase and the doping must decrease, resulting in roughly square relationship decrease in forward conduction vs. blocking voltage capability of the device.

By injecting minority carriers (holes) from the collector p+ region into the n- drift region during forward conduction, the resistance of the n- drift region is considerably reduced.

However, this resultant reduction in on-state forward voltage comes with several penalties:

- the additional PN junction blocks reverse current flow. This means that unlike a MOSFET, IGBTs cannot conduct in the reverse direction.

In bridge circuits where reverse current flow is needed, an additional diode (called a freewheeling diode) is placed in parallel with the IGBT to conduct current in the opposite direction.

The penalty is not as severe as first assumed though, because at the higher voltages where IGBT usage dominates, discrete diodes are of significantly higher performance than the body diode of a MOSFET;

- the reverse bias rating of the N-drift region to collector P+ diode is usually only of tens of volts, so if the circuit application applies a reverse voltage to the IGBT, an additional series diode must be used;
- the minority carriers injected into the N-drift region take time to enter and exit or recombine at turn on and turn off. This results in longer switching time and hence higher switching loss compared to a power MOSFET;
- the on-state forward voltage drop in IGBTs behaves very differently to that in power MOSFETS.

The MOSFET voltage drop can be modeled as a resistance, with the voltage drop proportional to current.

By contrast, the IGBT has a diode like voltage drop (typically of the order of 2V) increasing only with the log of the current.

Additionally, MOSFET resistance is typically lower for smaller blocking voltages, meaning that the choice between IGBTs and power MOSFETS de-

pends on both the blocking voltage and current involved in a particular application, as well as the different switching characteristics mentioned above.

In general, high voltage, high current and low switching frequencies favor IGBTs while low voltage, low current and high switching frequencies are the domain of the MOSFET.

A.3 IGCT (Integrated Gate Commutated Thyristor)

The IGCT is a power semiconductor electronic device, used for switching electric current in industrial equipment. It is related to the gate turn-off (GTO) thyristor. It was jointly developed by Mitsubishi and ABB.

Like the GTO thyristor, the IGCT is a fully controllable power switch, meaning that it can be turned both on and off by its control terminal (the gate).

Gate drive electronics are integrated with the thyristor device. An IGCT is a special type of thyristor similar to a GTO. They can be turned on and off by a gate signal, have lower conduction loss as compared to GTOs, and withstand higher rates of voltage rise (dv/dt), such that no snubber is required for most applications.

The structure of an IGCT is very similar to a GTO thyristor. In an IGCT, the gate turn off current is greater than the anode current.

This results in a complete elimination of minority carrier injection from the lower PN junction and faster turn off times.

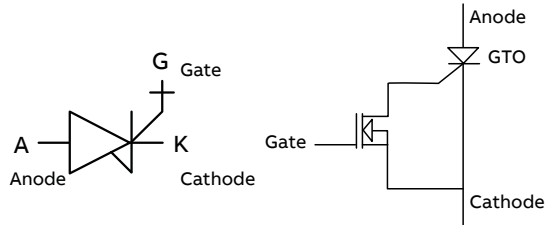
The main difference is a reduction in cell size, plus a much more substantial gate connection with much lower inductance in the gate drive circuit and drive circuit connection.

The very high gate currents plus fast di/dt rise of the gate current means that regular wires can not be used to connect the gate drive to the IGCT.

The drive circuit PCB is integrated into the package of the device. The drive circuit surrounds the device and a large circular conductor attaching to the edge of the IGCT is used.

The large contact area and short distance reduces both the inductance and resistance of the connection.

Figure A.3 – Circuit symbol and equivalent circuit of an IGCT



IGCT much faster turn-off times compared to GTO allows them to operate at higher frequencies—up to several kHz for very short periods of time. However, because of high switching losses, the typical operating frequency is up to 500 Hz. IGCT are available with or without reverse blocking capability. Reverse blocking capability adds to the forward voltage drop because of the need to have a long, low doped P1 region. IGCT capable of blocking reverse voltage are known as symmetrical IGCT, abbreviated S-IGCT. Usually, the reverse blocking voltage rating and forward blocking voltage rating are the same. The typical application for symmetrical IGCT is in current source inverters. IGCT incapable of blocking reverse voltage are known as asymmetrical IGCT, abbreviated A-IGCT.

They typically have a reverse breakdown rating in the tens of volt. A-IGCTs are used where either a reverse conducting diode is applied in parallel (for example, in voltage source inverters) or where reverse voltage would never occur (for example, in switching power supplies or DC traction choppers). Asymmetrical IGCTs can be fabricated with a reverse conducting diode in the same package.

These are known as RC-IGCTs, for reverse conducting IGCTs. Moreover, IGCTs capable of blocking reverse voltage are known as reverse blocking IGCTs (symmetrical IGCTs), abbreviated RB-IGCT. Usually, the reverse blocking voltage rating and forward blocking voltage rating are the same.

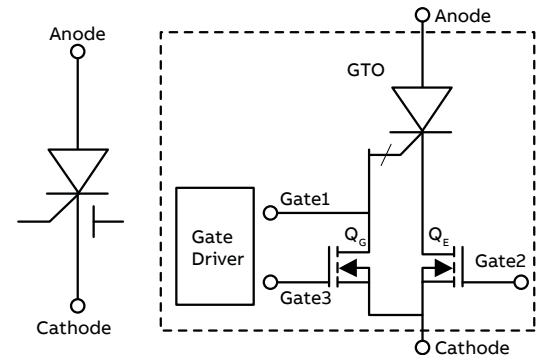
A.4 ETO (Emitter Turn-Off thyristor)

Based on the integration of the GTO thyristor and power MOSFET technology, the emitter turn-off (ETO) thyristor is a new type of superior high-power semiconductor device that is suitable for use in high-frequency and high-power converters.

By optimally integrating commercial GTOs and MOSFETs, the ETO has the advantages of fast switching speed, snubberless turn-off capability, voltage control, and built-in current sensing capabilities.

An ETO is formed by integrating a GTO in series with an emitter switch QE. A gate switch QG is also connected to the GTO gate, as shown in Figure A.4.

Figure A.4 – Circuit symbol and equivalent circuit of an ETO



During a normal forced turn-off transient, QE is turned off and QG is turned on.

The turn-off of the emitter switch QE cuts off the GTO's cathode current path, and all of the cathode currents are quickly transferred to the gate path. In this way, the latch-up mechanism of the GTO is broken and the ETO is turned off under a unity-gain turn-off condition (also known as a hard driven turn-off condition).

Therefore, the ETO has a wide reverse biased safe operation area (RBSOA) and snubberless turn-off capability. In real applications, a dv/dt turn-off snubber is usually applied to reduce the device turn-off loss and to improve its reliability.

With a dv/dt snubber, compared to the snubberless case, the ETO has a lower storage time and current fall time since the device current starts to drop once the anode voltage begins to rise.

During the turn-on transient, QE is turned on and QG is turned off. A high-current pulse is injected into the GTO gate by the integrated gate driver in order to reduce the turn-on delay time and to improve the turn-on di/dt rating. The built-in PNP and NPN transistors inside the GTO latch up quickly and the anode voltage of the ETO collapses to a low voltage. So the turn-on process of the ETO is similar to that of a GTO. Thanks to the ETO compact structure and low gate loop inductance (about 10 nH), a gate current pulse with high amplitude and rise rate can be applied; therefore an ETO can be uniformly turned on without current crowding problems.

Annex B: Switch-mode three-phase converters

The input/output to switch-mode converter is assumed to be a DC-voltage source, so such converters are referred to as voltage-source converters (VSCs). VSCs can be split into two macro-categories:

- Pulse-Width Modulated (PWM) – in these converters, the DC voltage is kept constant in magnitude, so the converter controls the magnitude and the frequency of the AC voltages. This is met by PWM of the converter switches and hence such converters are called PWM converters. There are various schemes to pulse-width modulate the inverter switches so as to shape the AC voltage to be as close to a sine wave as possible
- Square-Wave – in these converters, the DC voltage is controlled in order to control the magnitude of the AC voltage, so the converter has to control only the frequency of the AC voltage, whose waveform is similar to a square wave and hence these converters are called square-wave converters.

B.1 Pulse Width Modulated (PWM) switching mode

In a PWM control, so as to produce a sinusoidal AC voltage waveform at a desired frequency, a sinusoidal control signal (v_c) at the desired frequency is compared with a triangular waveform (v_t).

The frequency of the triangular waveform establishes the switching frequency (f_{sw}) and is generally kept constant with its amplitude.

The control signal is used to modulate the switch duty ratio and has a frequency (f_c), which is the desired fundamental frequency of the inverter voltage output.

The amplitude modulation ratio (m_a) is defined as the ratio between the peak amplitude of the control signal and the amplitude of the triangular signal (which is usually kept constant):

[B.1]

$$m_a = \frac{\hat{v}_c}{\hat{v}_t}$$

The frequency modulation ratio (m_f) is defined as the ratio between the switching frequency and the fundamental frequency:

[B.2]

$$m_f = \frac{f_{sw}}{f_1}$$

The harmonic spectrum of the phase voltage (v_f) shows three items of importance:

- the peak amplitude of the fundamental frequency component is [1]:

[B.3]

$$\hat{v}_{f1} = \frac{\hat{v}_c}{\hat{v}_t} \cdot \frac{V_{dc}}{2} = m_a \cdot \frac{V_{dc}}{2} \quad (m_a \leq 1)$$

- the harmonics in the voltage waveform appear as sidebands centered around f_{sw} and its multiples
- choosing m_f as an odd integer, only the coefficients of the sine series in the Fourier analysis are finite and only odd harmonics are present.

Because of the relative ease in filtering harmonic voltages at high frequencies, it is desirable to use as high a switching frequency as possible, except for one significant drawback: switching losses in the inverter switches increase proportionally with the switching frequency. Hence, in most applications, the switching frequency is up to 20 kHz.

With reference to the value of m_a , two behavior modes may occur:

- linear modulation ($m_a \leq 1$), in which the fundamental frequency component in the output voltage varies linearly with m_a .

Therefore, the line-to-line rms voltage at the fundamental frequency can be written as:

[B.4]

$$v_l = \frac{\sqrt{3}}{\sqrt{2}} \cdot m_a \cdot \frac{V_{dc}}{2} \cong 0.612 \cdot m_a \cdot V_{dc} \quad (m_a \leq 1) \rightarrow V_{dc} \cong \frac{1.63 \cdot v_l}{m_a}$$

- overmodulation ($m_a > 1$), in which the peak of the control voltage exceeds the peak of the triangular waveform. In this mode of operation the fundamental frequency voltage does not increase proportionally with m_a and for sufficiently large value of m_a , the PWM degenerates into a square-wave inverter waveform.

This results in the maximum value of the line-to-line rms voltage equal to:

[B.5]

$$v_l = \frac{\sqrt{3}}{\sqrt{2}} \cdot \frac{4}{\pi} \cdot \frac{V_{dc}}{2} = \frac{\sqrt{6}}{\pi} \cdot V_{dc} \cong 0.78 \cdot V_{dc} \rightarrow V_{dc} \cong 1.28 \cdot v_l$$

In overmodulation more sideband harmonics appear centered around the frequency of harmonic m_f and its multiples. However, the dominant harmonics may not have as large an amplitude as with $m_a \leq 1$.

B.2 Square-Wave switching mode

It should be noted that the square-wave switching is also a special case of the sinusoidal PWM switching when ma becomes so large that the control voltage waveform intersects with the triangular waveform. One of the advantages of the square-wave operation is that each inverter switch changes its state only twice per cycle, which is important at very high power levels where the solid-state switches generally have slower turn-on and turn-off speeds.

One of the serious disadvantages of this switching mode is that the inverter is not capable of regulating the AC voltage magnitude.

Therefore, the DC voltage to the inverter must be adjusted so as to control the magnitude of the AC voltage. The line-to-line voltage waveform contains harmonics ($h=6n\pm 1; n=1,2,\dots$), whose amplitudes decrease inversely proportional to their harmonic order:

[B.6]

$$v_l = \frac{0.78}{h} \cdot V_{dc}$$

B.3 Current regulated modulation

There are various ways to obtain the switching signals for the converter switches in order to control the AC current. Two of such methods are:

- tolerance band control – the actual phase current is compared with a sinusoidal reference current with the tolerance band around the reference current associated with that phase.

If the actual current tries to go beyond the upper tolerance band, the lower inverter switch of the actual inverter leg is turned on whereas the upper inverter switch is turned off.

Similar actions take place in the other two phases. The switching frequency depends on how fast the current changes from the upper to the lower limit and vice versa.

Moreover, the switching frequency does not remain constant but varies along the current waveform.

- fixed frequency control – the error between the reference and the actual current is amplified or fed through a proportional-integral (PI) regulator. The output control voltage of the amplifier is compared with a fixed frequency (switching frequency) triangular waveform. A positive error and, hence, a positive voltage control results in a larger inverter AC voltage, thus bringing the actual current to its reference value. Similar action occurs in the other two phases.

In the rectifier mode of operation of the converter the amplitude of the reference current should be such as to maintain the DC voltage at a desired or reference value V_{dc} , in spite of the variation of several DC loads.

B.4 Bidirectional power flow

In a single-phase converter (but the analysis may be extended to a three-phase converter remaining valid) with a rectifier mode of operation, the following formula is valid:

[B.7]

$$v_s = v_{conv} + v_l = v_{conv} + L_s \frac{di_s}{dt}$$

Assuming v_s to be sinusoidal, the fundamental frequency components of v_{conv} and v_s can be expressed as phasors

\bar{V}_s and \bar{V}_{conv} :

[B.8]

$$\bar{V}_s = \bar{V}_{conv} + \bar{V}_l = \bar{V}_{conv} + j\omega L_s \bar{I}_s$$

The real power P and the reactive power Q supplied by the source to the converter are [1]:

[B.9]

$$P = \frac{V_s^2}{\omega \cdot L_s} \cdot \left(\frac{V_{conv}}{V_s} \sin \delta \right)$$

[B.10]

$$Q = \frac{V_s^2}{\omega \cdot L_s} \cdot \left(1 - \frac{V_{conv}}{V_s} \sin \delta \right)$$

From these equations it is clear that for a given line voltage \bar{V}_s and inductance L_s , desired values of P and Q can be obtained by controlling the magnitude and phase of \bar{V}_{conv} . In particular, the magnitude of \bar{V}_{conv} can be varied by controlling the amplitude of the sinusoidal reference waveform v_c , whereas the phase of \bar{V}_{conv} can be varied by shifting the phase of v_c . Hence, the magnitude and direction of power flow are automatically controlled by regulating V_{dc} at its desired value.

Annex C: DC fault contribution of other types of converters

Hereunder several types of interface converters between the DC-Bus and DC/AC loads, ESS, renewable sources and gensets are analyzed from their DC fault contribution point of view. Since the converters are connected on one side to the LVDC microgrid, they have at their terminals the LVDC microgrid voltage.

This means that, in the absence of a separation transformer, the terminals of a generator or an ESS are isolated from the ground. For example, if a MV/LV transformer with the star point connected to the ground is considered, another connection to the ground of an active part, e.g. a PV plant or ESS terminal, creates a double active part ground connection with an unwanted trip of the residual current devices installed on AC side.

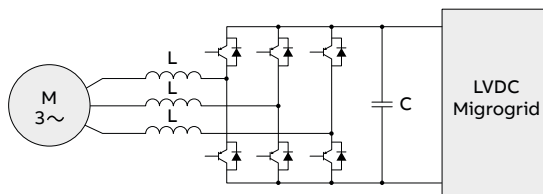
As a consequence, even a ground fault in the LVDC microgrid is seen by each converter as a short circuit at its DC terminals.

C.1 DC/AC interface converter for AC loads

This converter feeds those loads that require mandatorily an AC supply. A DC fault causes firstly the capacitor discharge current.

This capacitor is usually installed in most converters. Instead, the converter current contribution is negligible whether the loads are passive or it is limited at maximum the transient short circuit current fed by motors.

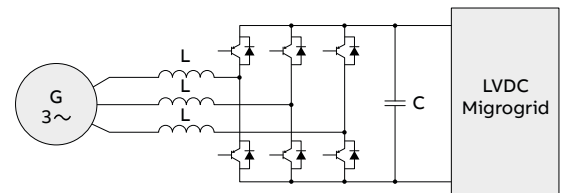
Figure C.1 – DC/AC interface converter for AC loads



C.2 AC/DC interface converter for Gen-sets or wind power plants

In case of a DC fault, besides the capacitor discharge, the converter behaves in similar manner of what analyzed in Chapter 2, but now the short circuit power on AC side is limited to the usual one supplied by an alternator.

Figure C.2 – AC/DC interface converter for Gen-sets or wind power plants



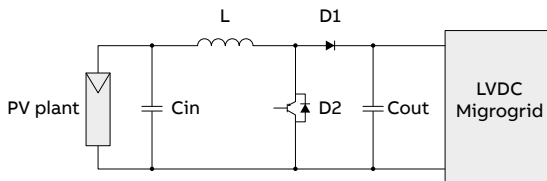
C.3 DC/DC interface converter for PV plants

This DC/DC converter has the double task of both to allow the PV plant to work at its own maximum power point and to adapt the DC array voltage to the DC-Bus voltage. With the common ratio between these voltages, usually the boost (step-up) converter configuration is used for medium-high power applications.

In case of a DC fault, this converter supplies firstly a peak current due to the DC capacitor discharge, then the boost converter continues to feed the fault with the whole available PV plant short circuit current (equal to 1.25 times the maximum current in standard conditions).

It is important to note that this type of converter is not able to limit such current, since in this situation the short circuit current flows through the diode D1 in series (Figure C.3) without any possible action by the converter control.

Figure C.3 – DC/DC interface converter between the PV plant and the LVDC microgrid

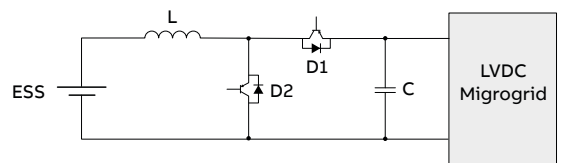


C.4 DC/DC interface converter for ESSs

The configuration of this DC/DC converter is the reversible one (Figure C.4), since it has to perform the double task to recharge and maintain the ESS charged and, when necessary, to allow the power flow toward the DC-Bus.

In case of a DC fault, a situation similar to that in Section C.3 occurs, because the presence of the freewheeling diode D1 allows the DC fault ESS contribution without any control by the converter.

Figure C.4 – DC/DC reversible interface converter between the ESS and the LVDC microgrid





—

ABB S.p.A.

5, Via Pescaria

I-24123 Bergamo - Italy

Phone: +39 035 395.111

www.abb.com